Universität Stuttgart

Institut für Wasser- und Umweltsystemmodellierung

Mitteilungen

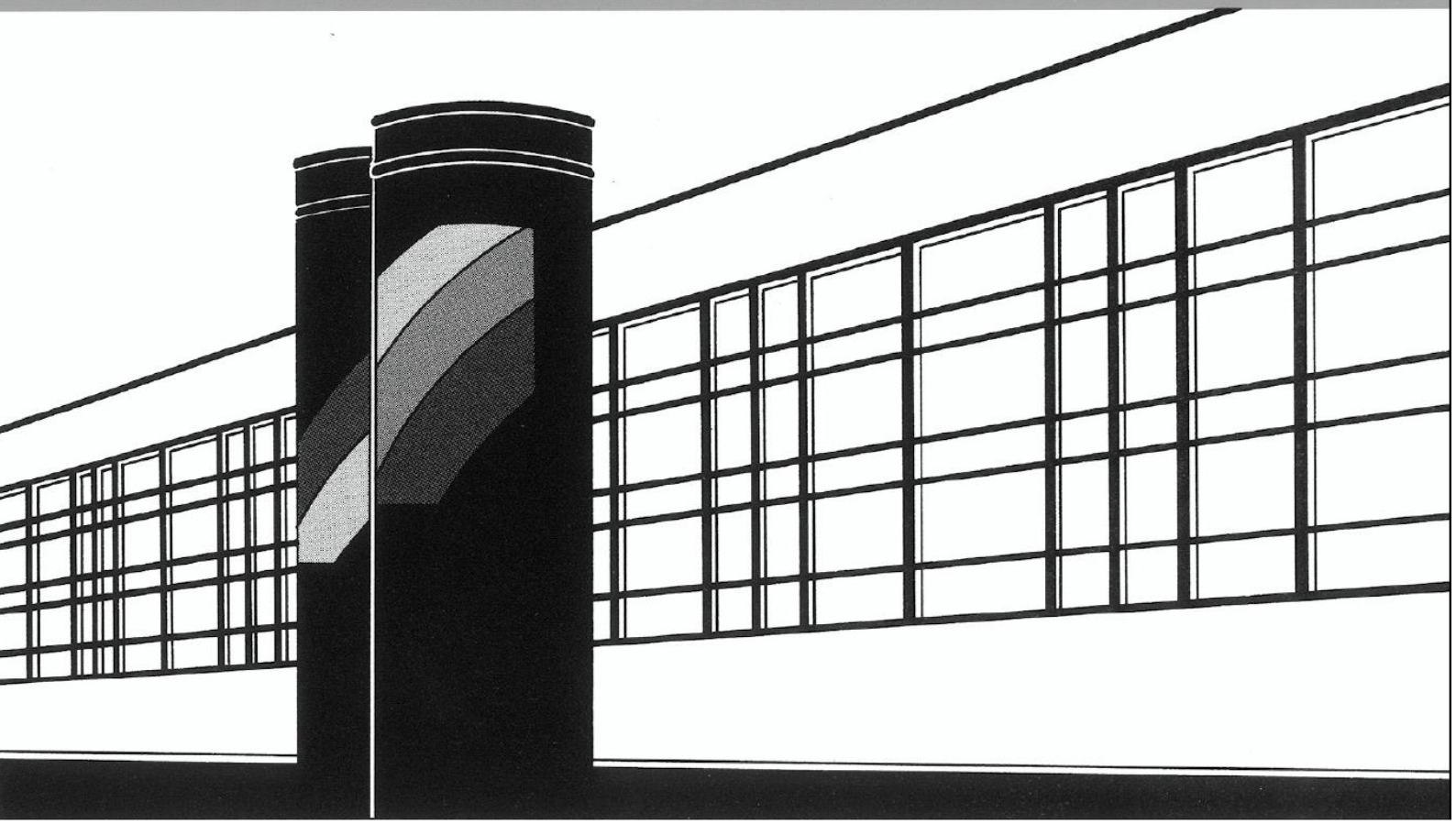

Heft 272 Abelardo Rodríguez Pretelín

Integrating transient flow conditions into groundwater well protection

Integrating transient flow conditions into groundwater well protection

Von der Fakultät Bau- und Umweltingenieurwissenschaften der Universität Stuttgart zur Erlangung der Würde eines Doktor-Ingenieurs (Dr.-Ing.) genehmigte Abhandlung

Vorgelegt von

Abelardo Rodríguez Pretelín

aus Mexiko Stadt, Mexiko

Hauptberichter:	Prof. Dr.-Ing. Wolfgang Nowak
Mitberichter:	Prof. Dr. Eric Morales Casique

Tag der mündlichen Prüfung: 12. March 2020

Institut für Wasser- und Umweltsystemmodellierung
der Universität Stuttgart
2020

Heft 272

Integrating transient flow conditions into groundwater well protection

von
Dr.-Ing.
Abelardo Rodríguez Pretelín

Eigenverlag des Instituts für Wasser- und Umweltsystemmodellierung
der Universität Stuttgart

D93 Integrating transient flow conditions into groundwater well protection

Bibliografische Information der Deutschen Nationalbibliothek
Die Deutsche Nationalbibliothek verzeichnet diese Publikation in der Deutschen Nationalbibliografie; detaillierte bibliografische Daten sind im Internet über http://www.d-nb.de abrufbar

Rodríguez Pretelín, Abelardo:
Integrating transient flow conditions into groundwater well protection, Universität Stuttgart. - Stuttgart: Institut für Wasser- und Umweltsystemmodellierung, 2020

(Mitteilungen Institut für Wasser- und Umweltsystemmodellierung, Universität Stuttgart: H. 272)
Zugl.: Stuttgart, Univ., Diss., 2020
ISBN 978-3-942036-76-4

NE: Institut für Wasser- und Umweltsystemmodellierung <Stuttgart>: Mitteilungen

Herausgegeben 2020 vom Eigenverlag des Instituts für Wasser- und Umweltsystem-modellierung

Druck: DCC Kästl e.K., Ostfildern

Contents

Notation

The following table summarizes the symbols used throughout this work.

Symbol	Definition	Dimension
Greek Letters:		
α_l	Longitudinal dispersivity	[L]
α_t	Transverse dispersivity	[L]
α_i	Average transient magnitude for i-th transient driver	
Γ	Boundary Condition	
δ	Dirac function	
ε	Amplitude percentage	
θ	Hydrogeological parameters influencing the WHPA delineation	
κ	Matérn shape parameter	
λ_j	Magnitude of the j-th transient driver influence at time t	
λ_x	Length scale on x-axis	[L]
λ_y	Length scale on y-axis	[L]
λ_z	Length scale on z-axis	[L]
μ_i^*	Absolute mean effect	
σ_i	Standard deviation	
ϕ	Hydraulic head	[L]
$\widehat{\phi}$	Predefined head	[L]
$\widetilde{\phi}_j$	Sensitivity of the head field solution with respect to the i-th transient driver	
τ_{crit}	Critical time related to the delineation	[T]
φ_n	Phase shift	
τ	Relevant time interval for capture analysis	[T]
τ_{past}	Relevant past time interval of already experienced transient flow behavior	[T]
τ_{dec}	Upcoming management period starting at the current time t	[T]
Ω	Domain	
ω_i	Frequency	
Latin Letters:		
A	Energy cost per pumped volume and vertical height	
$\hat{A}$	Ensemble mean over all WHPA realizations.	
A_{area}	Total capture area depicted by the number of map pixels inside each capture outline.	[L^2]
A_{dist}	Difference between the binary outline of a WHPA outline and the ensemble mean over all all WHPA realizations.	[L^2]
c	Concentration	[M/L^3]

$\widehat{c}$	Prescribed concentrations	[M/L^3]
D	Hydromechanic dispersion tensor	[L$^2/T$]
D_e	Effective diffusion coefficient	[L$^2/T$]
D_m	Molecular diffusion coefficient	[L$^2/T$]
E_{del}	Error measure that evaluates the disagreement between different approximation of reliability outlines of same magnitude.	
$\tilde{E}_r$	Monte Carlo approximation of the expected solution	
$\tilde{E}_s$	Subset approximation of the expected solution	
h_k	Time-dependent depth of the water level at each well location	[T]
h_{max}	Maximum allowed drawdown	[L]
I	Identity matrix	
I_s	Indicator map for the actually delineated WHPA	
$\widehat{J}$	Prescribed normal flux density	[L/T]
K	Hydraulic Cconductivity tensor	[L/T]
K_{dist}	Euclidean distance between each hydraulic conductivity realization and the ensemble average over all K-field realizations	[L]
$\hat{K}$	Ensemble average over all K-field realizations	[L/T]
L	Relevant length scale	[L]
	Randomly selected number of realizations used as cluster centers	
N	Number of Monte Carlo realizations	
N_s	Subset size of hydraulic conductivity realizations	
N_r	Size of the original ensemble of hydraulic conductivity realizations	
n	Outward-directed unit normal	
n_e	Effective porosity	[-]
n_j	Ensemble of batch-wise maps	
$\widehat{q}$	Predefined flux	[L$^3/TL^2$]
q	Darcy velocity	[L/T]
q_s	Source/sink terms	
q_{max}	Maximum allowed pumping rate	[L$^3/T$]
S_s	Specific storage	[1/L]
T^*	Time constant	[T]
T	Total simulation time	[T]
t	Time	[T]
t_j	Time step for particle release	[T]
t_l	Time step for the flow time domain	[T]
t_k	Time step for the reading of transport simulations	[T]
U	Uniform distribution	
v	Velocity	[L/T]
w	Set of random input parameters	
W_t	Chosen time-geological reliability outline	

Operators and Functions

$\nabla(\cdot)$	Nabla Operator
Δ	Difference Operator
∂	Partial derivative

Abbreviations

CDF	Cumulative Distribution Function
$DMOO$	Dynamic Multi Objective Optimization
EE	Elementary Effect
GSA	Global Sensitivity Analysis
GW	Groundwater
MOO	Multi Objective Optimization
$MOPSO$	Optimal Multi-Objective Particle Swarm Optimization
$WHPA$	Wellhead Protection Area

Functions:

$D(\tau_{dec})$	Expected groundwater demand
f_{cost}	Objective function: Involved costs
f_{del}	Objective function: Groundwater shortage
f_{gws}	Objective function: Exceedance area
$f_j(x_i)$	Boolean (yes/no) map
$F(x_i)$	Time frequency map
$q_k(\tau_{dec})$	Pumping rate at well k
$R_t(\mathbf{x}_i)$	Time reliability isoline

List of figures

List of tables

Abstract

Motivation and Goal

Groundwater is by percentage of availability the largest reserve of unfrozen fresh water on Earth [51]. Thus, there is an obvious concern about its protection against any source of potential contamination. At the same time, water scarcity increases due to polluted surface water or due to population growth. Thus, it forces entire regions to depend on groundwater as main or unique source of drinkable water. International organizations such as the World Health Organization [26] have enacted guidelines and regulations for groundwater protection. In these guidelines, Wellhead Protection Areas (WHPA) are presented as commonly used strategy to prevent groundwater pollution by restricting land use activities that could cause groundwater contamination.

Often, strong assumptions are made in WHPA delineation in order to simplify modelling. For instance, homogeneous geological conditions or steady-state flow conditions are used simplifications. Obviously, such assumptions inevitably invoke modelling and delineation errors. The former kind of simplifications has been profoundly studied in the literature, leading to probabilistic approaches for well vulnerability analysis and WHPA delineation. This has been a major advance towards realism and more robust risk control. However, the latter simplification lacks scrutiny: all existing approaches still neglect temporal variations in flow conditions.

The main goal of this thesis is to improve the protection of groundwater abstraction in order to provide safer water supply conditions. I achieve this goal by extending the existing framework for probabilistic well vulnerability analysis by including additional uncertainties caused by transient effects in flow and transport towards wells. Different directions are taken to accomplish this goal, leading to the four main contributions presented below.

Contributions and Conclusions

Groundwater flow model reduction Simulating transient flow conditions in WHPA analysis easily becomes highly expensive in terms of computational time. Even excessive, when addressing uncertainties through Monte Carlo simulation. Thus, I propose a numerical approximation of transient groundwater flow that uses dynamic superposition of steady-state flow solutions to reduce these costs.

From this transient analyses, now is possible to integrate transiency in WHPA delineation analysis which leads to the development of dynamic capture maps. These maps express the time frequency of well catchment membership for each location in the domain. To account for additional sources of uncertainty, such as aquifer heterogeneity, I wrapped up the WHPA transient simulation within a Monte Carlo frame. Now, the results are probabilistic WHPA maps that depict the probabilities of groundwater pollution due to geological and dynamic uncertainty.

Enhancing probabilistic WHPA analysis towards including transient flow Using the newly developed method described above, I evaluate the impact that transient flow conditions

have on (probabilistic) WHPA delineation. Thereby, I extend current methodologies and concepts in WHPA analysis so that transiency can be integrated as a new dimension in WHPA delineation. For illustration, I use a synthetic model scenario in which I address and analyze the effects of transiency and uncertainties on capture zones and WHPA delineation. The key conclusion from this chapter is that working under steady-state conditions is not enough. Transient analysis for probabilistic WHPA delineation provides additional information in terms of time reliability maps. Now, a WHPA can be defined by selecting both a reliability level for time and one for geological uncertainty.

Optimal control of pumping rates to reduce the influence of transient flow on actual abstraction zones The integration of transient flow conditions into probabilistic WHPA delineation might lead to a massive enlargement of required WHPAs. This could be problematic or even prohibitive in densely populated areas, especially with industrial activities, where larger WHPAs become difficult to implement. To address this problem, I propose a dynamic management model. With this tool, a decision maker can control changes in the actual abstraction outline (compared to the delineated WHPA) caused by transient flow conditions. This allows to reduce the influence of transient flow on the actual abstraction zone, such that abstraction remains within the delineated WHPA. My management approach employs multi-objective optimization (MOO) concepts, searching for compromise solutions that consider at least three objectives simultaneously: 1) to minimize the risk of pumping water from outside of a given WHPA, 2) to maximize groundwater supply, and 3) to minimize involved costs.

I conclude that WHPA programs and pumping management can benefit from multi-objective optimization concepts. The competitiveness among the selected objectives lead to Pareto-optimal solutions from which a decision maker can select the pumping strategy that suits upcoming management necessities and transient groundwater flow conditions best.

Computational cost reduction via unsupervised learning techniques The above two contributions assume that enough computational power is available for uncertainty quantification through Monte Carlo simulation. Yet, this is not always available, e.g., for some small-medium size companies.

Thus, I investigate how to detect a limited subset of hydraulic conductivity field realizations that best approximate the geological uncertainty conditions of a model ensemble used in WHPA delineation almost entirely. Thereby, the selection of representative realizations has to be achieved without running the expensive transient optimizations, i.e. as pre-processing of the most expensive step. For this purpose, I propose a classification methodology that clusters similar ensemble realizations according to pixel-wise commonalities among all generated hydraulic conductivity fields. Thus, I can approximate the aggregated capture probability map of the whole ensemble but at a much lower cost. I achieve this reduction using unsupervised learning techniques. This way, many subsequent analyses can also be performed on the condensed set of representative scenarios that would be computationally expensive otherwise.

The main conclusion is that, for probabilistic WHPA analysis, clustering is a suitable strategy to account for the influence of geological uncertainty while reducing the overall size of required realizations.

Looking back at the main goal of this thesis: to improve the protection of groundwater abstraction, it becomes clear that the integration of temporal variations in flow conditions during

WHPA analysis is indispensable. The problem of higher computational costs due to transient flow simulation was addressed by two approximation methodologies (groundwater flow model reduction and clustering analysis). Using these cost-reduction techniques, I propose to make groundwater abstraction safer by integrating directly (uncertain) transient effects into WHPA delineation or by controlling pumping rate conditions to counter dynamic changes.

Kurzfassung

Motivation und Ziel

Hinsichtlich der prozentualen Verfügbarkeit, Grundwasser die größte Reserve ungefrorene, Frischwassers der Erde [51]. Daher besteht ein offensichtliches Interesse an dessen Schutz vor jeglicher potentieller Verschmutzungsgefahr. Gleichzeitig steigt der Wassermangel aufgrund verschmutzter Oberflächenwassers oder des Bevölkerungswachstums. Daher sind ganze Regionen auf Grundwasser als hauptsächliche oder einzige Trinkwasserquelle angewiesen. Internationale Organisationen wie die Weltgesundheitsorganisation [26] haben Richtlinien und Regulierungen zum Grundwasserschutz erlassen. In diesen Richtlinien sind Wellhead Protection Areas (WHPA) als übliche Strategie zur Vermeidung von Grundwasserverschmutzung durch restriktive Bodennutzung vorgestellt, die im Falle eines Überlaufereignisses das Grundwasser verseuchen könnte.

Oft, wurden in des WHPA-Abgrenzung starke Annhamen gemacht um die Modellierung zu vereinforten. Zum Beispiel wurden homogene geologische Bedingungen oder ein zeitlich unveränderlichen Flieeßvorhalten als verein antrag verwendet. Offensichtlich führen solche vereinfachungen unweigerlich zu Modellierungs- und Abgrenzungsfehlern. Erstere Art von Vereinfachungen wurde in der Fachliteratur ausgiebig behandelt und führte zu probabilistischen Ansätzen bei der Analyse von Brunnenbeeinträchtigung und WHPA-Abgrenzung. Dies war ein maßgeblicher Fortschritt in Richtung realistischer Betrachtung und stabilerer Risikokontrolle. Letztere vereinfachung wird jedoch zu selten beleuchtet alle existierenden Ansätze vernachlässigen die zeitliche Variabilität des Fliessverhaltens.

Das Hauptziel dieser Arbeit besteht darin, den Schutz der Trinkwassergewinnung zu verbessern und damit für eine sichere Wasserversorgung zu sorgen. Ich erreiche dieses Ziel, indem ich den existierenden Rahmen der probabilistischen Brunnenbeeinträchtigungsanalyse erweitere, und zwar durch Einfügung der zusätzlichen unsicherheiten durch transiente Fliess und Transporteffekte in Richtung Brunnen. Zum Erreichen dieses Ziel wurden verschiedene Ansätze angewendet, die zu den folgenden vier Hauptbeiträgen führten.

Beiträge und Schlussfolgerungen

Vereinfachung des Grundwasserflussmodells Die Simulation von transienten Strömungsbedingungen innerhalb einer WHPA-Analyse wird leicht äußerst zeitaufwendig sogar ausufernd, wenn man Unsicherheiten über eine Monte-Carlo-Simulation erfasst. Daher schlage ich eine numerische Annäherung transienter Grundwasserströmungen vor, die auf dynamischer Überlagerungen von zeitlich unveränderlichen Strömungslösungen beruht um diesen Aufwand zu reduzieren. Die Schlussfolgerung dieses Kapitels lautet, dass die Einbettung transienten Verhaltens in der WHPA-Abgrenzungsanalyse dynamische Einzugskarten ergibt. Diese Karten zeigen die zeitliche Brunneneinzugsgebiet um zusätliche quellein von Unsicherheit wie Aquifer-heterogenität mit einzubeziehen, habe ich die transiente WHPA-Simulation in einer Monte-Carlo Analyse eingebettet. Daraus ergeben sich nun probabilistische WHPA-Karten, die die Wahrscheinlichkeit von Grundwasserverschmutzung aufgrund geologischer und dynamischer Unsicherheit beschreiben.

Erweiterung probabilistischer WHPA-Analyse unter Einbezug transienter Strömungen Die oben genannte neu entwickelte Methode nutzend, bewerte ich nun den Einfluss transienter Strömungsbedingungen auf (probabilistische) WHPA-Analysen. Dadurch erweitere ich gegenwärtige Methodologien und Konzepte der WHPA-Analyse um zeitliche Variabilität als neue Dimension in der WHPA-Abgrenzung zur veranschaulichung nutze ich ein synthetisches Modellszenario, um die Effekte zeitlich Variabilität und Unsicherheit auf Einzugsgebiete und WHPA-Abgrenzung zu erfassen und zu analysieren. Die wichtigste Schlussfolgerung hierda ist dass die alleinige Betrachtung zeitlich unveränderlich Bedingungen nicht ausreicht. Transiente Analysen für probabilistische WHPA-Abgrenzung bieten zusätzliche Informationen bezüglich Zuverlässigkeit bei Dynamik der Karten. Von nun an kann eine WHPA über die Auswahl von beidem definiert werden, des Zuverlässlichkeits-Levels bei zeitlicher Dynamik und der geologischen Unsicherheit.

Optimale Kontrolle von Pumpraten zur Reduzierung des Einflusses transienter Strömungen auf Wasserentnahmezonen Der Einbezug transienter Strömungsbedingungen in probabilistische WHPA-Abgrenzungen kann leicht zu einer massiven Vergrößerung der benötigten WHPAs führen. Dies wäre für dicht bevölkerte Gebiete problematisch, besonders im Fall zusätzlicher industrieller Tätigkeiten, wo größere WHPAs nur schwer bis unmöglich realisiert wurden können. Um dieses Problem anzugehen, schlage ich ein dynamisches Management-Modell vor: Mit diesem Werkzeug können Entscheidungsträger die durch transiente Strömungsbedingungen verursachte Änderungen im tatsächlichen Einzugs-gebiet (verglichen mit dem abgegrenzten WHPA) kontrollieren. Dies ermöglicht es, den Einfluss transienter Strömungen auf konkrete Trinkwasserentnahmezonen zu reduzieren, sodass die Entnahme innerhalb des abgegrenzten WHPA-Rahmens bleibt. Mein Managementansatz beruht auf Multikriterielle Optimierung (MOO) und ich suche damit nach Kompromisslösungen, die mindestens drei Ziele gleichzeitig verfolgen: 1) das Risiko zu minimieren, Wasser von außerhalb eines gegebenen WHPA abzupumpen, 2) den Grundwasserertrag zu maximieren und 3) die anfallenden Kosten zu minimieren. Ich schlussfolgerne dass WHPA-Programme und Pump-Management von multikriterieller Optimierung profitieren können. Der Wettbewerbzwischen unter den ausgewählten Zielen führt zu Pareto-optimalen Lösungen, von denen ein Entscheidungsträger die Pumpstrategien auswählen kann, die zu bestehenden Managementanforderungen und transienten Grundwasserströmungsbedingungen am Besten passen.

Berechnungskostenreduzierung über unbeaufsichtigte Lerntechniken Die beiden obigen Beiträge setzen voraus, dass genügend Rechenpower für Unsicherheitqualifizierung hin Monte-Carlo-Simulationen vorhanden ist. Jedoch steht ohne nicht immer zur Verfügung, z. B. bei kleine und mittlere Unternehmen. Daher untersuche ich, wie man eine begrenzte Teilmenge hydraulischer Leitfähigkeitsfelder findet, die die geologische Unsicherheit eines in WHPA-Abgrenzungen benutzten Modelles nahezu vollständig abbilden. Die Auswahl repräsentativer Realisierungen muss jedoch ohne Einsatz von aufwändiger transienter Optimierung erreicht werden, d.h. als Vorbearbeitung des aufwendigsten Schritts. Zu diesem Zweck schlage ich eine Klassifizierungsmethodologie vor, die ähnliche Realisierungen im Ensemble gemäß pixelweser Übereinstimmung hydraulischer Leitfähigkeitsfelder zusammenfasst. Auf diese Weise kann ich mich den aggregierten Karten von Einzugsgebietwahrscheinlichkarten, die auf dem gennanten Ensemble bestünden annähern, aber bei wesentlich geringeren Aufwand. Ich erreiche diese Reduzierung mit Techniker des unbeaufsichtigte maschine Lernens. Auf diese Weise können viele subsequente Analysen auf dem kondensierten Set repräsentativer Realisierungen

durchgeführt werden die indem falls zu aufwändig wären. Die hauptsächliche Schlussfolgerung besteht darin, dass, Clustering angemessene Strategie für probabilistisch WHPA-Analyse darstellt, um den Einfluss geologischer Unsicherheit bei gleichzeitiger Reduzierung der Gesamt anzahl benötigter Realisierungen zu erfassen. Rückblickend auf das Hauptziel dieser Arbeit, -wie man den Schutz von Grundwasserentnahme verbessern kann-, wird nun klar, dass der Einbezug zeitlicher Variabilität des Strömungsbedingungen während einer WHPA-Analyse unerlässlich ist. Das Problem der höheren Berechnungsaufwanden von transienten Strömungssimulationen wird durch zwei Annäherungmethodologien (Reduzierung des Grundwasserströmungsmodells und cluster-Analyse) angegangen. Durch Gebrauch dieser aufwandsreduzierenden Techniken schlage ich vor Grundwasserentnahme sicherer zu machen, entweder durch Integration direkter (unsicherer) transienter Effekterer in die WHPA-Abgrenzung oder durch die Kontrolle von Pumpraten, um dynamischen veränderungen zu entgegnen.

1. Introduction

1.1 Motivation and goal

Groundwater represents the largest amount of available unfrozen freshwater on Earth [51]. The increasing demand due to population growth together with the pollution of most surface freshwater sources, have lead in many places to depend on groundwater as the main source for drinkable water. Therefore, there is an obvious necessity to protect its abstraction against any source of pollution.

For this purpose, the World Health Organization [26] have enacted international standards and guidelines for drinking water quality. The 2004 guideline edition introduced a "preventive safety management approach for Safe Drinking-water" [103]. One of its main components, the Safe Water Plan, recommended to implement preventive protection measures in order to avoid and control risk sources of contamination due to land use activities which could compromise the groundwater quality that could threat the human health.

A commonly used strategy to prevent groundwater pollution in drinking water well catchments is to delineate Wellhead Protection Areas (WHPA) around drinking water wells. The objective is to restrict land use activities that could pollute the groundwater flowing towards a well in case of a spill event. In most cases, the delineation of WHPAs relies on simplifications, such as assuming homogeneous or zonated aquifer conditions or considering steady-state flow scenarios.

Obviously, such assumptions on homogeneous aquifer conditions and steady-state considerations inevitably invoke errors. Such errors lead to inappropriate delineation of WHPA, such that the goal of safeguarding water quality is not fulfilled. While uncertainty due to aquifer heterogeneity has been extensively studied in the literature (e.g. [125], [45], [66], [126], [116], [36], [35]), the impact of transient flow conditions has received yet very little attention. For instance, WHPA maps in the offices of water supply companies are fixed maps derived from steady-state models although the actual catchment out there is transient. The way how WHPA delineation can be adapted to account for transient conditions is not yet understood.

This lack of understanding is what took me to develop, as main research goal of my thesis, to provide better safety conditions of drinking water from groundwater wells in spite of transient groundwater flow currently neglected in WHPA analysis. Rephrased as a fundamental and open research question: this main objective becomes: "How does transiency of groundwater flow influence the actual capture are of wells and what strategies allow me to properly address such influence?" To solve this question, I will propose and investigate different strategies that can be categorized into three main groups, which I discuss in the following section: 1) Accounting for transient WHPA delineation, 2) counteracting transience by optimal control and 3) efficient machine learning simulation of transient systems as a prerequisite for the former two.

1.2 Research Questions and Approaches

The overall set of methodologies and concepts I present in this thesis, in order to address transience in groundwater flow, can be categorized into three main groups: *Transient WHPA*

delineation, *Optimal control* and *Efficient transient simulation*. Each of these groups leads to the formulation of research questions, that are presented within each group.

Transient WHPA delineation.

Most groundwater protection programs use WHPAs to safeguard groundwater abstraction against pollution. For instance, Fig. 1 highlights in black a typical WHPA of a well gallery composed of eight drinking wells. The drawn WHPA assumes known heterogeneous aquifer conditions (hence the asymmetry in the delineation) and steady-state conditions. Likewise, Fig. 1 highlights in red an additional outline for the same well gallery, but now accounting for transient flow conditions within the WHPA analysis. Obviously, covering all possible capture outlines that occur under transient flow conditions leads to a greater outline that is not considered by the steady-state solution. Transient conditions are triggered, for example, during consecutive periods of dry and rainy seasons, where pumping wells might increase and decrease their water abstraction, respectively, to meet the corresponding demand. This, combined with changes in the mean ambient groundwater flow caused by same dynamic weather environment (e.g., changes in the regional flow direction or the regional hydraulic gradient) might trigger a variation over time of the water abstraction zone of the well. This can lead to a risk scenario, where locations with dangerous land use conditions (e.g., gas stations or agricultural lands) might be actually included within the abstraction zone, during particular time intervals. Furthermore, besides the uncertainty in WHPA delineation attributed to transient flow considerations, additional uncertainty might be triggered due to (a) imprecise information regarding aquifer parameters and (b) inexact knowledge about the behavior of the different transient drivers.

Furthermore, the delineation of WHPAs influenced by transient flow conditions is computationally more expensive in comparison to their steady-state solutions, even more, if they are coupled with Monte Carlo analysis for obtaining probabilistic WHPAs [36].

Thus, as first contribution, I propose a reliable probabilistic delineation rule for WHPAs in the presence of (uncertain) transient conditions and geological uncertainty. The final output is again a fixed WHPA outline, but based on probabilistic concepts and transient considerations. Additionally, to reduce the computational cost of transient flow simulation, I present a methodology to simulate transient groundwater flow at reduced computational costs. Considering both objectives, I formulate the following two research questions:

1. How can I formulate a methodology which makes possible to achieve faster but asymptotically (for large aquifer hydraulic diffusivity) valid transient flow conditions?

2. What is the overall influence and principal differences when compared to steady-state (probabilistic) WHPAs, of WHPA solutions integrating transience effects?

Optimal control.

Expanding the actual steady-state outline solution due to the influence of transient flow conditions might become unfeasible for well galleries located in urban areas. For instance, the obvious integration of industrial areas into the new urban water supply WHPA raises concerns and trigger the implementation of strong regulations not yet considered. For such cases, an alternative possibility is to use engineered pumping management schemes that reduce the influences and deliver control to the decision maker of the changes in the actual abstraction

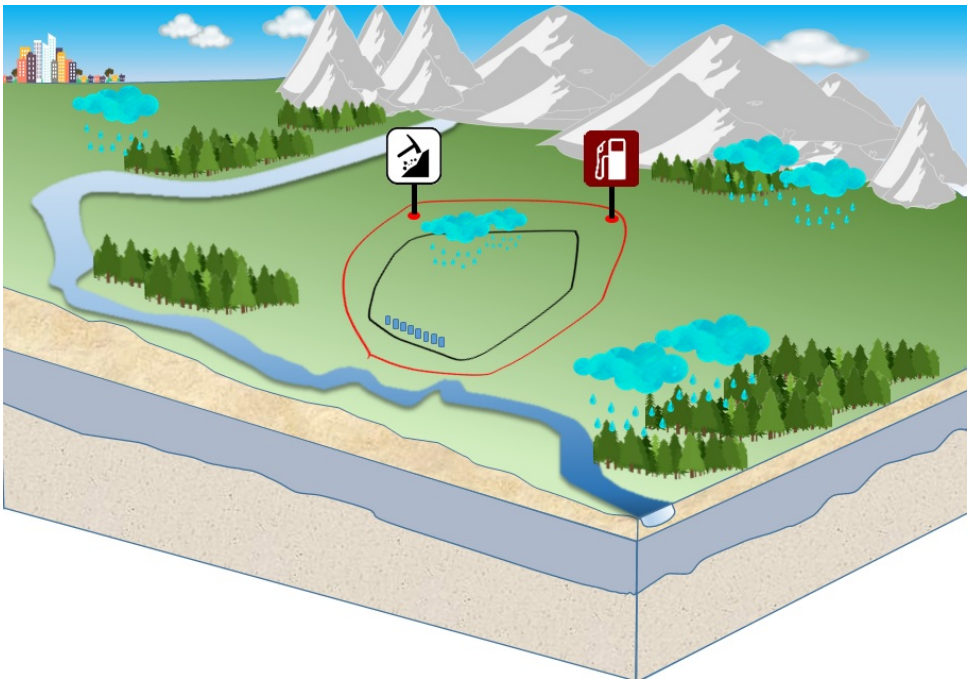

Figure 1.1: Problem sketch: The influence of transient flow conditions in WHPA delineation. The black and the red outlines depicts the WHPA of a well field assuming steady-state and transient flow conditions, respectively. The transient influence not considered by the former outline leads towards a risk scenario where locations with dangerous land use conditions (e.g., a gas station or a quarry) might be pulled within the actual groundwater abstraction zone during some time intervals.

outline (compared to the delineated WHPA) caused by transient flow conditions. Thus, model-based steady-state WHPAs together combined with active pumping management can represent a robust and still valid solution against the dynamic flow environment.

To achieve this, I propose a well gallery management scheme that dynamically adapts and re-distributes pumping rates of individual wells in a well gallery. To avoid unfeasible decisions, it works with trade-off solutions among the following three objectives: 1) To minimize the actual abstraction form outside the given WHPA, 2) to satisfy the groundwater demand and 3) to minimize the related costs of pumping. Until now, the use of optimal control for well galleries has been constrained to only few cases. None of them considered the effect of time-variant flow conditions affecting the actual abstraction. Hence, the next two especific research questions are:

1. How to integrate transient flow conditions into the optimization problem so that transient flow conditions are properly handled?

2. What are the achievable results if optimal control is implement and how do they differ from conventional management alternatives?.

Efficient Monte-Carlo simulation of transience

So far, I have introduced a *carrot-stick* approach to deal with transient flow conditions, by either expanding the current WHPA delineation (*carrot*) to account for time-varying conditions

in the abstraction zone or by restricting transiency via optimal control of the pumping rates in the well gallery (*stick*). In either case, both methodologies are prohibitively expensive in terms of computational time if geological uncertainty, (through Monte Carlo simulation) is considered.

Thus, the purpose of this last contribution is to formulate and develop a methodology, based on unsupervised learning, in order to recognize a subset of model realizations that represent relevant statistics of interest for WHPA analysis under the influence of geological uncertainties. To avoid clustering in a high-dimensional space, I will find a problem-specific low-dimensional space and appropriate distance metrics for clustering. The distances I suggest are a combination of pixel-wise commonalities between hydraulic conductivity fields (permeability-based representation) and respective WHPA outlines (transport-based representation). Accordingly, the last specific research question is formulated:

1. What clustering approach is adequate for my methodology and what feature distances should I consider to reduce the high-dimensional representation of hydraulic conductivity fields and respective WHPA solutions?

1.3 Structure of this thesis

The structure of this thesis is divided into three main sections:

Section 1 is composed of chapters 1 and 2, both chapters represent the introduction to this thesis and do not provide any novelty or contribution. The current Chapter presents the motivation of this thesis. Chapter 2 introduces the physical equations for groundwater flow simulation as well as the set of methodologies used during my research.

The second section includes chapters 3, 4, 5 and 6. These chapters represent the main body of this thesis, and are aligned with the three groups and my five specific research questions:

1. In chapter 3, I present as integrated part of my first contribution, a methodology that makes it possible to achieve faster but asymptotically (for large aquifer hydraulic diffusivity) valid simulations for transient flow conditions (R.Q. 1). Otherwise, the delineation of WHPAs influenced by transient flow conditions is computationally too expensive in comparison to their steady state solutions, even more, if they are coupled with Monte Carlo analysis for obtaining probabilistic WHPAs.

2. In chapter 4, I improve as part of first main contribution, the protection of wells against (uncertain) transient flow conditions by proposing a probabilistic delineation rule for WHPAs in the presence of (uncertain) transient conditions and geological uncertainty (R.Q. 2). The final output is again a fixed WHPA outline, but based on probabilistic concepts and transient considerations.

3. In chapter 5, as third main contribution, I formulate and develop a multi-objective dynamic management model with the goal to reduce and deliver control to the decision maker of the changes in the actual abstraction outline (compared to the delineated WHPA) caused by transient flow conditions (R.Q. 3 and 4). This approach helps stabilize the dynamic capture zone within the static WHPA through dynamically adapting and

re-distributing pumping rates of individual wells in a well gallery. Thus, model-based steady-state WHPAs together with controlled pumping can represent a robust and still valid solution against the otherwise unconsidered dynamic flow environment.

4. In chapter 6, as fourth main contribution, I develop a methodology, based on unsupervised learning concepts, that reduces the computational time required to take into practice expensive transient flow simulations (R.Q. 5).

Finally, in chapter 7 I summarize and conclude my overall work, while additionally giving an outlook for possible future research.

2. Methods

In this section I briefly introduce the methodology used during the elaboration of this thesis. Section 2.1 presents the governing equations for groundwater flow and transport, and numerical methods for their solution are presented in Section 2.2. Sections 2.3 and 2.4 briefly discuss Monte Carlo simulation to address different sources of uncertainty in WHPA analysis and the concepts behind sensitivity analysis and the Morris methodology. Section 2.5 introduces optimization and the use of the particle swarm optimization technique to solve multiobjective optimization problems. Finally, Section 2.6 introduces clustering approaches to address fast integration of geological uncertainty in highly expensive simulations.

2.1 Governing equations for flow and transport in groundwater modeling

2.1.1 Transient groundwater flow

The general governing equation for transient groundwater flow in heterogeneous and isotropic conditions for 3D confined aquifers is:

$$S_s \frac{\partial \phi}{\partial t} - \nabla \cdot (K \nabla \phi) = q_s(\mathbf{x}, t) \quad \text{in} \quad \Omega \tag{2.1}$$

With hydraulic transmissivity K, hydraulic head ϕ, specific storage S_s and sink/source term $q_s(\mathbf{x}, t)$ in the domain Ω. The boundary conditions for Eq. (2.1) are:

$$(K \nabla \phi) \cdot \mathbf{n} = -\widehat{q}(t) \quad \text{on} \quad \Gamma_1 \qquad\qquad \phi = \widehat{\phi}(t) \quad \text{on} \quad \Gamma_2. \tag{2.2}$$

Where $\widehat{q}$ and $\widehat{\phi}$ are predefined fluxes and heads on Neumann Γ_1 and Dirichlet Γ_2 boundaries, respectively, and $\mathbf{n}$ is the outward-directed unit normal to Γ, where Γ=$\Gamma_1 \cup \Gamma_2$.

2.1.2 Advective-diffusive (dispersive) transport

The advective-dispersive transport of a conservative tracer is given by:

$$\frac{\partial c}{\partial t} + \nabla \cdot (\mathbf{u}c - \mathbf{D} \nabla c) = 0 \quad \text{in} \quad \Omega \tag{2.3}$$

Here, c is concentration, t is time, $\mathbf{u} = \mathbf{q}/\ n_e$ is velocity, $\mathbf{q}$ is Darcy velocity, effective porosity n_e (assumed constant in this study) and $\mathbf{D}$ is the hydromechanic dispersion tensor [100] given by:

$$\mathbf{D} = (\alpha_t ||\mathbf{u}|| + \mathbf{D}_e)\mathbf{I} + (\alpha_l - \alpha_t)\frac{\mathbf{u}\mathbf{u}^T}{||\mathbf{u}||} \tag{2.4}$$

With longitudinal and transversal dispersivities α_l and α_t, respectively, effective diffussion coefficient D_e and the identity matrix **I**. Eq. 3.6 is subject to the boundary conditions:

$$\mathbf{n} \cdot \mathbf{u}c + \mathbf{n} \cdot (\mathbf{D}\nabla c) = \widehat{J} \quad \text{on} \quad \Gamma_1, \tag{2.5}$$

$$c = \widehat{c} \quad \text{on} \quad \Gamma \backslash \Gamma_1. \tag{2.6}$$

Here, $\widehat{J}$ is a prescribed normal flux density and $\widehat{c}$ represents prescribed concentrations.

2.2 Lagrangian solution to transport simulation

In this thesis a Particle Tracking Random Walk (PTRW) algorithm [25] is used in order to simulate the advective/dispersive transport of contaminants moving throughout the aquifer domain. I choose this Lagrangian approach over Eulerian methods since it overcomes the numerical dispersion problems and artificial oscillations that plagues Eulerian transport models [96]. To solve the transport equation (Eq. 2.3), the PTRW represents the mass of a contaminant with a large number of virtual particles. Once a group of particles is injected into the domain, they stay in motion driven by advection and dispersion. The particle displacement through the aquifer is represented by:

$$\mathbf{X}_p(t + \Delta t) = \mathbf{X}_p(t) + (\mathbf{u}(\mathbf{X}_p, t) + \nabla(\mathbf{X}_p, t))\Delta t + \mathbf{B}(\mathbf{X}_p, t) \cdot \boldsymbol{\xi}(t)\sqrt{\Delta t} \tag{2.7}$$

Here, $\mathbf{X}_p$ is the particle position for particle p at time t and Δt is the chosen time step that discretizes the particle movement. **B** is the displacement matrix tensor that defines the strength of diffusion/dispersion and has to fulfill $\mathbf{B} \cdot \mathbf{B}^T = 2\mathbf{D}$.

$\boldsymbol{\xi}$ (t) are normally distributed random numbers with zero mean and unit variance. Salamon et al. (2006) [96] defines the 3D form of matrix **B** like:

$$\mathbf{B} = \begin{pmatrix} \frac{u_x}{|\mathbf{u}|} w_l & -\frac{u_x u_z}{|\mathbf{u}|\sqrt{u_x^2+u_z^2}} w_t & -\frac{u_y}{|\mathbf{u}|\sqrt{u_x^2+u_y^2}} w_t \\ \frac{u_y}{|\mathbf{u}|} w_l & -\frac{u_y u_z}{|\mathbf{u}|\sqrt{u_x^2+u_z^2}} w_t & -\frac{u_x}{|\mathbf{u}|\sqrt{u_x^2+u_y^2}} w_t \\ \frac{u_z}{|\mathbf{u}|} w_l & \frac{\sqrt{u_x^2+u_y^2}}{|\mathbf{u}|} w_t & 0 \end{pmatrix} \tag{2.8}$$

Here, $w_t = \sqrt{2(\alpha_t|\mathbf{u}| + D_m)}$ and $w_l = \sqrt{2(\alpha_t|\mathbf{u}| + D_m)}$.

2.2.1 Backward Particle Tracking Random Walk

My methodology for WHPA delineation relies on a backward-in-time formulation, where the flow velocity field is reversed and the injection of particles starts at the pumping well [81]. The Backward Particle Tracking Random Walk formulation reduces the computational time of solving individual Monte Carlo realizations for WHPA delineation by directly solving the WHPA outline with a single model run. Otherwise, the computational time to simulate the transport of particles from each possible spill location within the model domain would lead to unfeasible computational times within the Monte Carlo framework.

2.3 Wellhead Protection Area delineation

2.3.1 Regulations on WHPAs

In order to reduce the risk of pumping contaminated groundwater at drinking water wells, a common strategy is to restrict land use activities surrounding these wells. According to many national regulations, these Well Head Protection Areas (WHPAs) [124] envelope theoretical "time-of-travel capture zones" specifying the travel time required for a contaminant to reach a pumping well. Such delineations frequently rely on modeled 2D or 3D scenarios based on conceptual assumptions and approximations using either analytic (e.g., fixed-radius method) or numerical methods (e.g., particle tracking method) [64]. However, there is a tendency to favor numerical simulations in order to implement arbitrary hydro(geo)logical parameters and boundary conditions [43].

For instance, in Germany, the German national standard DVGW (2006) [33] bases the protection of groundwater production on a WHPA subdivided into 4 differentiated sub-zones. Zone I depicts the smallest delineation, and ensures the protection of the water abstraction point by fencing the drinking well gallery. Zone II depicts a time-of-travel distance of 50 days to ensure microbiological safety. Zone III is divided into Zone IIIa which defines a 2km radius area around the pumping well and Zone IIIb which depicts the complete well catchment.

2.3.2 Sources of uncertainty in WHPA delineation: Geological vs Temporal uncertainty

To answer the question made by Evers and Lerner (1998) [39] *How Uncertain Is Our Estimate of a Wellhead Protection Zone?*, Stauffer et al. [117] presented a list of parameters and conditions that have great impact in WHPA analysis. Aside from uncertainty sources that concern local information gathered during the exploration campaign (e.g., local borehole measurements) or groundwater simulation (e.g., the extension of the flow domain or the location of the boundary conditions), most of the sources triggering uncertainties in WHPA analysis can be broadly grouped into two main sources: (1) spatial heterogeneity and (2) time-varying boundary and flow conditions.

The first main influence denotes the variability of hydrogeological parameters that describe the aquifer geological conditions. The effect of heterogeneity on groundwater flow causes irregular contour lines and streamlines [53], thus influencing contaminant transport processes. Considering that a complete characterization of the aquifer at the field scale is prohibitively expensive, the limited available information about aquifer geological conditions leads to an associated uncertainty during the delineation of WHPAs and pumping well capture zones. Together with its uncertainty, the influence of heterogeneity on pumping well protection zones, has been extensively covered in the literature (e.g. [125], [45], [66], [126], [116], [36], [35]). However, these studies did not explore the effect of transiency; instead they base on steady-state considerations.

Thus, the second main challenge includes all those forces producing transiency in the flow field towards the well. Transient flow behavior is triggered by stochastically occurring weather conditions, seasonal variations and demand-adjusted pumping rates. In general, several studies have been conducted about temporal variability and its influence on aquifer response (e.g. [121], [105], [122], [83]) and on transport processes (e.g. [50], [92], [18], [34], [67]).

Recently, Libera et al. [70] explored the effects that known time-varying pumping rates have on key features of contaminant transport in a randomly heterogeneous aquifer. They showed that such dynamic conditions have a significant impact on the temporal behavior of contaminant breakthrough curves observed at pumping wells. Furthermore, in a subsequent study, Libera et al. [71] showed that these fluctuations hold regardless of different geostatistical models (multi-Gaussian and non-multi-Gaussian) used to represent heterogeneity. Despite recognizing transiency as an important influence, in both studies, they did not consider the impact of other transient drivers (other than pumping rates), nor the effects of uncertainty associated to transient flow behavior.

In general, there is only a limited number of studies addressing the impact of transiency on required pumping well protection zones. Early studies addressing WHPA transiency due to pumping regimes have been conducted since the nineties. Ramanarayanan et al. [88] used numerical models to contrast a WHPA between steady-state and transient conditions. They concluded that seasonal variations seem "not to average out with time" and that they increase the WHPA extension by approximately 30%. Musa and Kemblowski [80] defined an effective capture zone under time-varying velocity fields caused by temporal evolution of the cone of depression under constant pumping rates. They tracked particles through a time sequence of steady-state analytical solutions for flow towards a well. The works of Masterson et al. [74] and Starn et al. [60] analyzed the influence of transient pumping regimes in real site conditions for capture zone delineation. They showed how temporal variations in the flow field caused by unsteady pumping rates can induce flow from new contributing areas to the well, as well as to introduce significant changes on the mean transport process.

In addition to transient pumping regimes, changes in the size and shape of capture outlines due to transient natural groundwater recharge have been initially investigated by Lerner [68]. Later, numerical analyses were implemented by Reilly and Pollock [91] and Barry et al. [8].

Other studies have investigated the influence of transient behavior in the ambient groundwater flow. Festger and Walter [41] showed that changes in the regional hydraulic gradient have a significant effect on expanding and shrinking the capture zone once compared to its steady-state solution. Rock and Kupfersberger [93] showed how a solution under transient conditions differs from steady-state outlines driving high and low groundwater level conditions. All previous studies neglected the influence of uncertain transient conditions, instead they identified transient capture zones based on given time series of groundwater levels.

Although both sources of uncertainty (transient conditions and geological uncertainties) depict two relevant sources of uncertainty for WHPA delineation, I have found only a few WHPA studies exploring their joint effect. Stauffer et al. [117] qualitatively listed both sources of uncertainty among a set of parameters and conditions that cause uncertainty in the characterization of capture zones. Franssen et. al [44] used Monte Carlo analysis in order to measure the impact on capture delineation of spatiotemporally variable natural recharge for moderately heterogeneous transmissivity fields. In summary, none of those studies that address transient effects in WHPA provide a corresponding decision rule for delineation. Only two consider jointly effects of transience and uncertainties from heterogeneity and none of them recognizes uncertainty in describing transient drivers.

2.3.3 Representation of transient and geological uncertainty conditions

The focus of this thesis is to investigate the combined impact that both transient flow (and related uncertainties) and inexact aquifer characterization have on WHPA analysis. According to the framework presented by Walker et al. [127], both sources depict the so called *Input uncertainty* type. This type of uncertainty is associated with the description of the reference system (e.g., permeability field) and to the external forces that are driving changes in the reference system (e.g., seasonal conditions in pumping rate conditions). Besides this types of uncertainty, Walker et al. [127] recognize additional type of uncertainties, according to their location in the modelling process: 1) *Context uncertainty* that is related to uncertainties about problem and purposes of the model. 2) *Model uncertainty* which refers to the selection of the governing equations to be chosen to describe the reference system as well as the selected computer model, i.e. the conceptual model description. 3) *Parameter uncertainty* which describes uncertainty driven by the data used for calibration purposes as well as the selected calibration methodology. 4) *Model Outcome uncertainty* which represents the discrepancy, that driven by the previous types of uncertainty types, depicts the *prediction error* between the data measured in field and the model's predicted outcome.

However, in this thesis such additional types of uncertainty were not considered. For instance, I assume that the governing equations used to build the computer model accurately describe the system (*Model uncertainty*). Further studies should consider the implication of these types of uncertainties in order to evaluate its impact into the proposed methodology and presented findings. In the following, I define how I represented both sources of input uncertainties.

First, to represent geological uncertainty conditions, I depict hydraulic conductivity as a Multi-Gaussian random space function described by a Matérn covariance function [77]. I treat the parameters of the structural model (e.g. covariance parameters) as uncertain, following uniform distributions.

In the case of time-variant groundwater flow, I considered seasonal variations of the groundwater flow behavior. Several studies rely on sinusoidal time series to represent the behavior of natural transient flow conditions (e.g. [3], [41], [106], [87]). This arrangement resembles the cyclic pattern of natural phenomena. The same pattern can be representative of $dynamic$ pumping rates in response to seasonal fluctuations (e.g. [57], [23], [9]). Hence, I represent the transiency of all transient model forcing sinusoidal patterns:

$$\lambda_i(t_l) = \alpha_i + \varepsilon_i sin(\omega_i t_l + \varphi_i) \tag{2.9}$$

Here, $\lambda_i(t_l)$ is the magnitude of the transient driver to be used in Eq. (2.1).

To represent transient flow conditions, I utilize four transient drivers that often appear on the seasonal scale: (I) regional groundwater flow direction, (II) strength of the regional hydraulic gradient, (III) natural recharge to the groundwater and (IV) pumping rate. The pumping strength and natural conditions are representative from case scenarios found in the literature. Specifically, I base the amplitude of the strength of the regional hydraulic gradient on the values given in Festger and Walter (2002) [41]. For the natural recharge, I consider values given in Franssen et al. (2002) [44]. For pumping rate conditions, the actual choice of distribution is meaningful because there is often a legal or regulated upper bound to pumping. Therefore, I stick to the magnitudes given in Frind et al. (2002) [46].

Uncertainty in transiency is represented by treating amplitudes and phase shift as random variables. For randomizing amplitudes, I multiply the literature values with random numbers drawn independently from the uniform distribution U[0,1]. For instance, a pumping well will be at steady-state if its amplitude value is multiplied by zero, while it would be imposing a fully transient regime with amplitude equal to 100%. Any value in-between will control the strength of the amplitude. The choice of uniform distributions is arbitrary, and represents a simple uncertainty scenario that is specific to each study. I treat pumping rates as random, although they may be perceived as controllable parameters of well operation. However, I argue that future pumping rates are unknown because they react to the joint influence of future water demand and future weather conditions.

Likewise, I randomize the phase shift uniformly between zero and π. The only assumption made about phase shifts in the transient behavior is that the pumping rate acts precisely opposite to natural recharge, i.e., stronger pumping takes place during the dry season (phase-shifted by half of the used period) because *"the recovery from pumping begins at the end of the irrigation season, before the beginning of the rainy season"* [23].

2.3.4 Probabilistic WHPA delineation

The classical approach for dealing with uncertainties in WHPA analysis is through probabilistic methods, solving repeatedly the deterministic WHPA outline (each one using a distinctive set of randomly generated input parameters) by means of Monte Carlo simulation [49].

The aggregation over several (in the order of thousands) steady-state deterministic WHPA solutions results in a well capture probability map that, ranging on a scale from zero to one, displays the pixel-wise probability of pixels to be inside the well's catchment or not. In this way, the Monte Carlo simulation extends to probabilistic terms what used to be binary outline solutions [117]. This extension provides additional information to water stakeholders and decision makers, such as the probabilistic level of exposure risk for advective–dispersive intrinsic well vulnerability criteria ([36], [35]) or the temporal catchment membership induced by time-varying flow-field conditions ([95]). Furthermore, Monte Carlo simulation represents a straightforward methodology, since the stochastic representation of each parameter can be generated in numerous ways, and sophisticated groundwater models can be integrated easily [15].

However, the underlying problem of using stochastic techniques in WHPA analysis is that high safety levels against uncertainty lead to an unconventionally large increase in the extent of WHPAs ([36], [115]). In order to reduce uncertainty caused by, for example, limited aquifer characterization, it is common among practitioners to use data assimilation and conditioning techniques [35]. As Prof. Andre Journel from Stanford University said in a talk in 1992, *...if I ever find myself crossing paths with somebody using unconditional realizations, I will cross the street* [99].

Conditional simulation techniques integrate catchment-specific data (e.g., piezometric head, hydraulic conductivity) gathered during the exploration campaign to generate a set of conditional realizations, each presenting statistically equally likely parameter sets [37]. There are various methods that addresses conditional simulation, for example, PEST [30], Ensemble Kalman Filters [84] or Bayesian GLUE [42], to name a few. Specifically, in this thesis, I rely on the FFT-based geostatistical tool described in Fritz. et al. (2009) [47] to condition realizations of log-conductivity to conductivity data at high computational efficiency.

2.4 Sensitivity Analysis

The following introduction to sensitivity analysis is based on the books of Smith [113] and Saltelli et al. [97] and on the work of Borgonovo and Plischke [13]. In the field of uncertainty quantification, Sensitivity Analysis has the objective to quantify the relative contribution that input parameter uncertainties have on the model outcomes. Commonly, sensitivity analysis focuses on answering the following questions:

1. To quantify the robustness of the modeling outputs in the presence of uncertainty.
2. To simplify modeling by fixing input variables with null or limited influence on the model output.
3. Highlighting regions in the input variable space leading to optimal model solutions.
4. Guide the discussion between modelers and decision makers towards problem-specific recommendations by indicating the most important factors to consider during simulation.

In general, the methods used for sensitivity analysis [98] can be divided into two main groups: local and global sensitivity techniques.

2.5 Sensitivity Analysis Techniques

2.5.1 Local sensitivity analysis

Local Sensitivity Analysis (LSA) measures the variability of the model outcome with respect to a set of given nominal values. Achieving this by measuring the partial derivative of the model outcome respect to each input variable, the local sensitivity approach does no attempt to explore the complete input space. Instead, it searches for sensitive parameters by measuring small perturbations for one parameter at the time.

However, one problem with LSA is that it does not take into account the possibly non-linear character of model responses over the global admissible parameter space [113]. Additionally, it does not measure the interaction between input variables since the obtained partial derivative is only informative at the fixed point of computation. Thus, it does not provide any insight about additional interaction at some other point of the input space. To overcome both limitations, a global sensitivity analysis is implemented, which I describe in the following.

2.5.2 Global sensitivity Analysis

In general, Global Sensitivity Analysis (GSA) evaluates the degree of influence that a given set of input parameters has over the model outcome. The difference when compared to LSA is that GSA explores the entire admissible input parameter space delimited by the range of each input value, while additionally addressing the existing non-linear response between input variables and model outcomes. Thus, GSA becomes the appropriate tool to use for highly non-linear model simulations. One example of such models is the non-linear relation between the transport modeling of contaminant through the aquifer and the consequent WHPA delineation.

For highly-complex models, GSA approaches can be divided into two main groups; those using the law of total variance (variance-based methods) and those implementing screening designs techniques. In the following a brief explanation of both approaches is given:

Variance-based GSA

The Sobol method [114] is the most commonly used technique among the distinctive variance-based frameworks. Its core methodology uses the variance decomposition formula in order to quantify the contribution to the model output variance caused by a given set of input variables. To determine each individual contribution, the Sobol technique decomposes the total output variance into fractions which are then assigned to the individual or combined influence of input parameters.

Under this methodology, the variance that can be attributed to the sole influence of an input parameter is called the main effect or first Sobol index. Higher orders of the Sobol indexes depict the effects of many variables interacting among each other (e.g., a fifth Sobol index indicates the interaction among five input variables). For highly parametrized models, the calculation of the total-effect index describes the fraction of the output variance that can not be explained yet by the current Sobol index order. Total-effect index value computation is used in order to avoid the computational burden of evaluating subsequent order effects.

An alternative framework for the Sobol method is the *Fourier amplitude sensitivity test* (FAST). The FAST algorithm was initially introduced by Cuckier et al. (1973a and 1973b) to compute the first Sobol index of large sets of coupled nonlinear rate equations. It was later expanded to account for higher-order indexes [131]. Using the Fourier transform, the FAST framework decomposes the model output variance into fractional variance magnitudes, each one depicting the individual input variable contribution. To obtain each individual contribution, the FAST approach uses Fourier series to periodically sample each input variable on the parameter space. Then, using the Fourier transform, each individual contribution to the output model variance is computed using the frequency differences of the sampling procedure.

Both GSA approaches provide quantitative measurements (Sobol indexes) to assess the degree of influence of each input value over the model outcome. Often they are implemented using Monte Carlo techniques. This is a major drawback if we assess highly parametrized models or models with long computational times where thousand of realizations are needed in order to achieve convergence of the Sobol indexes [82]. As an alternative, screening methods are used to reduce the computational cost while still accounting for non-linear conditions.

Screening Techniques

As mentioned above, screening techniques help to identify the most important parameters from a large set of input variables while requiring a reduced (when compared to variance-based solutions) number of model evaluations [97]. However, what is gained in computational speed is lost in accuracy. Screening techniques provide qualitative sensitivity measures that rank the order of importance of a set of variables. The most well-known screening technique is the Morris approach.

The Morris approach, originally developed by Morris in 1991 [78], computes two sensitivity measurements per randomized variable. Here, each variable is known as input factor i and

the computed sensitivity measure is the Elementary Effect (EE_i). First, it calculates the absolute mean effect μ_i^* to describe the global influence of each input factor. Second, it computes the standard deviation σ_i to point out whether a factor exhibits a non-linear behavior or interactions with other factors. An input factor can be acknowledged as unimportant if both Morris measures show low values (i.e., both sensitivity measures are located near to the origin). Linear effects depict high values of μ_i^* and low values of σ_i, while non-linearity or interactions with other factors are indicated by high magnitudes in both measurements.

Adaptation of the Morris technique

One objective of this thesis is to evaluate the impact that different transient drivers have on the WHPA delineation. Among the different existing methodologies for GSA, I chose the Morris technique given its simplicity and straightforward implementation (e.g. compared to the FAST technique).

My adapted Morris technique computes the difference of outcomes between a reference solution (e.g. time reliability capture map) and a second solution using identical values but with a first variable of interest drawn (from the transient driver parameters) randomly. Then, it measures sensitivity by dividing this difference by the change of the variable of interest. Subsequent analyses repeat the same process by randomizing a next variable of interest, until all variables of interest k have been modified. The most important modification necessary here is that we want to compare elementary effects on average over random conductivity fields, which multiplies the total number of simulation calls by a number N of conductivity realizations. Here, the $k+1$ realizations define a row of Monte Carlo iterations n, with each $n(k+1)$ realizations utilizing same randomly generated n hydraulic conductivity field. This procedure is repeated for $N(k+1)$ simulations with $n = 1, ...N$ representing both the number of rows of Monte Carlo iterations and the amount of different hydraulic conductivity fields. As a second modification in my analysis, I use the absolute difference in order to avoid compensations of opposite signs [16]. I refer to Saltelli et al. [97] for a more detailed explanation of the method.

To compute the absolute mean effect μ_i^* I average the absolute value of EE_i over all N realizations:

$$\mu_i^* = \frac{1}{N} \sum_{j=1}^{N} \left| EE_i^{(j)} \right| \tag{2.10}$$

Second, the standard deviation σ_i, which points out whether a factor depicts a non-linear behavior or interactions with other factors:

$$\sigma_i = \sqrt{\frac{1}{N-1} \sum_{j=1}^{N} \left(EE_i^{(j)} - \mu_i \right)^2} \tag{2.11}$$

Here, μ_i is the mean effect value per factor, not accounting for compensations.

2.6 Clustering

Until now, the implementation of transient probabilistic WHPA analysis requires to generate a large set of Monte Carlo realizations in order to achieve numerical convergence. However, for large and complex hydrosystems, the generation and simulation of such a large set of Monte Carlo realizations might lead to cost prohibitive conditions. To overcome this problem, I propose to use cluster analysis in order to identify a limited subset of Monte Carlo realizations that still represent the overall larger set.

The following is a brief introduction about clustering based on the book of Witten et al. [130] and on the work of Steinbach et al. [118]. In unsupervised learning, cluster analysis or clustering has the objective to divide data into groups (named clusters) in such a way that instances inside a cluster (data points) bear stronger resemblance to other instances of the same cluster than to other remaining instances [130]. Whenever I talk about data points, it refers to low-dimensional representation of each Monte Carlo realization of conductivity. In this way, the resulting clusters capture the natural structure of the data [118] (i.e., here, of the random conductivity ensemble).

A good clustering solution can be interpreted as the one that maximizes the difference between clusters and minimizes the differences (high similarity) among instances within the cluster. This is what is called a *well-separated cluster*.

Obviously, in most real situations, such interpretation of clustering is not present. Instead, data points at the edge of cluster A might present greater similarity to closer instances of cluster B. To account for this particularity, cluster algorithms subdivide the data set following different approaches.

Center-based clustering methods define a data point as the center of a cluster (centroid) and assign whether an instance belongs to the cluster depending on the distance between the data point and the centroid. Transitive clustering assigns cluster membership based on the distance between instances of a data set, with instances away from the current group becoming part of another cluster. Additionally, besides distances criteria, the density on the data set can be used as well to assign cluster membership (Density-based clustering). This criterion is preferred for grouping instances of an irregular or intertwined data set. An extension of this framework is Similarity-based clustering, that bases clustering using additional properties such as geometry, local properties, etc.

Independently of the criterion chosen for clustering, there are different ways to express the obtained partition of the data set.

For instance, exclusive partitioning assigns a unique cluster membership to each data point. The opposite is to assign some degree of membership to each instance. This overlapping partitioning allows data points to belong to more than one cluster, with the degree of membership based on probabilities. Hierarchical partitioning subdivides a single initial cluster (i.e., the dataset) into a nested sequence of partitions. From the top to the bottom, each partitioning exercise subdivides the current number of clusters into two or more sub-clusters. This partitioning continues until the lowest instance at the bottom represents each individual dataset as distinctive cluster. Finally, Partitional techniques create a one-level (unnested) partitioning of the data points using some previously defined number of clusters K. Partitioning can be seen as one instance of the hierarchical approach that subdivides the data set, but without taking care of upper-instance subdivision and instead using K for splitting the dataset. Clustering is

not a trivial task. Besides the aforementioned criteria for subdividing the dataset, additional possibilities might be to consider only one attribute at the time (*monothetic partitioning*) when subdividing the data set or consider all attributes simultaneously (*polythetic partitioning*).

A problem that has to be taken care of, especially for distance-based clustering, is the curse of dimensionality [11]. This is a well-known problem that affects the analysis and organization of data in high-dimensional spaces. The greater the dimensionality of the dataset (here, the number of pixels used to discretize conductivity fields), the greater the volume of the space thereof. For high-dimensional datasets, due to this sparsity, clustering becomes a non-trivial exercise, since to obtain a meaningful clustering solution, the size of the dataset should increase exponentially with the dimensionality. Otherwise, the obtained clusters might result in meaningless information.

One possibility to solve this problem is through the reduction of the dataset dimensionality by using feature extraction techniques [14]. The central idea behind feature extraction is to characterize the high-dimensional dataset using artificial features constructed from the original dataset which still depict the relevant information and characteristics thereof. Which features are important or how many features to use (feature selection) is a problem-dependent decision.

Once the data set has been properly treated, the next step is to select the adequate clustering algorithm that subdivides the (artificial) dataset into meaningful clusters. In the following section, I briefly describe the K-medoid algorithm which is used, in this thesis, to improve Monte Carlo efficiency.

2.6.1 Clustering techniques: K-medoid algorithm

The *K-medoid algorithm* [62] belongs to the centroid-based polythetic and exclusive clustering techniques that partition the dataset into clusters such that there is a high degree of similarity between a data point belonging to a cluster and the center of such cluster. The *K-medoid algorithm* divides the dataset into a predefined number K of clusters. It evaluates the degree of similarity using the distance (commonly Euclidean) between each data point and the center of the cluster or medoid. Its selection for cluster analysis (see Section 6) relies on the straightforward understanding and selection of representative Monte Carlo realizations (medoids), ease of application and fast and efficient in terms of computational efficiency. Obviously, the selection of how many K clusters use to subdivide the data set is a clear disadvantage of the K-medoid algorithm. However, it is well managed by introducing an specific-metric for WHPA result interpretation (see Section 6). Although, it is not a goal of this thesis, future research could investigate the efficacy and improvement of computational efficiency of different cluster techniques. For instance, the Agglomerative Hierarchical Clustering, Expectation-Maximization Clustering using Gaussian Mixture Models, mean-shift clustering, density-based spatial clustering of applications with noise.

The K-medoid procedure starts by selecting randomly an initial number K of data points used as medoids. Then, by computing the distance d between each medoid and the dataset, it assigns each data point to the closest medoid. Using Eq. 2.11, a new medoid for each cluster is assigned. The process is repeated using the new computed medoids until each cluster center converges.

$$\mathbf{x_{medoid}} = \underset{\mathbf{y}\in\{\mathbf{x_1},\ldots,\mathbf{x_n}\}}{\arg\min} \sum_{i=1}^{n} d(y, x_i) \tag{2.12}$$

The number of medoids required to represent the desired statistic from the total dataset is an indicator for the structure of knowledge in the chaos of uncertainty, and a small set of representations, each one at the center of each cluster can be used as a condensed, yet comprehensive, set of hypothesis to represent the relevant aspects of uncertainty that exist in the dataset. Hence, the clustering analysis aggregates the larger dataset into a limited set of representative meta-concerns. Furthermore, with the selection of a unique medoid per cluster, I emphasize that each medoid is equiprobable, i.e., each medoid has same importance or weight for describing the dataset. Due to these properties, K-medoid will be used in chapter 6 to speed up Monte Carlo simulation by selecting a limited but representative set of Monte Carlo realizations that depict the behavior of a greater set of Monte Carlo realizations.

2.7 Optimization

The introduction to optimization problems given in this section is based on the book of Coello-Coello et al. [20]. Overall, a single-objective global optimization problem is the process of finding the global minimum of an objective function within the feasible region Ω of the search space S. This is mathematically expressed by:

$$\mathbf{x_{opt}} = \underset{\mathbf{x}\in\Omega}{\arg\min} f(x) \tag{2.13}$$

$$f : \Omega \subseteq S = \mathbb{R}^n \to \mathbb{R} \tag{2.14}$$

Here, the function f is called objective function and x_{opt} is a global minimum with:

$$\forall \vec{x} \in \Omega : f(\vec{x}^*) \leq f(\vec{x}) \tag{2.15}$$

Then, $\vec{x}^*$ is the global minimum solution of the objective function f. When $f(x)$ describes several objectives and hence is a vector-valued function, the problem of searching for the global minimum solutions is named Multiobjective optimization problem (MOO). Now, the goal of a MOO is to find optimal trade-offs solutions, called Pareto optimal, rather than searching for the single global optimal solution. A solution $\vec{x}^*$ is acknowledged as Pareto optimal if there exist no feasible solution $\vec{x}$ which improves the quality of one of the objective functions $f(x)$ while being at least equally good in all other objectives f_k. In other words, a solution $\vec{x}^* \in \Omega$ is Pareto optimal if for every $\vec{x} \in \Omega$ and $I = \{1, 2, ..., k\}$ either:

$$\forall_{i\in I} = (f_i(\vec{x}) = f_i(\vec{x}^*)) \tag{2.16}$$

or, there is at least one $i \in I$ that improves current solutions:

$$f_i(\vec{x}^*) < f_i(\vec{x}) \tag{2.17}$$

and is equal for the rest:

$$f_1(\vec{x}^*), f_{i-1}(\vec{x}^*), f_{i+1}(\vec{x}^*), \cdots, f_k(\vec{x}^*) = f_1(\vec{x}), f_{i-1}(\vec{x}), f_{i+1}(\vec{x}), \cdots, f_k(\vec{x}) \tag{2.18}$$

Then, to find the set of Pareto optimal solutions, it is necessary to compare among vectors of objective function values. A vector $\vec{f} = (f_1, \cdots, f_k)$ is said to *dominate* $\vec{g} = (g_1, \cdots, g_k)$ (represented mathematically as $(\vec{f} \preceq \vec{g})$), if and only if $\vec{f}$ is partially less than $\vec{u}$. Finally, for a given set of Pareto optimal solutions ($\mathcal{P}^*$) discovered during the MOO procedure, the Pareto front ($\mathcal{PF}^*$) is defined as:

$$\mathcal{PF}^* := \{\vec{f} = (f_1(x), \cdots, f_k(x)) \mid x \in \mathcal{P}^*\} \tag{2.19}$$

A MOO model can be divided into two main categories: Linear programming (LP) and non-linear programming (NLP) problems. This division bases on the degree of non-linearity of the objective functions and constraints that constitute the MOO problem. In LP problems, the series of linear constrains produces the so called convexity of the feasible domain. This desired characteristic, produces that the optimum obtained solutions, located at the edge between the feasible solution domain and the entire domain Ω, depict the global minimum (concave) or global maximum (convex) of the problem, i.e., the smallest and largest value of the objective function. Because of convexity, LP problems can be solved efficiently through a variety of methods such as the simplex algorithm which provide of precise solutions.

On the other hand, in NLP problems, the objective function is non linear and/or the feasible domain is determined by non-linear constrains. Many physical systems are inherently non-linear, for instance, the WHPA delineation is defined via nonlinear transport modeling. This example implies that NLP problems are more difficult to optimize. Reasons of this could be that exist multiple disconnected feasible regions or to the difficulty of distinguishing a local optimum from global optimum. One possibility to solve NLP problems, is through heuristic optimization techniques which drive the search towards regions of expected optima but without guarantee of finding the global optimum. In the next section, I give a brief introduction about different heuristic optimizations techniques with emphasis on the Particle Swarm algorithm and its adaptation to solve MOO problems.

2.7.1 Multiobjective Optimization Particle Swarm algorithm

In this section I briefly introduce some selected heuristic methods with focus on Particle swarm Optimization and its modification for solving MOO problems. The use of heuristic optimization techniques on this thesis is due to the high non-linearity of the multiobjective optimization problem (see Sec 5).

Simulated Annealing. The simulated annealing (SA) algorithm was developed by Kirpatrick et al. (1983) [65]. SA gets its name from the process of heating and controlled annealing (cooling) of a material in metallurgy. The concept of controlled annealing is represented

in the SA algorithm as slowly decreasing the probabilities of accepting worse solutions as the algorithm searches throughout the solution space for better solutions. Whether a new solution replaces the current one depends on a probabilistic rule and considers the current changes in the objective function and the progress along the optimization procedure.

Evolution-based and genetic methods. As their name suggests, Evolutionary strategies (ES) simulate evolution through mutation and selection of the fittest to solve optimization problems. ES, introduced by Rechenberg (1965) [89], produces an initial population P of solutions which at each iteration mutate randomly into new solutions (offspring). From the combined population of solutions (Parents and offspring) only the best are selected, becoming the parents of the new generation of solutions (iteration).

The Genetic Algorithm (GA) [58] makes use of evolutionary strategies and assigns probabilities for the generation of new offspring solutions. Using the principle of the *survival of the fittest*, those with overall current better performance within the population are attributed higher probabilities for generating the new offspring and vice versa. Then, after selection, the "chromosomes" of the survival solutions are recombined in order to generate the new solutions. This cross-over operation started using binary strings but later was modified to account for alternative representations given the initial and non-trivial binary representation of continuos problems by binary chromosomes.

Memetic algorithms. The Memetic optimizer (MA), introduced by Moscato in 1989 [79] is a hybrid algorithm that combines the population-based strategy of having several coexisting solutions (GA), each one performing a local search as in the SA procedure. While for producing new solutions the MA uses the cross-over approach for depicting cooperation, the replacement of the current solutions by the new ones follows the acceptance criterion of the SA approach.

The Particle Swarm Optimization. (PSO) algorithm is based on the book of Clerc [19] and its adaption to address multiobjective optimization problems is based on the work of Coello et al. [21] and Sierra and Coello [109], [22]. Although there is no superior individual heuristic optimizer that provides better optimization performance, the selection of PSO (and its MOO adaption) to solve my MOO problem relies mainly on its simplicity to implement and on the straightforward update of the vector of continuous decision variables (e.g., pumping rates) rather than encoding solutions depicted in binary representation (0s and 1s) such as in GA.

PSO was originally proposed by Kennedy and Eberhardt (1995) for solving global optimization problems. PSO belongs - along with the Ant Colony Optimization [32] and Stochastic Searching networks [12]- to the category of swarm intelligence systems known for replicating the behavior and self-organizing interaction among agents such as a bird flocking [75] rather than imitating the natural selection used by evolutionary optimizers such as GA [28].

In the PSO algorithm, a particle represents a point in the parameter space that links a set of (randomly) chosen decision variables with the corresponding solution of the optimization problem. After generating several particles, each one depicting a distinctive solution, the particle swarm *flies* throughout the parameter space, searching for particular zones of expected improved performance of the problem solution. The motion of each particle is driven by a velocity vector that updates each particle's position based on its own experience, and on that of its neighbors [109]:

$$v_d = c_1 v_d + c_2(p_d - x_d) + c_3(g_d - x_d) \tag{2.20}$$

$$x_d = v_d + x_d \tag{2.21}$$

Here, v_d is the velocity vector that modifies the current particle's position x_d. The confidence coefficients c_i are values chosen randomly (using a linear distribution between [0 c_{max}]) that depict the particle's confidence on its own movement c_1, on the particle's best-own performance c_2 and on the best solution found so far by the entire swarm c_3. While p_d is the best position found up to now by each particle, g_d expresses the best solution found so far by the particle's neighborhood.

Although the original PSO algorithm was initially developed to solve single-objective optimization (SOO) problems, further modifications have been made [21] for dealing with multi-objective optimization (MOO) problems.

Unlike the single-objective version, the multiobjective particle swarm optimization (MOPSO) procedure has to deal with three issues which are not present in the original PSO algorithm: leadership, propagation of the non-dominated solutions and diversity.

Leadership. refers to the selection of the particle with the best solution found so far. For SOO problems, the leading particle is one of two parts that influences the motion, through the velocity vector of the particle swarm. However, in MOO problems, the solution is a set of non-dominant solutions, each one equally likely to become the leading particle. To select the leading particle among non-dominant solutions, one possibility is to use a quality value based on density measures. Among several techniques existing in the literature, the *Nearest neighbor density estimator* [28] and the *Kernel density estimator* [27] are two of the most commonly used. The former quantifies as density the number of particles inside a cuboid formed around a given particle. The latter defines a radius around a given particle (called niche), and selects as leading solution the particle that has the fewest possible particles inside its perimeter.

Propagation of the non-dominated solutions. In MOO problems, besides searching for new non-dominant solutions, it is necessary to keep a track of the non-dominated solutions discovered so far. The usual approach is to retain the information of the non-dominated particles using an external file. At each iteration, the particle's solutions are evaluated and if a new non-dominated solution is found, the particle's information is added to the external file. Additionally, if such particle's solution becomes dominant over a number of particles solutions contained in the external file, the latter are discarded. In general, the comparison is carried out utilizing an ϵ dominance approach that helps to keep the external file small. Using this strategy, a cube of size ϵ is generated at each particle's solution and if more non-dominant particles are found inside the cube, only one remains.

Diversity refers to the swarm being spread over the solution space in order to warrant global search. There may be a loss of diversity within the swarm due to the fast convergence feature of the PSO algorithm. Two main approaches are used to maintain diversity within the swarm: 1) Use of different topologies for depicting particle neighborhoods. Here, a topology represents the group of particles to which a particle shares information. If the particle communicates with the entire swarm it will lead to a fast propagation of the information among particles. However, this will lead to a rapid decay in the diversity, since all particles will follow a unique leader. Hence, to reduce the loss of diversity, it is preferable to use topologies that define a smaller neighborhood to the particle. 2) Another strategy to maintain diversity, is through the correct treatment of the confidence value c_1 in the PSO equation. A large confidence magnitude indicates that the particle effectuates a global exploration of the solution space (a big jump), which

is preferred at the beginning of the optimization procedure. On the other hand, a small magnitude indicates that the particle would perform a local exploration due to its reduced velocity, which is preferred at the final stages of the MOPSO procedure.

To address the aforementioned issues, several strategies have been proposed by the distinctive MOPSO techniques that currently exist in the literature. For example, the original MOPSO algorithm [21] included a *mutation operator* strategy that improves the exploration capabilities of the swarm while avoiding the particle's stagnation at zones of assumed local optima. To achieve this, the position of each particle is randomly modified, to some limited extent, at the beginning of the optimization procedure, reducing the number and extent of the mutation for later iterations. The Optimal MOPSO algorithm (OMOPSO) [109] combines three strategies for improving the MOPSO procedure: A *crowding factor* that filters out the list of available leaders (leadership), a *mutation operator* strategy based on uniform and non-uniform variation of the decision variables (diversity) and an ϵ *Dominance* approach for the propagation of the non-dominated solutions.

2.7.2 Dynamic Optimization problems

In a dynamic environment, the MOO formulation (regardless of the optimization algorithm used to obtain the Pareto front) has to permanently search for new Pareto optimal solutions whenever the environmental conditions change. By tracking the moving optima, the Pareto front evolves over time, presenting new solutions that continuously fulfill the conditions of the predicted state of the dynamic system. These changes can be attributed to dynamic objective functions or constraints that change over time [40], [56], [55].

When solving a Dynamic Multiobjective optimization (DMOO) problem, the goal is to find for each time step a new Pareto front. By modifying Eq. 2.19 this is expressed like:

$$\mathcal{PF}^* := \{\vec{u} = \vec{f} = (f_1(\mathbf{x}, \mathbf{w}(t)), \cdots, f_k(\mathbf{x}, \mathbf{w}(t)) \mid \mathbf{x} \in \mathcal{P}^*(t)\} \tag{2.22}$$

Above, $\mathbf{w}(t)$ denotes the influence on time-variant conditions (objective functions) of the Pareto front. DMOO problems can be found by sequential solution of MOO problems over time, and this strategy will be used to solve a DMOO problem with OMOPSO in chapter 5.

3. Efficient transient simulation of well capture areas by quasi-steady-states

Parts of this chapter have been published in the Journal ADVANCES IN WATER RESOURCES under the title *Integrating transient behavior as a new dimension to WHPA delineation* [95]. I am reusing parts of the text and figures from this publication by the kind permission of the publisher Elsevier]

In accordance to the challenge expressed in Chapter 1, the simulation of transient flow conditions becomes highly expensive in terms of computational time. Even more, when addressing uncertainties through Monte Carlo simulation. Thus, it becomes necessary to develop more efficient simulations for transient flow conditions. The concept of quasi-steady states developed here is an efficient approximation. With this technique, I still can achieve asymptotically valid transient flow conditions for large aquifer hydraulic diffusivity in effective linear systems.

Domenico and Schwartz [31] presented a time constant ($T^* = S_s L^2/K$) derived from dimensionless analysis of Eq. 2.1 (neglecting q_s), relating the aquifer hydraulic diffusivity term $(S_s/K)^{-1}$ to a relevant length scale L such as the distance between the aquifer boundaries. This diffusivity term is applicable to fully saturated aquifers where the saturated thickness remains constant and thus is aimed principally at confined aquifers. For practical purposes, however, one can use this concept for unconfined aquifers if the change in the saturated thickness does not exceed, for instance, 10% of the initial saturated thickness [7]. They proposed to compare this time constant T^* to the time scale t at which I wish to observe the aquifer. Here, T^* depicts the time required to reach equilibrium after some hydraulic perturbation [2]. Thus, for times $t > T^*$, the aquifer would appear to be at steady state, where the influence of the storage term in Eq. (2.1) is negligible:

$$\left| S_s \frac{\partial \phi}{\partial t} \right| << \left| \nabla \cdot (\mathbf{K} \nabla \phi) \right| \quad \forall t > T^* \tag{3.1}$$

This equation is a common approximation that has been used in previous studies (e.g. [10]). Consequently, Eq. (2.1) can be reformulated without the storage term following the same boundary conditions as before in Eq. (2.2):

$$-\nabla \cdot (K \nabla \phi) = \sum_{i=1}^{N_i} q_i(x,t) \quad \text{in} \quad \Omega \tag{3.2}$$

Eq. (3.2), when applied to fully saturated confined aquifers, becomes a linear differential equation [90]. Thus, I can write (without further loss of generality) the solution ϕ and its boundary conditions as a linear superposition of the influences from external driving forces:

$$\phi(\mathbf{x},t) = \tilde{\phi_0}(\mathbf{x}) + \sum_{j=1}^{N_j} \lambda_j(t) \cdot \tilde{\phi_j}(\mathbf{x}) \tag{3.3}$$

Here, $\tilde{\phi}_0(\mathbf{x})$ is the solution of Eq. (3.2) under time-averaged boundary conditions and without internal sources and sinks. $\lambda_j(t)$ is the magnitude of the j-th transient driver influence in the solution of Eq. (3.2) at time t. The functions $\tilde{\phi}_j(\mathbf{x})$ are the sensitivities of the solution $\phi(\mathbf{x}, t)$ with respect to the i-th transient driver. Further sensitivities result from the likewise treated boundary conditions. Similarly, I decompose (again without loss of further generality for fully saturated confined aquifers) the changes over time for the boundary conditions and internal source/sink terms. The source/sink terms become:

$$q_s(\mathbf{x}, t) = \tilde{q_0} + \sum_{i=1}^{N_i} \lambda_i(t) \cdot \tilde{q_i}(\mathbf{x}) \tag{3.4}$$

I apply the same treatment as in Eq. (3.4) to the boundary conditions of Eq. (2.2). As an example, the influence from a pumping well is represented by:

$$q_{pw}(\mathbf{x}, t) = \lambda_{pw}(t) \cdot \tilde{q}_{pw}(\mathbf{x}) = Q_{pw}(t) \cdot \delta(\mathbf{x} - \mathbf{x}_i) \quad \text{on} \quad x_i \in \Omega \times [t_0, \infty) \tag{3.5}$$

Here, $q_{pw}(\mathbf{x}, t)$ is the point-like sink term, $Q_{pw}(t)$ is the pumping rate with negative values and δ is the Dirac function being zero at all $\mathbf{x}$ except at the position of the well $\mathbf{x}_i$. All boundary conditions (transient drivers) are treated likewise.

I solve the proposed dynamic superposition of steady-state solutions using a standard Galerkin finite element code as used by Nowak et al. [85]. The same mathematical treatment holds approximately for unconfined aquifers where the changes in the saturated thickness are small compared to the steady-state saturated thickness. In the following, I present the numerical implementation of the superposition approach to obtain time frequency maps of well capture areas as well as the probabilistic WHPA formulation and delineation rules used for dealing with both transience and geological uncertainties.

3.1 Transport formulation under transient conditions

The advective-dispersive transport of a conservative tracer is given by:

$$\frac{\partial c}{\partial t} + \nabla \cdot (\mathbf{v}c - \mathbf{D}\nabla c) = 0 \quad \text{in} \quad \Omega \tag{3.6}$$

Here, c is concentration, t is time, $\mathbf{v} = \mathbf{q}/\ n_e$ is velocity, $\mathbf{q}$ is Darcy velocity, effective porosity n_e (assumed constant in this study) and $\mathbf{D}$ is the hydromechanic dispersion tensor [100] given by:

$$\mathbf{D} = (\alpha_t ||\mathbf{v}|| + \mathbf{D}_e)\mathbf{I} + (\alpha_l - \alpha_t)\frac{\mathbf{v}\mathbf{v}^T}{||\mathbf{v}||} \tag{3.7}$$

With longitudinal and transversal dispersivities α_l and α_t, respectively, effective diffusion coefficient D_e and the identity matrix $\mathbf{I}$. Eq. 3.6 is subject to the boundary conditions:

$$\text{-}\mathbf{n} \cdot \mathbf{v}c + \mathbf{n} \cdot (\mathbf{D}\nabla c) = \widehat{J} \quad \text{on} \quad \Gamma_1, \tag{3.8}$$

$$c = \widehat{c} \quad \text{on} \quad \Gamma \backslash \Gamma_1. \tag{3.9}$$

Here, $\widehat{J}$ is a prescribed normal flux density and $\widehat{c}$ represents prescribed concentrations. Our methodology to solve Eq. (3.6) relies on a backward-in-time formulation where the source of contaminants starts at the pumping well [81]. I choose a particle-tracking random walk scheme due to its absence of numerical dispersion [63], [96]. In comparison to steady-state flow scenarios, when particles are released under transient conditions, they experience a sequence of velocity fields throughout their entire life time. Hence, I define points in time $t_j \in [0, T]$ at which batches of particles are released in order to discretize the continuous injection in time. Particles are tracked until they reach a life time τ_{crit} that is relevant for WHPA analysis. Then I use the transient time-of-travel capture zone analysis described in section 2.3 at points in time t_k that discretize the solution of Eq. (3.6). Thus, our approach involves three time discretizations: (1) one for the flow time domain to discretize the flow conditions of different stress periods at points in time t_l, (2) another for the particle release at times t_j, and (3) a discretization with time points t_k on which I read out the transient transport simulations for capture analysis. The latter runs from t_j to t_j + τ_{crit} for each particle batch, where τ_{crit} is the critical time related to the delineation of WHPAs.

3.2 Time frequency map representation of capture areas

The backtracking of each particle batch j results in a batch-wise (and hence time-dependent) map of mean travel time towards the well. The mean refers to the respective mean over all particles (subject to hydrodynamic dispersion) that pass through the pixels of the map. I generate each particle age map using the same grid as for the flow discretization. Then, using Eq. 3.17 (see Algorithm in Table 1), I convert each travel time map to a boolean (yes/no) map $f_j(x_i)$ that indicates whether the mean travel time is below the critical value τ_{crit}. This map expresses, for each pixel x_i, whether it represents a risk to the well in case of contaminant spills. Finally, I assess the frequency (across all n_j batch-wise maps, i.e., over the transient behavior of the system) how often each map pixel has a critical or smaller mean travel time. This yields a frequency map F($\mathbf{x}_i$) of WHPA membership:

$$F(\mathbf{x}_i) = \frac{1}{n_j} \sum_{j=1}^{n_j} f_j(\mathbf{x}_i), \tag{3.10}$$

$$f_j(\mathbf{x}_i) = \begin{cases} 1, & \text{if } [\tau(\mathbf{x}_i, t_j) \leq \tau_{crit}]. \\ 0, & \text{otherwise.} \end{cases} \tag{3.11}$$

Lower values represent a smaller temporal window for possible contamination, which is inversely proportional to how urgently a pixel should be included in the WHPA. Therefore, I convert from frequency map to reliability map by:

$$R_t(\mathbf{x}_i) = (1 - F(\mathbf{x}_i)) \times 100[\%] \tag{3.12}$$

I use the index t for these reliability maps to distinguish the time/frequency-related reliability from the probabilistic reliability that I will discuss later. The time-related reliability

expresses how likely the production well remains safe in case of an instantaneous spill event happening in each map pixel $\mathbf{x}_i$, as the resulting transient contaminant plume may bypass the well under the current transient flow conditions. For instance, for a total simulation time T of 360 days, the area outlined by the 90% time reliability isoline R_{90} is safe in 324 = 360 $\times$ 90% days of the year. Thus, time reliability denotes a different kind of risk in WHPA analysis. A lack of time reliability means that I *know* that such location will put the well at risk. The only remaining question is for how many days per year, and this question is answered through the pixelwise time reliability values.

3.3 Probabilistic WHPA formulation and delineation rules

Besides the uncertainty in capture delineation attributed to transient flow considerations additional uncertainty might be triggered due to (a) imprecise information regarding aquifer parameters and (b) inexact knowledge about the behavior of the different transient drivers. I tackle both sources of uncertainty via Monte Carlo simulation of time reliability maps:

$$R_t(\mathbf{x}_i) = R_t(\mathbf{x}_i, w) \tag{3.13}$$

Above, w denotes the dependence on random input parameters. The ensemble of time reliability maps represents the joint probability distribution of pixel-wise frequencies in transient flow conditions and under uncertain aquifer parameters. The above formulation resembles the probabilistic framework for WHPAs given by Enzenhoefer et al. (2012) [36], but now extended for transience-related frequencies. It is important to emphasize the difference between time reliability and geological reliability values. While both handle risk in the face of uncertainty (time and geological, respectively), a lack of geological reliability defines that I *do not know* whether the well is safe. This is a different risk condition compared to the lack of time reliability, which means that I *acknowledge* that the well is already at risk for a certain fraction of days per year.

The resulting decision rule for delineating WHPAs requires two decision parameters: a desired time/frequency reliability level and a desired geological/uncertainty reliability level. How different transient drivers and the choice of these parameters affects the area consumed by the WHPA will become clear in chapter 4. The proposed approach for the time frequency map representation of capture areas and its probabilistic WHPA delineation is outlined in Algorithm 1.

Algorithm 1 Probabilistic WHPA delineation

1: **for** Ensemble realization 1:$\hat{N}$ **do** ▷ $\hat{N}$ depicts either N or N_s

2: Construct the time frequency map $F(\mathbf{x}_i, \theta_k)$

3:

4: **for** Time interval $1 : n_l$ **do**

5: Convert each travel time map j to a boolean (yes/no) map $f(\mathbf{x}_i, \theta_k)$

$$f_j(\mathbf{x}_i, \theta_k) = \begin{cases} 1, & \text{if } [\tau(\mathbf{x}_i, t_j, \theta_k) \leq \tau_{crit}]. \\ 0, & \text{otherwise.} \end{cases} \tag{3.14}$$

6: **end for**

7: Compute for realization k the time frequency map: $F(\mathbf{x}_i, \theta_k)$

$$F(\mathbf{x}_i, \theta_k) = \frac{1}{n_j} \sum_{j=1}^{n_j} f_j(\mathbf{x}_i, \theta_k), \tag{3.15}$$

8: Compute the time reliability map $R_t(\mathbf{x}_i, \theta_k)$

$$R_t(\mathbf{x}_i, \theta_k) = (1 - F(\mathbf{x}_i, \theta_k)) \times 100[\%] \tag{3.16}$$

9: Convert each time reliability map to a boolean (yes/no) map

$$r(\mathbf{x}_i, \theta_k, t_r) = \begin{cases} 1, & \text{if } [t_p(\mathbf{x}_i, \theta_k) \leq t_r]. \\ 0, & \text{otherwise.} \end{cases} \tag{3.17}$$

10: Compute the probabilistic WHPA transient delineation

$$W(\mathbf{x}_i, \theta_k, t_r) = (\frac{1}{\hat{N}} \cdot r(\mathbf{x}_i, \theta_k, t_r)) + W(\mathbf{x}_i, \theta_k, t_r) \tag{3.18}$$

11: **end for**

3.4 Summary

Transient conditions in groundwater flow have received only little attention regarding their effects in WHPA delineation. Instead, most WHPA solutions are derived from steady-state models. One cause is the high computational cost of addressing transiency during WHPA analysis. For instance, most WHPA programs from water supply companies base their decision making on fixed maps although the catchment to protect is in fact transient.

In this chapter, I propose a numerical approximation of transient groundwater flow that uses dynamic superposition of steady-state flow solutions. The integration of transiency in WHPA delineation analysis leads to the development of dynamic capture maps. These maps express the time frequency of well catchment membership for each location in the domain. To account for additional sources of uncertainty, such as aquifer heterogeneity, I wrapped up the WHPA transient simulation within a Monte Carlo analysis. The resulting solutions, are Probabilistic WHPA maps that depict the probabilities of groundwater pollution due to geological uncertainty and temporal uncertainties.

4. Integrating transient behavior as a new dimension to WHPA delineation

Most of the content of this chapter has been published in the Journal ADVANCES IN WATER RESOURCES under the title *Integrating transient behavior as a new dimension to WHPA delineation* [95]. I am reusing parts of the text and figures from this publication by the kind permission of the publisher Elsevier

In this chapter I evaluate the impact that transient flow conditions have on (probabilistic) WHPA delineation. By doing this, I extend current methodologies and concepts in WHPA analysis so that transiency can be integrated as a new dimension to WHPA delineation. To achieve and illustrate this, I use the newly developed method described in chapter 3 in a synthetic model scenario which is described below.

4.1 Model scenario

I set up a synthetic model scenario in order to address and analyze the effects of transiency and uncertainties on capture zones and WHPA delineation. Here, I describe the model domain. The transient drivers considered were already presented in Section 2.3

4.1.1 Set up of the synthetic base model

The geometry used for the synthetic base model resembles a single geological layer. It is confined only by a leaky layer that permits recharge. The model uses prescribed fluxes and heads for the Neumann and Dirichlet boundary conditions (see Fig. 4.1). The model domain has a size of 3,500 m $\times$ 3,500 m $\times$ 50 m, discretized with 10 m $\times$ 10 m $\times$ 10 m cells. I select τ_{crit} = 180 days, setting the total simulation time for transport to 360 days, ensuring at least 180 days of simulation for any batch of particles injected over the half-year period of system time. The quasi-steady flow is discretized in time steps of 20 days (see Chapter 3), and I release a new batch of particles every day into a single fully penetrating well located at $x = 2800$ m and $y = 1750$ m in the domain. Additionally, I highlight four locations (see Fig. 4.1) within the domain in order to analyze how the results of our approach (i.e., time reliability and geological reliability) can be used in decision making.

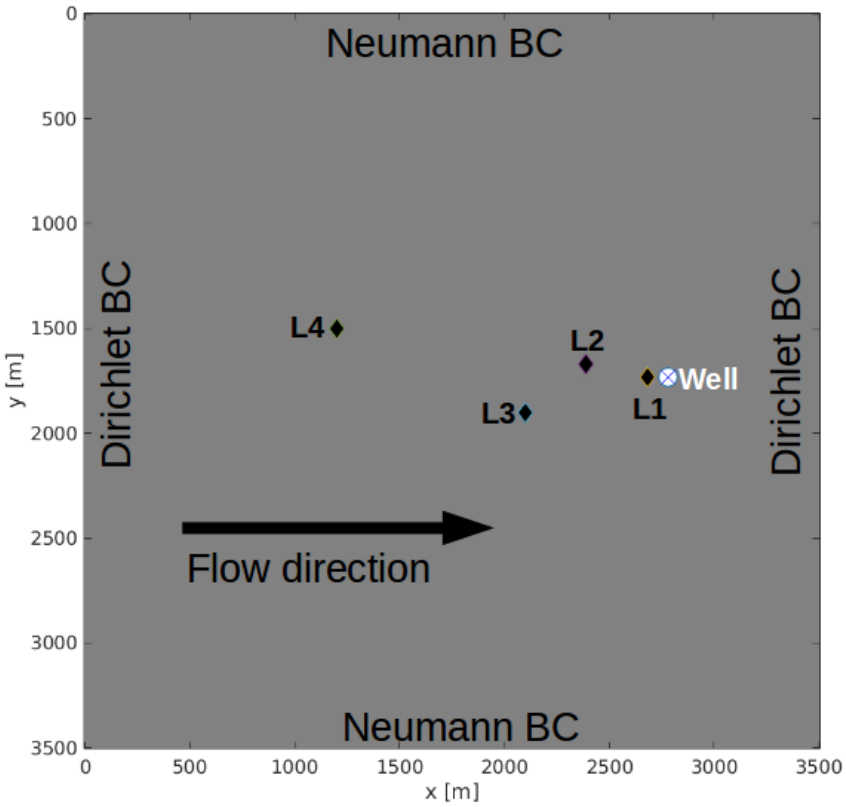

Figure 4.1: Synthetic base model showing the boundary conditions, pumping well position and the four locations (L) with analyzed time reliabilities

Table 4.1: Transient flow, transport and covariance model parameters

Scenario	Full Amplitude $\alpha \pm \varepsilon$	Steady-state condition α
Flow direction (°)	[170 - 190]	180
Gradient strength (-)	[0.0015 - 0.0065]	0.004
Pumping rate (m^3/s)	[0.005 - 0.050]	0.0275
Natural recharge (mm/yr)	[50 - 500]	275
Frequency ω (π/year)		
Amplitude percentage ε (%)	U[0 - 100]	
Phase shift φ_n (-)	U[0 - π]	
Porosity n (-)	[0.30]	
Molecular diffusion coefficient (D_m m^2/s)	[1$\cdot$ 10^{-9}]	
Longitudinal dispersivity α_l (m)	[1]	
Transversal dispersivity α_t (m)	[0.1]	
Mean Log Hydraulic Conductivity K (m/s)	U[-5.5 - -7.5]	
Variance σ^2 (-)	U[2 - 5]	
Shape parameter κ (-)	U[0.55 - 0-75]	
Length scale on x-axis λ_x (m)	U[510 - 1025]	
Length scale on y-axis λ_y (m)	U[220 - 515]	
Length scale on z-axis λ_z (m)	U[35 - 55]	

In my scenario, I assumed a specific storage of $1 \cdot 10^{-6}$. Utilizing the distance between

boundaries (L = 3500 m) and both extreme values of mean K (see table 4.1), I obtain time constants T^* ranging from 0.034 to 0.26 days. Thus, the groundwater system will reach equilibrium after the introduction of a new set of transient conditions on a time scale of 369 min at the latest. Table 4.1 lists all relevant parameters for transient flow, transport and the covariance model.

4.2 Influence of transient conditions in single WHPA delineations

In my investigation, I distinguish between the influence of transient flow conditions on deterministic WHPA delineation (Eq. 3.12) and its impact on probabilistic WHPA solutions (Eq. 3.13). In this first section, I investigate the changes in WHPA delineation triggered by the individual influence of each considered transient driver. Based on this, I examine and rank their individual influence on the WHPA outlines.

4.2.1 Each transient driver has a distinct pattern

How does a transiency-driven WHPA outline differ from a steady-state WHPA delineation? Fig. 4.2 displays an example of the individual contribution that heterogeneous aquifer conditions and each considered transient driver can cause in WHPA delineation. All transient realizations utilize the same amplitude (100%), phase shift (0) and period (π/year) values. Each figure shows the isolated influence of a single transient driver or heterogeneity as specified in the figure headings, while all other drivers are fixed to their average steady-state values. Additionally, I show the equivalent solution for a homogeneous aquifer under fully steady-state conditions. For comparison in each figure, I outline in white the steady-state WHPA, as well as the corresponding 100% time reliability WHPA in red. The blue cross indicates the pumping well location.

At first, I look at steady-state cases as a basis for comparison. Fig. 4.2a presents the straightforward WHPA solution based on steady-state assumptions and homogeneous aquifer conditions. Fig. 4.2b shows the influence of aquifer heterogeneity in a single aquifer realization under steady-state assumptions that, depending on the individual realization of hydraulic conductivity, deforms the theoretically required WHPA outline. The absence of transiency and assumption of complete knowledge of aquifer heterogeneity in these two cases should result in a deterministic WHPA outline.

Now I look at the influence of seasonal changes in the regional groundwater flow direction in a homogeneous aquifer, i.e., ignoring all aspects of heterogeneity and uncertainty. Fig. 4.2c shows the corresponding frequency map of WHPA membership through dynamic changes. A transient direction results in a narrower guaranteed-membership area (yellow) in the transverse direction, but with increasing WHPA area for higher time reliability levels. Compared to the homogeneous steady-state case in Fig. 4.2a, there is minimum impact on the WHPA downgradient (right) of the pumping well position. Overall, transiency in regional flow direction mainly calls for a laterally expanded WHPA at the upstream and middle sections.

The pattern caused by seasonal changes in the strength of the regional hydraulic gradient is shown in Fig. 4.2d. Two system states arise during its temporal variations: 1) during periods of larger magnitudes, the hydraulic gradient will have a higher influence on the velocity field than the current pumping rate. This extends the required WHPA into the upgradient flow direction,

leading to a larger, although narrower, WHPA. 2) Periods of weaker gradients, on the other hand, permit a stronger relative influence from current pumping rate conditions, leading to a shorter, yet wider, WHPA. The combination of both effects induce an extended WHPA at almost all sections of the outline, but only at large time reliability values. Hence, a visual ranking between the factors may be misguiding.

Next, in Fig. 4.2e, we look at the effects of seasonal changes in the natural groundwater recharge. Among all analyzed transient drivers, natural recharge causes the smallest variations in WHPA delineation. Our scenarios are inspired by moderate climates, so the importance of natural recharge variations may be more pronounced in regions with a rain season followed by a clearly arid season. However, I postpone the discussion of quantitative statements about significance of the drivers to section 4.1.2.

Finally, in Fig. 4.2f, I look at the pattern caused by variations in pumping rates. The influence of transient pumping conditions and the resulting pattern can be understood as the exact opposite of the two effects mentioned for the strength of the regional gradient. When comparing the time frequency patterns between the transient pumping case (Fig. 4.2f) and the transient hydraulic gradient scenario (Fig. 4.2d), it shows a smaller variation in the time frequency pattern. This smaller variation, however, is attributed to the assumed pumping rate amplitude, rather than to the transient driver effect by itself. Nevertheless, in both WHPA solutions I used magnitudes from real-case scenarios (Festger and Walter [41] and Frind et al. [46]) that represent realistic situations from the literature. Overall, I conclude that each individual transient driver has a distinct pattern of temporal catchment memberships. They lead to different WHPA shapes than the steady-state case, and they have their own regions of increased (frequency-related) uncertainty.

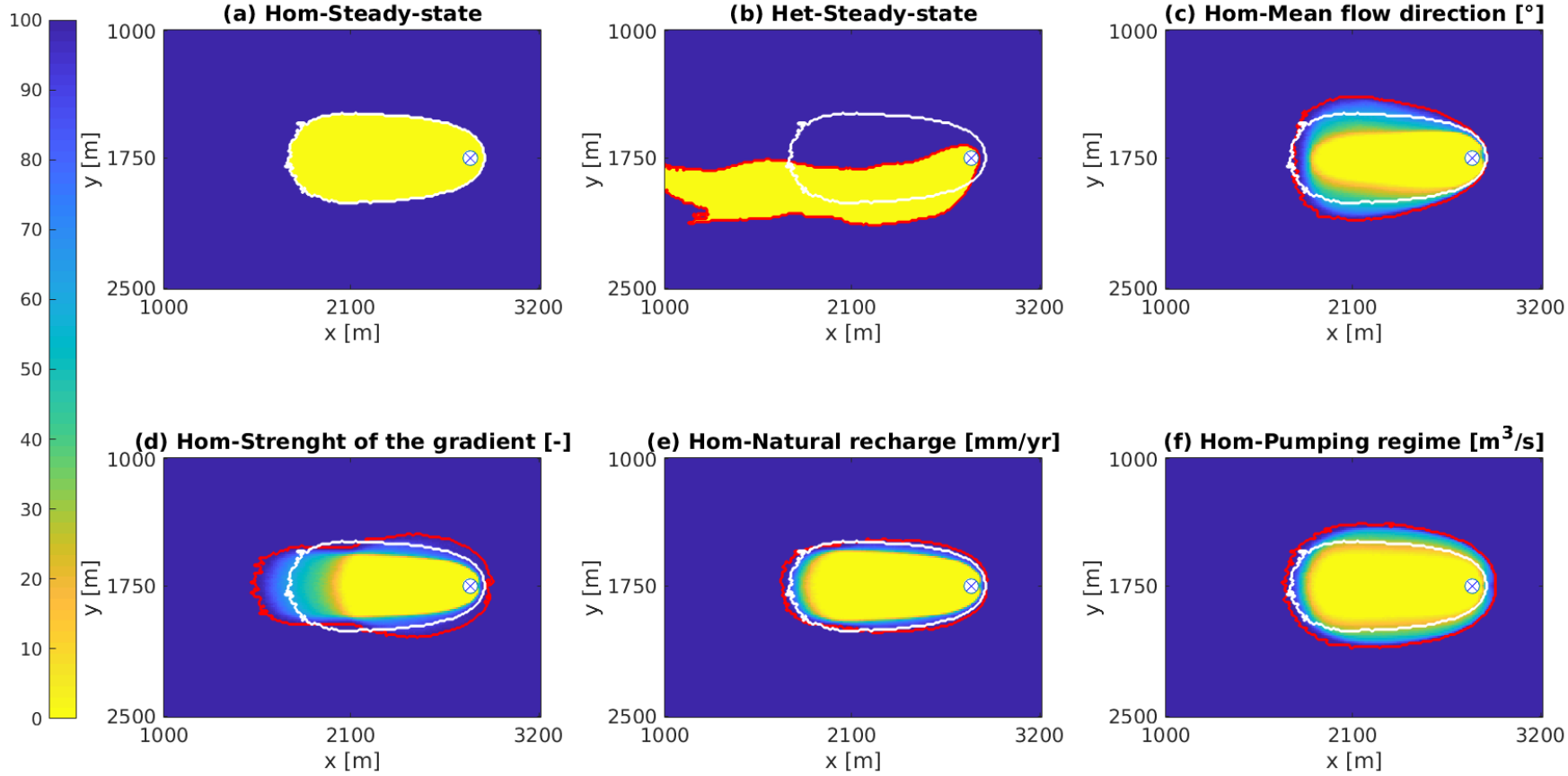

Figure 4.2: Example of the impact in WHPA delineation due to aquifer heterogeneity and transient flow conditions. The color scale defines the pixelwise time reliability values for each WHPA scenario. WHPA delineation assuming steady-state conditions in homogeneous (a) and heterogeneous aquifer conditions (b). WHPA delineation on a homogeneous aquifer influenced by a single transient driver, holding other transient conditions to average magnitudes: (c) angle of regional flow direction, (d) strength of the regional hydraulic gradient, (e) seasonal natural groundwater recharge, (f) seasonal pumping rate.

4.2.2 Ambient flow direction is the dominant driver

Which transient driver has the most important influence in our analyzed scenario? In order to answer this question beyond the visual impression from section 4.2.1 and in combination with uncertainty in the strength and phase shift of each transient and in combination with uncertain conditions in aquifer characterization (geological uncertainty), I carried out a global sensitivity analysis (GSA) based on the Morris method [78]. To analyze sensitivities, the GSA computes two sensitivity measurements per randomized variable (known as factors within the Morris framework). First, it calculates the absolute mean effect μ_i^* to describe the global influence of each input factor. Second, it computes the standard deviation σ_i to point out whether a factor depicts a non-linear behavior or interactions with other factors. A factor can be acknowledged as unimportant if both Morris measures show low values (i.e., both sensitivity measures are located near to the origin). Linear effects depict high values of μ_i^* and low values of σ_i, while non-linearity or interactions with other transient drivers are indicated by high magnitudes in both measurements. In our analysis, I consider the sensitivities with respect to four amplitude and three phase shift values (because pumping depends on recharge), using 5,000 Monte-Carlo repetitions per transient driver.

In our assessment, I investigate three different sensitivity aspects. Case A depicts changes in time reliabilities for each pixel within the WHPA. Case B compares the total areal demand (land surface area delineated by arbitrarily selected reliability levels) inside the 100% time reliability. Finally, case C measures changes in delineation by counting the number of pixels left that flip from "inside WHPA" to "outside" and vice versa.

Fig. 4.3 displays, for cases A (red), B (blue) and C (black), the sensitivity measures due to changes in the regional flow direction (circles), regional hydraulic gradient (diamonds), pumping rate (triangles) and natural recharge (squares). First, I analyze the overall behavior from all transient drivers for the three mentioned cases. As expected, each transient driver introduces a change in WHPA delineation indicated by $\mu_i > 0$, while additionally showing a non-linear behavior or interaction expressed by $\sigma_i > 0$. The location of all transient drivers on the diagonal of the plot indicates the importance of transient flow conditions during WHPA analysis.

Next, I analyze the relation between both sensitivity measures μ_i^* and σ_i for each transient driver. Apparently, I can group their overall influence into two main clusters. The first cluster groups all sensitivities attributed to changes in the regional groundwater flow direction (circles). Case A (Areal demand) becomes the most sensitive case in comparison to the other two cases, as seen by the larger values in both sensitivity measures.

The second cluster groups all transient drivers that modify in some extent the velocity field. Here, transient pumping rate conditions (triangle) depict for all three cases an overall greater influence than the remaining two transient flow behaviors. In general, changes of the regional hydraulic gradient are described as the third most influential condition, although only for cases A (red) and C (black). Dynamic behavior in the natural recharge is ranked in general as the least influential transient driver.

Although this analysis is specific to the used range of transient driver magnitudes, it allows us to formulate tentative recommendations about the treatment of transient drivers: First, in the presence of dynamic fluctuations of the regional flow direction, one should account for these variations during WHPA delineation, rather than introducing a mean flow direction into simulation. Second, pumping regimes and dynamic changes in the regional hydraulic gradient can represent an important source of transiency which should not be neglected. However,

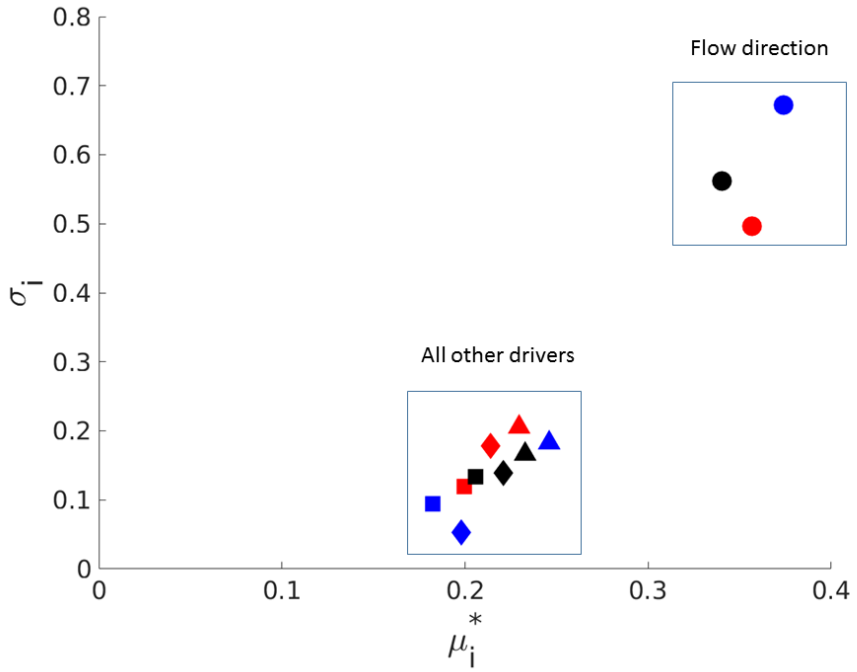

Figure 4.3: Normalized sensitivity values for the four analyzed transient drivers: 1) Changes in the regional flow direction (circle), Regional hydraulic gradient (diamond), Pumping rate (triangle) and Natural recharge (square). Red, blue and black colors identify Cases A, B and C, respectively

pumping regimes can be easier to predict, because they are under control of the operator (see Chapter 5). Finally, dynamic variations in the natural groundwater recharge might be viewed as a mean value in case other transient conditions are strongly pronounced.

4.3 Transient analysis improves probabilistic WHPA delineation

In the previous section I discussed how the individual effects of each considered transient driver modify the conventional WHPA outline. Now, in this section, I introduce uncertainty in WHPA delineation, attributed to the insufficient knowledge about parameters of transient drivers in Eq. 2.9 and also to inexact characterization of aquifer heterogeneity. I investigate this issue via Monte Carlo analysis.

4.3.1 The difference between transient and steady-state probabilistic analysis

How does our probabilistic transient analysis and decision rule (including uncertainty in transient drivers and in heterogeneity) differ from probabilistic steady-state WHPA analysis? To investigate this question, I compare the solution of our fully uncertain transient analysis with an equivalent scenario that considers only geological uncertainty and replaces transient flow conditions by their long-term average (see Table 5.1). Fig. 4.4 shows, for both analyses, the delineation for a 50% geological reliability level using 100% time reliability in the transient analysis (larger white contour line) and in the steady-state analysis (smaller white contour line). Of course, the transient analysis leads to the larger outline. This is because the transient analy-

sis integrates all locations that, due to transient flow conditions, might contribute groundwater to the well at any time of the year.

The transient analysis provides richer information than conventional probabilistic analyses in the form of time reliability outlines. For example, Fig. 4.4 highlights in red the 10%, 50% and 90% time reliability outlines for the same 50% geological reliability level. These outlines include all locations in the WHPA that contribute to the pumped water quality in 10%, 50% and 90% of all days in the year. The larger the time reliability value, the larger the corresponding outline. The observable increase in areal demand of the WHPA is a combination of the individual patterns discussed in section 4.2. With the help of these time reliability outlines, a decision maker can elucidate (here: for a chosen geological reliability value), the time frame of protection against groundwater contamination that the WHPA should provide. Of course, there will be trade-offs between choosing higher geological reliability versus higher time reliability, as will be discussed in section 5.2.2. In section 5.2.4, I show how the richer information provided by time reliability maps is useful in decision making about WHPA delineation.

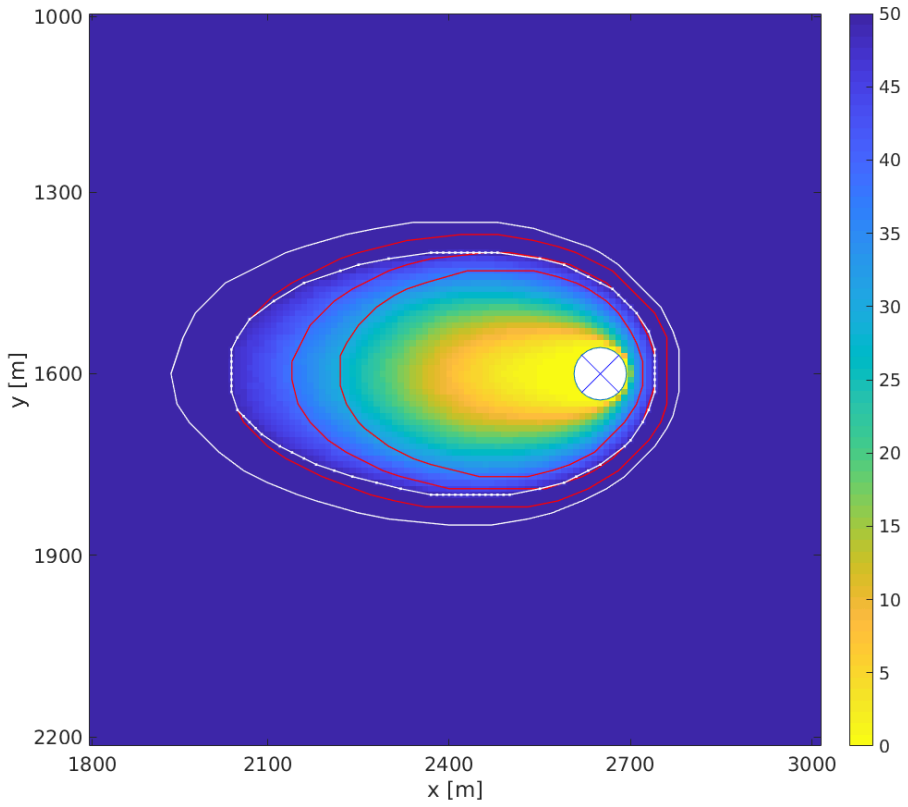

Figure 4.4: Comparison of probabilistic capture delineation assuming transient and steady-state solutions. The smaller white contour line denotes the WHPA delineated in the steady-state scenario at 50% geological reliability level, while the greater white contour shows the result for the transient analysis (combining uncertain transiency and geological uncertainty) at 100% time reliability and 50% geological reliability. The red contour lines highlight time reliability levels of 10%, 50% and 90% in the same transient scenario. The background shows the steady-state solution for values $\leq 50\%$

4.3.2 Choosing higher time reliability levels is much cheaper than increasing geological reliability

How does the overall areal demand for WHPA delineation depend on the chosen reliability and what is the trade-off between geological and time reliability? Fig. 4.5 shows the corresponding areal demand for combinations of geological and time reliability levels $\geq 50\%$. The greater these levels are, the greater the safety and the corresponding areal demand, reaching the maximum protection and area at the 100%-100% (time-geological) combination. For instance, the curve for areal demand for a fixed 100% time reliability value indicates the area required for full temporal protection as a function of geological reliability.

Do time and geological reliability behave differently in demanding area? First, I compare the steepness of the slopes in areal demand with increasing time reliability for the fixed 50% and 100% geological reliability levels. While both curves seem to increase linearly with increasing time reliability, the steeper increment in areal demand at the 100% geological reliability level shows that the greater transient influence occurs when requiring larger geological reliability. Now I look at the slopes along the geological reliability axis, e.g. for fixed time reliability levels of 50% and 100%. Here, I see a strong increase in slope over the last 10% of geological reliability for both time reliability levels. By comparing the behavior along the two directions, I can conclude that the additional areal demand for more time reliability is always smaller than the additional areal demand for larger geological reliability. Thus, there is an obvious preference for choosing larger time reliability over larger geological reliabilities, especially at high reliability levels.

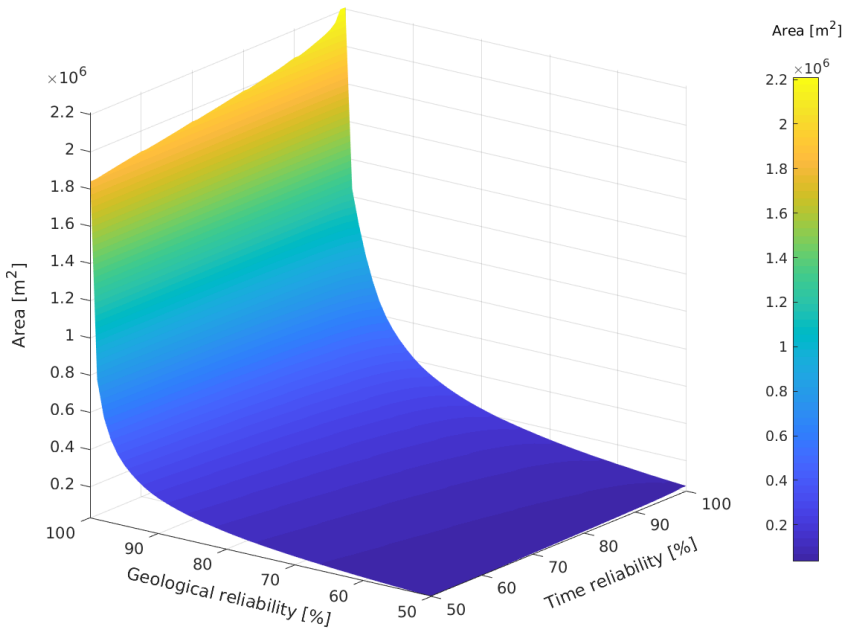

Figure 4.5: Areal demand for combined time and geological probabilistic delineations $\geq 50\%$

4.3.3 Time reliability information can help to prioritize protection

In this analysis, I investigate how time reliability information improves decision making in WHPA delineation and when deciding on individual protection measures for sensitive locations

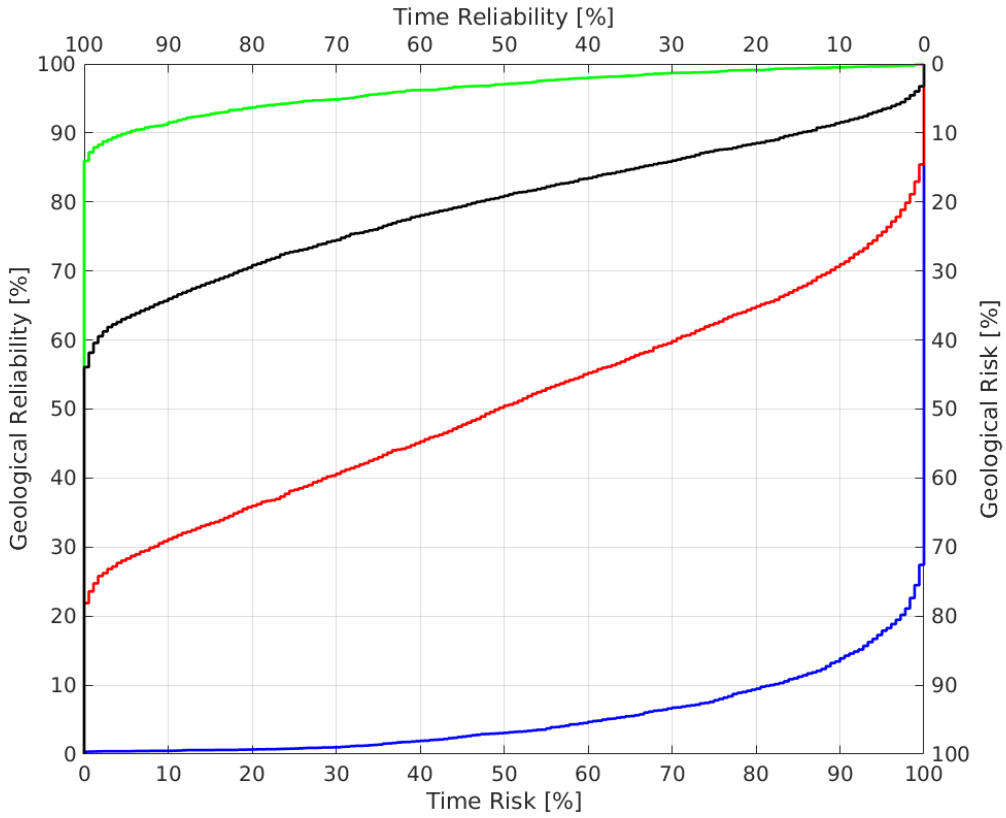

Figure 4.6: Cumulative distribution functions for locations: 1(blue), 2(red), 3(black) and 4(green)

within the WHPA. For our analysis, I utilize the Cumulative Distribution Function (CDF) of time reliability values over all realizations. I extract their CDF at the four different locations marked in the Fig. 4.6 as blue, red, black and green lines for locations L1, L2, L3 and L4, respectively. In addition, for reasons of clarity, I add axes of opposite magnitude to indicate risk. If I look at the lower-right corner of the plot, the combined 100%-100% time-geological risk scenario will represent the worst case for any location, since it indicates a 100% probability risk for groundwater contamination at all times. Vice versa, the 100%-100% time-geological reliability conditions in the upper left corner describe that the location under analysis represents zero risk at all times.

The probability that a spill at any time will impact the well (0% time reliability) is less than 3% for L3 and less than 1% for L4. But our analysis also shows a continuous release at L3 (looking at close to 100% time reliability) will impact the well at some days of the year with more than 40%.

For a good decision, I can look at the type of land use of the featured locations. For instance, if there is industrial activity at L3, the need to implement strong regulations is obvious, and L3 should be treated just like L1. However, if locations L3 and L4 show only limited human activity such as a forest area, I would be willing to discuss rather mild and cost-effective strategies for risk reduction. In this way, I enhance the decision making about the treatment of sensitive locations within the WHPA by introducing our transient analysis.

4.4 Conclusions and Outlook

In this study, I implement four chosen transient conditions and analyze how they influence WHPA delineation. My key analysis tools are joint frequency/probability maps that indicate the degree of membership to the area that should be protected. In the end, my analysis results in a fixed WHPA map, but the construction of the map explicitly considers transiency and uncertainty. I am aware that the results and conclusions of my study are specific to the analyzed scenario, i.e., to the used set of parameters and employed models to represent geological uncertainty conditions. For example, the choice of sinusoidal dynamics, the selection of dynamic drivers and the adequacy of geostatistical models will differ from site to site (e.g. [70], [71]). However, I expect that on a qualitative level, the effects and the ranking between heterogeneity and transiency generalizes. In summary, my findings are:

1. The influence of every considered transient driver resulted in a distinctive pattern how WHPA maps are affected. The ambient flow direction drives most of the changes in WHPA delineation.

2. Working under steady-state conditions is not enough. Transient analysis for probabilistic WHPA delineation provides additional information in terms of time reliability maps. Now, a WHPA can be defined from this analysis by selecting a reliability level for time and one for geological uncertainty.

3. Time reliability relates to a different kind of risk when compared to geological reliability. A lack of time reliability denotes that I *know* that the well is at risk for a certain fraction of days per year, while a lack of geological reliability means that we *do not know* whether the well is at risk.

4. In the presence of uncertain transient and geological conditions, selecting a higher time reliability level becomes much cheaper than increasing geological reliability.

5. Transient analysis enhances decision making for sensitive locations within a WHPA. The use of time-geological reliability information, combined with land use information, helps to take more targeted risk reduction measures that align with the two different types of risk added by time reliability and geological reliability.

5. Dynamic re-distribution of pumping rates in well fields to counter transient problems in groundwater production

Most of the content of this chapter has been published in the Journal GROUNDWATER FOR SUSTAINABLE DEVELOPMENT under the title *Dynamic re-distribution of pumping rates in well fields to counter transient problems in groundwater production* [94]. I am reusing parts of the text and figures from this publication by the kind permission of the publisher Elsevier

As previously explained in Chapter 1, groundwater modelers usually delineate Wellhead protection areas (WHPAs) assuming steady-state flow conditions. However, time-varying groundwater flow conditions dynamically change the area from which the water is actually pumped, as it is discussed in chapters 3 and 4. For instance, seasonal changes in the ambient flow direction might bring locations with hazardous land use activities (e.g., gas stations or agricultural lands) into the actual abstraction zone for some time periods during the year. Thus, steady-state WHPA solutions can become inadequate for reliable drinking water well protection. Of course, one might simply enlarge the delineated WHPA to account for all seasonal conditions, but this can lead to a massive enlargement of required WHPAs (see Chapters 3 and 4).

In this context, I present a novel pumping management scheme that reduces the influence of transient flow conditions on the actual abstraction zone, so that abstraction remains within the delineated WHPA. Thus, steady-state WHPAs together with old schemes can represent a robust solution against dynamic environments. To formulate my management approach, I use multi-objective optimization (MOO) concepts, searching for compromise solutions that consider at least three objectives: 1) to minimize the risk of pumping water from outside of a given WHPA, 2) to maximize groundwater supply and 3) to minimize involved costs.

5.1 Introduction

In WHPA analysis, one of the main assumptions usually taken by groundwater modelers is to neglect the impact of time-varying flow conditions during WHPA analysis. Instead, the standard routine is to assume steady-state flow conditions. However, nature is transient, and thus the actual time-of-travel capture area has a dynamic outline with no guarantee to remain within the delineated WHPA.

Transiency in groundwater flow can be triggered by several sources. For instance, the transition between dry and rainy seasons can lead to a dynamic water demand that increases and decreases, respectively, the required groundwater abstraction of a well field. The influence of transient pumping conditions on WHPA analysis has been analyzed by Ramanarayanan et al. (1995) [88]. They observed how unsteady pumping rate conditions expand the required WHPA outline compared to its equivalent steady-state delineation. They concluded that transient pumping seems "not to average out with time", and thus should be included in WHPA

analysis. Furthermore, seasonal dynamics and stochastically occurring weather conditions can also lead to changes in the outline of the actual abstraction area, triggered by changes in both the regional flow direction and the regional hydraulic gradient. Festger and Walter [41] analyzed the influence of both conditions and concluded that such variations influence the size of the actual abstraction zone by shifting, expanding or shrinking its outline.

Recently, Rodriguez-Pretelin and Nowak [95] (see Chapter 4) investigated the effects of (uncertain) transient flow conditions in (probabilistic) WHPA delineation. They showed, through four selected transient drivers, how the involved transience triggers significant changes in WHPA delineation when compared to equivalent-steady state solutions. From this, they concluded that *working under steady-state conditions is not enough*. Instead, they showed how a transient capture area calls for delineation of larger WHPAs to reduce the fraction of time per year where water is pumped from outside the delineated area.

They also provided a combined probabilistic/frequentistic delineation rule as a way out. However, the obtained WHPAs are always larger than steady-state-based WHPAs. Enlarging a WHPA might not be an issue when a well or well field is located in rural areas dominated by forests or with non-intensive farming. But in densely populated areas, especially with industrial activities, larger WHPAs become difficult to implement. Even in domestic areas, oil tanks for heating or major motorways are an issue. Therefore, alternative solution strategies to handle transience are required.

I argue that, once one starts caring about transient flow, one could just as well use tailored, dynamic pumping schemes within the well field to counteract natural fluctuation and thus reduce the dynamic changes in the actual abstraction outline. Dynamically managed pumping schemes are the most straightforward way out, since natural transient effects (e.g., regional gradients) cannot be brought under human control, but pumping is controlled by management. Many research papers about optimal pumping management schemes can been found in the literature. Most of these studies address sustainable management of groundwater resources involving quantity and quality issues ([111], [110], [112], [48], [24]) or solutions for groundwater remediation ([5], [59], [76], [69], [86]). When adapting such schemes to WHPA management, one should consider at least three objectives: 1) to minimize groundwater abstraction from outside of a predefined WHPA, 2) to minimize groundwater disparity between demand and supply and 3) to minimize the involved costs of pumping.

These three objectives seem to conflict with one another: for example, a pumping scheme that rigorously restricts the actual abstraction zone to an existing WHPA may not meet the water demand. Additionally, a strong redistribution of pumping rates can lead to locally stronger drawdown and hence increases the energy costs for pumping. Therefore I propose to utilize multi-objective optimization (MOO) concepts [72]. Using this formulation, if a management solution improves at least one of the aforementioned objectives without being worse in any of the other objectives, it is acknowledged as a so-called non-dominated solution. The set of all non-dominated solutions forms what is called a Pareto Front. The Pareto front is a list of all meaningful trade-off options between the three selected objectives, and the final selection for a specific solution is based on decision rules or discussions that reflect the preferences of the decision maker. Furthermore, given the dynamic behavior of our groundwater system, my dynamic multi-objective optimization (DMOO) problem [6] has to continuously search for new optimal pumping decisions that address the current state of a dynamic system, so that the Pareto front changes (and has to be tracked) over time. Hence, my management scheme requires to solve the MOO problem in a dynamic way, e.g., by re-optimizing at a sequence of time steps.

Additionally, it is essential to consider the impact that spatial variability and uncertainty of aquifer properties (e.g., hydraulic conductivity) have on WHPA analysis. The impact of geological uncertainty has been widely analyzed in the literature (e.g., [45], [66], [126], [116], [36], [35])). Consequently, dynamic pumping strategies that would not consider uncertainty could not be considered robust. Instead, they would represent over-confident management strategies that perform worse in practice than what is expected during the optimization and decision making. In this chapter, I address robustness through Monte Carlo simulation over conditioned hydraulic conductivity fields.

The contribution of this chapter is to formulate and develop a multi-objective dynamic management model with the goal to reduce and deliver control to the decision maker of the changes in the actual abstraction outline (compared to the delineated WHPA) caused by transient flow conditions. Thus, model-based steady-state WHPAs together with analytic scheme outlines can represent a robust and still valid solution against unconsidered dynamics of the flow environment. The proposed scheme achieves this via dynamically adapting and re-distributing pumping rates of individual wells in a well field. To avoid infeasible decisions, it works with trade-off solutions among the aforementioned competitive three objectives.

The remainder of this chapter is structured as follows. First, in section 5.2, I describe my intended management scheme and formulate the corresponding dynamic multiobjective optimization problem. Later, I extend my MOO problem to provide robustness over geological uncertainty (see Section 5.2.3). Finally, in section 5.2.4, I extend to a dynamic MOO problem and explain the decision rules I use for selecting Pareto solutions at each time interval. In section 5.3, I present the used methodology to carry out our novel pumping management approach. Section 5.5 describes a 3D synthetic application model and provide implementation detail. Results and corresponding discussions are found in section 5.5, while the conclusion and outlook are presented in section 5.6.

5.2 The proposed pumping rate management strategy

In the present section, I describe the novel approach for the optimal dynamic re-distribution of pumping rates to counter transient problems in groundwater production while additionally accounting for geological uncertainty.

5.2.1 Management problems in safe groundwater production due to transient flow conditions

Most groundwater protection programs use WHPAs to safeguard groundwater abstraction against pollution. Retaking Figure 1.1 from Chapter 1, it highlights in black a typical WHPA of a well field composed of eight drinking water wells. During WHPA analysis, this WHPA assumed a complete knowledge about heterogeneous aquifer conditions (hence the irregular WHPA geometry) and steady-state conditions. Likewise, this Figure highlights in red a larger additional outline for the same well field that accounts for transient flow conditions influencing the WHPA analysis [95].

Thus, the goal of my suggested pumping management approach is to optimally re-distribute pumping rates so that the adapted capture area remains within the original steady-state WHPA solution even in a transient environment, and so to avoid the WHPA enlargement sketched in

Fig 1.1. To achieve this, I investigate, over a defined time horizon, whether the predicted abstraction zone driven by transient flow and pumping rate conditions exceeds the given WHPA. If yes, I counter this exceedance by re-adjusting, for the analyzed time-horizon, the pumping rates.

I use the indicator map $I_s(\mathbf{x}, \theta)$ for the actually delineated WHPA. This indicator map marks all locations $\mathbf{x}$ inside the WHPA with $I_s = 1$, and $I_s = 0$ otherwise. θ are hydrogeological parameters influencing the WHPA delineation such as hydraulic conductivity or porosity. Likewise, for the predicted transient time-of-travel abstraction area, I use the indicator map $I_d(t, \mathbf{x}, \theta, \mathbf{q}(\tau), \boldsymbol{\alpha}(\tau))$.

Additional for being dependent on aquifer parameters θ, the dynamic capture zone predicted at time t into the future depends on pumping rates at $\mathbf{q}(\tau)$ and groundwater transient conditions $\boldsymbol{\alpha}(\tau)$ acting over some relevant time interval τ. For the latter indicator map, to simplify notation, I use its shorter expression $I_d(t, \mathbf{x}, \theta, \cdot)$. The predicted abstraction zone results from the combined influence of past ambient transient flow conditions and past pumping (either optimally rearranged or not) with forecasted ambient flow behavior and suggested pumping rate management. Thus, the time interval τ starts in the past of t and extends into the future of t. To evaluate whether the WHPA currently delineated remains valid as protection measure for the forthcoming stress period, my framework compares, for any suggested future pumping rate, $I_s(\mathbf{x}, \theta)$ to $I_d(t, \mathbf{x}, \theta, \cdot)$. In plain words, I measure the extent of area in I_d that is not protected by I_s.

I base the evaluation of a suggested pumping management on three aspects of relevant interest in WHPA analysis: (1) its *quality*, which describes the extent of area in $I_d(t, \mathbf{x}, \theta, \cdot)$ that currently contributes with groundwater to the well field without being protected by I_s. (2) the *quantity* of actual groundwater demand not fulfilled by the suggested pumping strategy and (3) the *efficiency* of the suggested management scheme interpreted as the costs for pumping operation over the studied time horizon. These three metrics are in fact competing among each other. For example, a pumping rate management strategy that always fulfills the actual groundwater demand will necessarily violate the given WHPA outline when compared to a solution with lesser groundwater supply, and of course it will represent a more expensive management strategy. However, different management strategies producing the same quantity of groundwater would not necessarily lead to the same size and shape of the actual abstraction zone as I can re-distribute the pumping rate within the well field. In order to find pumping management conditions that represent optimal management solutions in the face of transient flow behavior and geological uncertainty, I use multi-objective optimization (MOO) concepts [72], searching for compromise solutions among the considered three aspects.

5.2.2 Multi-objective optimization formulation

Based on the approach described above, I formulate the following MOO problem:

$$\mathbf{q_{opt}}(\tau_{dec} \mid \boldsymbol{\theta}, \boldsymbol{\alpha}(\tau_{dec}), \boldsymbol{\alpha}(\tau_{past}), \boldsymbol{q}(\tau_{past})) = \\ \underset{\mathbf{q}\in\mathbf{Q}}{\arg\min} \begin{bmatrix} f_{del}(\boldsymbol{q}(\tau_{dec}) \mid \boldsymbol{\theta}, \boldsymbol{\alpha}(\tau_{dec}), \boldsymbol{\alpha}(\tau_{past}), \boldsymbol{q}(\tau_{past}) \\ f_{gws}(\boldsymbol{q}(\tau_{dec}) \mid \boldsymbol{\theta}, \boldsymbol{\alpha}(\tau_{dec}), \boldsymbol{\alpha}(\tau_{past}), \boldsymbol{q}(\tau_{past}) \\ f_{cost}(\boldsymbol{q}(\tau_{dec}) \mid \boldsymbol{\theta}, \boldsymbol{\alpha}(\tau_{dec}), \boldsymbol{\alpha}(\tau_{past}), \boldsymbol{q}(\tau_{past}) \end{bmatrix} \\ \forall\, t \in\ t_0\ + \Delta\tau_{dec} \tag{5.1}$$

Here, $\mathbf{q}_{opt}(\tau_{dec} \mid \cdot)$ is an optimal pumping rate solution $\mathbf{q}$, for the upcoming management period τ_{dec} starting at the current time t. The suggested pumping-rates $\boldsymbol{q}(\tau_{dec})$ are subject to the constraints $\mathbf{q} \in \mathbf{Q}$, such as being positive, satisfying a minimal required groundwater supply or remaining below maximal admitted values. Each optimal pumping solution aims to reduce the influence of forecasted groundwater transient flow conditions $\boldsymbol{\alpha}(\tau_{dec})$ (e.g., regional changes in the hydraulic gradient or seasonal groundwater recharge) while conditioned to past pumping rates $\boldsymbol{q}(\tau_{past})$ and past groundwater transient flow conditions $\boldsymbol{\alpha}(\tau_{past})$. The sum of these two time intervals (τ_{past} and τ_{dec}) defines a time interval τ which I use for capture analysis. For instance, if I want to provide an optimal pumping rate management for the upcoming 30 days ($\tau_{dec} = 30$) of a one-year time-of-travel WHPA outline (τ = 365 days), $\tau_{past} = 335$ days represents the relevant past time interval of already experienced transient flow behavior. These time intervals are illustrated in Fig. 5.4.2. Hence, in order to solve Eq. 5.1, I would run, for each suggested pumping management alternative, the same natural transient flow and pumping rates over time τ_{past}. Once each alternative reaches time τ_{past}, the suggested pumping rate alternative would run over $\tau_{dec} = 30$ days, until it reaches the total time simulation $\tau = \tau_{past} + \tau_{dec}$. Then, for each suggested pumping rate management, I evaluate its performance through three objective functions: f_{del}, f_{gws} and f_{cost} which are explained in the following:

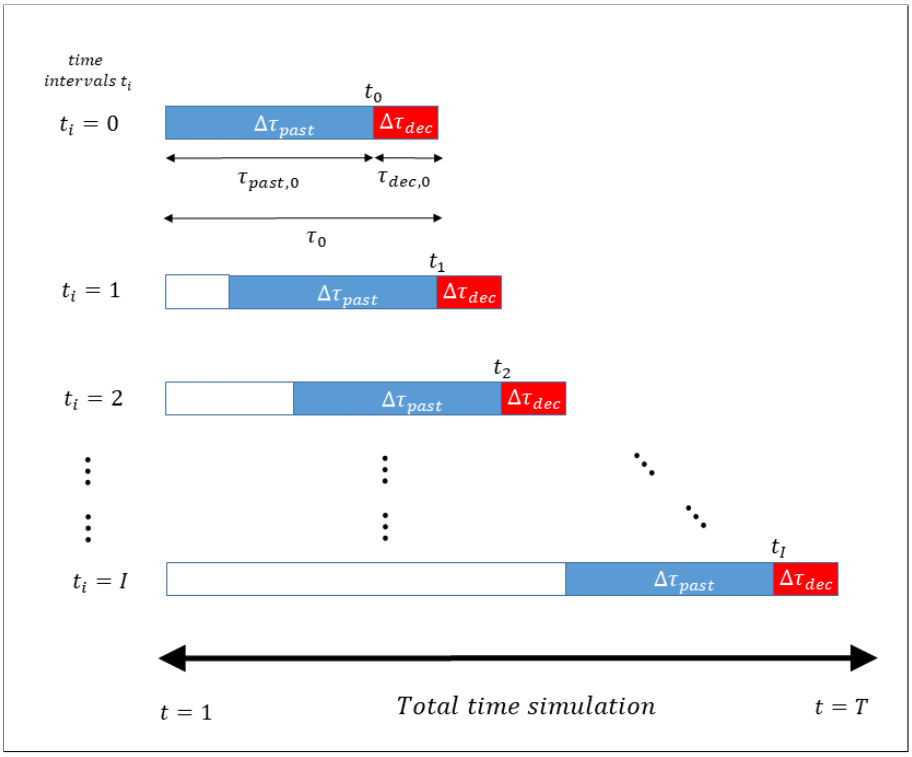

Figure 5.1: Conceptual visualization of the time discretization in the proposed method.

Exceedance area (f_{del}): Eq. 5.2 describes (integrated over time) the extent of area in the overall domain Ω that is within the predicted transient groundwater abstraction area $I_d(t, \mathbf{x}, \theta, \cdot)$ and exceeds the WHPA outline highlighted by $I_s(\mathbf{x}, \theta)$. To compute this exceedance area, I solve a transport problem for the suggested pumping rate strategy, using an available WHPA transient simulator (see Section 5.4.2). For instance, if $f_{del} = 0$, then the predicted capture zone will fully remain inside the given WHPA during all of τ_{dec}. Minimizing f_{del} corresponds to the quality goal (1) formulated in section 5.2.1.

$$f_{del}(\theta, \mathbf{q}(\tau_{dec})) = \int_{t}^{t+\Delta\tau_{dec}} \int_{\Omega} (1 - I_s(\mathbf{x}, \theta)) \cdot I_d(t, \mathbf{x}, \theta, \cdot)\, dx\, dt \tag{5.2}$$

Groundwater shortage(f_{gws}): The objective function for groundwater shortage depicts the difference in the water volume between the expected groundwater demand $D(\tau_{dec})$ and the suggested groundwater supply $S(\mathbf{q}(\tau_{dec}))$ that corresponds to a suggested pumping scheme $\mathbf{q}(\tau_{dec})$. In my analysis, I discard any pumping management alternative that would lead to undersupply in case of sufficient groundwater availability within the given WHPA, and formulate this as part of the constraints $\mathbf{q} \in \mathbf{Q}$. Minimizing f_{gws} represents the quantity goal (2) from section 5.2.1:

$$f_{gws}(\mathbf{q}(\tau_{dec})) = D(\tau_{dec}) - S(\tau_{dec}, \mathbf{q}) \tag{5.3}$$

$$S(\mathbf{q}(\tau_{dec})) = \sum_{k=1}^{n_k} \int_{t}^{t+\Delta\tau_{dec}} q_k(\tau_{dec})\, d\tau \tag{5.4}$$

Here, $q_k(\tau_{dec})$ is the pumping rate at well k during time interval τ_{dec} and n_k is the number of wells in the well field. As additional constraints, our optimization problem is subject to a maximum allowed pumping rate q_{max} for each well and to the prohibition of injection ($0 \leq q_k(\tau_{dec}) \leq q_{max}$).

Involved costs(f_{cost}): We evaluate the energy costs of the management scheme over the considered time horizon τ_{dec} using the following expression:

$$f_{cost}(\mathbf{q}(\tau_{dec})) = A \cdot \sum_{k=1}^{n_k} \int_{t}^{t+\Delta\tau_{dec}} q_k(\tau_{dec}) \cdot h_k \, d\tau \tag{5.5}$$

As stated by Katsifarakis et al. (2018) [61], Eq. 5.5 can be used for any aquifer type with A describing the energy cost per pumped volume and vertical height, which for the sake of simplicity is assumed constant in this study. Here, $h_k(\tau_{dec})$ is the time-dependent depth of the water level at each well location that is predicted from the simulated groundwater flow conditions over time τ_{dec}. As additional constraint within $\mathbf{q} \in \mathbf{Q}$, I constrain the dynamic drawdown at each well $h_k(\tau_{dec})$ to $h_k(\tau_{dec}) \leq h_{max}$ at all times, where h_{max} is a maximum allowed drawdown.

The solution of Eq. 5.1 provides a set of all non-dominated solutions that forms a Pareto Front. Each of these solutions depicts an optimal pumping management alternative because at least one of its objectives improves over other alternatives without sacrificing the performance of the remaining objectives [72].

5.2.3 Integrating Model uncertainty into the Multi-objective optimization

In practice, any optimal management strategy from Eq. 5.1 will represent an over-confident management alternative that deviates from the expected performance. This is due to the high sensitivity that capture analysis has towards geological uncertainty. In order to achieve robustness against this uncertainty, the water supply company will evaluate my MOO formulation over an ensemble of N Monte Carlo realizations that represents the uncertainty triggered by the limited knowledge I have about the model parameters θ. After computing the objective function for each Monte Carlo realization, I average over them and then solve the MOO problem again to get a Pareto front of expected goal attainment levels. Thus, I replace the objective functions in Eq. 5.1 with their expected objectives functions: ($\langle f_{del} \rangle_{\boldsymbol{\theta}}$, $\langle f_{gws} \rangle_{\boldsymbol{\theta}}$, $\langle f_{costs} \rangle_{\boldsymbol{\theta}}$):

$$\mathbf{q_{opt}}(\tau_{dec} \mid \theta, \cdot) = \underset{\mathbf{q} \in \mathbf{Q}}{\arg\min} \begin{bmatrix} \langle f_{del} \rangle_{\boldsymbol{\theta}}(\boldsymbol{q}(\tau_{dec}) \mid \boldsymbol{\theta}, \cdot) \\ \langle f_{gws} \rangle_{\boldsymbol{\theta}}(\boldsymbol{q}(\tau_{dec}) \mid \boldsymbol{\theta}, \cdot) \\ \langle f_{cost} \rangle_{\boldsymbol{\theta}}(\boldsymbol{q}(\tau_{dec}) \mid \boldsymbol{\theta}, \cdot) \end{bmatrix} \quad \forall \, t \in \, t_0 \, + \Delta\tau_{dec} \tag{5.6}$$

Although, in this study, the implemented concept of robustness rests on expected values, alternative statistics such as percentiles or the use of extreme scenarios can be implemented.

5.2.4 Dynamic decision making within the Dynamic Multi-objective Optimization

The obvious dynamic nature of our groundwater system makes the Pareto front evolve over time, resulting in dynamic optimal pumping rate management. My MOO formulation will permanently search for new pumping management alternatives whenever the groundwater flow conditions change. Therefore, a decision maker will dynamically need to select, from the evolving Pareto front, the pumping management strategy to use. I discretize the dynamic decision making with piecewise constant pumping rates in each time horizon τ_{dec}. To select from these Pareto alternatives in every time step, one possibility is to use the actual decision maker's preferences inside the simulation-optimization loop to select the best-ranked alternatives. However, for automation of our analysis, I emulate four decision rules that allow me to construct dynamic decision paths that any decision maker can easily understand and implement:

1. Decision rule A (meeting the demand): To prioritize groundwater supply, I select among Pareto solutions with the smallest penalties for groundwater shortage, the one that achieves the lowest penalty in exceedance area.

2. Decision rule B (risk aversion): We pick, from all solutions that minimize penalty in exceedance area, the Pareto alternative that achieves the lowest penalty in supply shortage. This decision criterion switches priorities with respect to the previous one. This management alternative will inevitably require to rely on external water sources to cover the missing gap in water supply.

3. Decision rule C (best compromise) is to select the Pareto solution with the so-called best compromise alternative between the three considered objective values. This optimal solution has the smallest Euclidean distance to an idealistic unattainable scenario situated at the coordinates origin of the objective values [120].

4. As Decision rule D (conventional), I select the Pareto solution that always follows the demand (like A) but uses spatially uniform pumping for all wells in the well field. I use this management alternative for contrasting optimal pumping (i.e., the previous decision rules) with a management alternative considered as non-optimal.

5.3 Methodology

In the present section I describe the methodology used to carry out my novel pumping management approach. Furthermore, I explain how to achieve robust Pareto fronts in the face of geological uncertainty.

5.3.1 Optimal management of pumping rate conditions in groundwater production

To start with my DMOO analysis, I define and store the given WHPA solution $I_s(\mathbf{x})$ that defines the quality compliance criterion f_{del}. Then, for each pumping scheme $\boldsymbol{q}(\tau_i)$ suggested by my DMOO at the current time interval t_i, I conduct the following steps:

First, for the current stress period under analysis, I solve a forward advective-dispersive transport problem. Batches of particles are continuously injected at times t_j in the entire domain

outside the given WHPA. To save computational time of tracking particles injected over the entire domain [93], it is sufficient to restrict particle release to a compliance testing zone around the WHPA. Then, based on the grid used for flow discretization, I inject one particle at the center of each grid cell in the buffer zone. Afterwards, particles from previous times τ_{dec} and recently injected, move throughout the domain for the current τ_{dec} or until they completed their life-time τ_i or when they reach the well field.

The transport of particles under transient conditions requires a brief explanation about the different time discretizations used for flow and transport simulation and how they couple with my DMOO formulation. In comparison to steady-state flow scenarios, when particles are released under time-varying flow conditions, these particles experience during their life cycle sequences of different velocity fields. Hence, to tailor my DMOO formulation with the available model (see Chapter 3), I use Δt_{dec} to discretize the transient flow time domain. Thus, states of transient boundary conditions are discretized into piecewise constant changes at points in time t_{dec}. Likewise, I use times $t_j \in [t, t + \Delta t_{dec}]$ to discretize the continuous injection of particles in time, at which I release a new batch of particles. Each batch of particles is tracked until it reaches a maximum relevant life time, which for purposes of our optimization analysis, it is the time-of-travel-capture distance τ or Δt_{dec}.

Second, using the information of the previous particle tracking analysis, I generate the Boolean (yes/no) capture map representation $I_d(t, \mathbf{x}, \theta, \cdot)$ of the predicted transient groundwater abstraction area. Within this Boolean capture map, each map pixel x_i receives an indicator value of one if a particle released in it at time t_j reaches the well field within the current τ_{dec}.

Third, I compute the respective objective values according to the suggested pumping rate and obtained capture map (see Section 5.2.2).

Fourth, I solve a MOO problem using Eq. 5.1 to find compromise solutions between the three considered objective functions. This uses the algorithm to be explained in section 4.2 and requires to repeat steps 1, 2 and 3 many times.

Finally, as the fifth step, I select (using the decision criteria explained in 5.2.4) and implement the preferred optimal pumping strategy. Then the WHPA transient simulation continues with the evaluation of the next time interval τ_{dec} until the total simulation time is completed. The overall used methodology is outlined in Algorithm 2.

5.4 Test case scenario and numerical implementation

For the sake of clarity, I demonstrate and discuss my proposed methodology using a synthetic model scenario. First, I describe the model domain. Then, I introduce the numerical methods and implementation used in my novel DMOO formulation.

5.4.1 Test case scenario

As already used in chapter 4, my model scenario resembles a rectangular 3D domain that is confined by a leaky aquifer on top that permits recharge (see Fig. 5.2). My synthetic model is equally discretized by $dx = dy = dz = 15$ m and has an extent of 5,250 m $\times$ 5,250 m $\times$ 60 m. I represent a well field, located in the eastern part of the model, with a row of eight fully

Algorithm 2 Dynamic re-distribution of pumping rates in well fields to counter transient problems in groundwater production

1: Delineate WHPA $I_s(\mathbf{x}_i, \theta)$ ▷ Use Algorithm 1

2: **for** time interval 1:n_l **do**

3: Evaluate suggested pumping rate scheme $q(\tau_{dec})$

4: Solve a forward transport problem for the current batch of particles present in the domain Ω

5: Delineate the predicted transient time-of-travel abstraction area $I_d(t, \mathbf{x}_i, \theta, \mathbf{q}(\tau), \boldsymbol{\alpha}(\tau))$

6: Compute objective functions: f_{del}, f_{gws} and f_{cost}

7: **if** $(\langle f_{del} \rangle_{\boldsymbol{\theta}}, \langle f_{gws} \rangle_{\boldsymbol{\theta}}, \langle f_{costs} \rangle_{\boldsymbol{\theta}}) < \eta$ **then**

8: $t_i = t_i + 1 \leftarrow$ Continue with the next time interval

9: **else**

10: Compute $\mathbf{q_{opt}} \leftarrow$ Set of optimal pumping rate solutions

$$\mathbf{q_{opt}}(\tau_{dec} \mid \theta, \cdot) = \underset{\mathbf{q} \in \mathbf{Q}}{\arg\min} \begin{bmatrix} \langle f_{del} \rangle_{\boldsymbol{\theta}}(\boldsymbol{q}(\tau_{dec}) \mid \boldsymbol{\theta}, \cdot) \\ \langle f_{gws} \rangle_{\boldsymbol{\theta}}(\boldsymbol{q}(\tau_{dec}) \mid \boldsymbol{\theta}, \cdot) \\ \langle f_{cost} \rangle_{\boldsymbol{\theta}}(\boldsymbol{q}(\tau_{dec}) \mid \boldsymbol{\theta}, \cdot) \end{bmatrix} \quad \forall\, t \in\ t_0\ + \Delta\tau_{dec} \tag{5.7}$$

11: **end if**

12: Select the optimal pumping rate strategy from $\mathbf{q_{opt}}$ to use for current time interval t_i

13: **end for**

penetrating wells depicted in Fig. 5.2 as blue circles with 160 m separation distance between each other.

In my approach, I do not infer transient flow behavior from observed data neither do I forecast future transient flow conditions; both are beyond of the scope of this study. Instead, I assume that there is an accurate characterization of transient drivers. Sufficient knowledge of transient drivers is an acceptable assumption for WHPA programs that actively survey groundwater flow behavior.

My model represents transiency via three transient conditions that are often observed on seasonal scale: (I) changes in the regional groundwater flow direction, (II) varying strength of the regional hydraulic gradient and (III) changing natural recharge to the groundwater. For simplicity, all three transient drivers will follow again sinusoidal patterns of given frequency (ω = π/year) and phase shift values (φ_n = 0) as was explained in Chapter 2. Likewise, I address the time-variant groundwater demand following a sinusoidal behavior but using a phase shift value of opposite magnitude to groundwater recharge ($\varphi_n = 180$), with stronger pumping taking place during the dry season and vice versa [23].

The model uses prescribed fluxes and heads for the Neumann and Dirichlet boundary conditions (see Fig. 5.2). I set the total simulation time for the DMOO formulation to 720 days, with $\tau = 360$ days, thus outlining WHPAs of 360 days of total travel time. The time length of every decision time step is $\tau_{dec} = 40$ days. To simulate transient transport, I release every four days (Δt_j) a new batch of particles into a delimited area. To reconcile my model with the time discretization of my optimization approach (see Sections 5.2.2 and 5.2.3), I set each aquifer stress period (used to approximate the transient environment) to last time τ_{dec}. Ergo, each decision interval τ_{dec} represents a stress period influenced by different transient flow and pumping rate conditions at which I search for optimal pumping rate management.

In Fig. 5.2 the black outline depicts the fixed steady-state WHPA delineation using the mean magnitude of pumping and transient drivers while the red outline defines the WHPA that accounts for transient flow conditions computed according to Rodriguez-Pretelin and Nowak [95] with 100% time reliability (See Chapter 4). Due to transient influence, the total area of the red transient delineation is 30% bigger than the fixed steady-state WHPA solution. The goal of my DMOO framework is to cope with the fixed, too small WHPA.

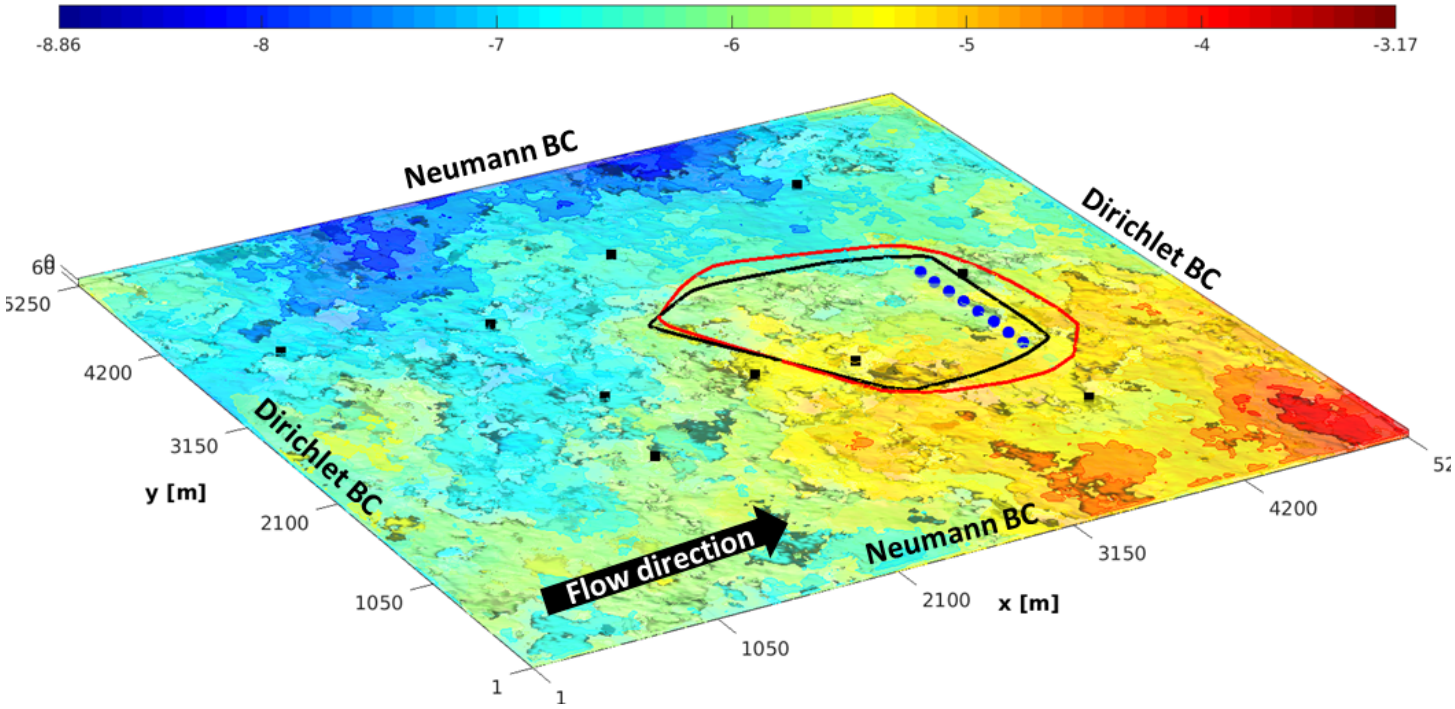

Figure 5.2: Synthetic base model of my well field catchment highlighting the log-K field used for Case 1. The solid black outline depict the steady-state WHPA solution. The red delineation represents the WHPA delineation influenced by seasonal groundwater flow behavior. The blue circles show the locations of eight production wells constituting our well field. The black squares show the locations of hydraulic conductivity measurements used later for conditioning.

.

I treat hydraulic conductivity as a random space function described by a Matérn covariance function [77] using the parameters listed in Table 5.1. Fig. 5.2 shows the realization of the hydraulic conductivity field used as "synthetic truth" scenario in order to evaluate my DMOO formulation (see Section 5.5.1). Then, to analyze my DMOO problem against geological uncertainty conditions (see Section 5.5.3), I use the same set of geostatistical covariance parameters to generate an ensemble of 100 hydraulic conductivity realizations. Each hydraulic conductivity field is conditioned to a set of 40 hydraulic conductivity measurements which were taken at ten different locations (4 measurements per location, each measurement is taken at each of the four grid cells representing depth) of my initial "synthetic truth" realization. The position of each taken measurement is highlighted with black squares in Fig. 5.2. To generate my ensemble of conditioned hydraulic conductivity fields, I use the FFT-based geostatistical tool described in Fritz et al. (2009) [47].

Table 5.1: Transient flow, transport and covariance model parameters

Scenario	Full Amplitude $\alpha \pm \varepsilon$	Steady-state condition α
Flow direction (°)	[160 - 200]	180
Gradient strength (-)	[0.0015 - 0.0065]	0.0040
Pumping rate (m^3/s)	[0.005 - 0.050]	0.0275
Natural recharge (mm/yr)	[50 - 500]	275
Porosity n (-)	[0.30]	
Molecular diffusion coefficient D_m (m^2/s)	[$1 \cdot 10^{-9}$]	
Longitudinal dispersivity α_l (m)	[1]	
Transversal dispersivity α_t (m)	[0.1]	
Mean log. hydraulic conductivity lnK (m/s)	[-6]	
Log. hydraulic conductivity variance σ^2 (-)	[1]	
Matérn shape parameter κ (-)	[0.90]	
Geostatistic length scale on x-axis λ_x (m)	[500]	
Geostatistic length scale on y-axis λ_y (m)	[600]	
Geostatistic length scale on z-axis λ_z (m)	[25]	

5.4.2 Numerical implementation

To simulate groundwater transient flow conditions and contaminant transport (with continuous injection) I use the methodology described in Chapter 3, where the available WHPA transient simulator uses a dynamic superposition of steady-state flow solutions.

Based on the discussions in Chapter 2.3, I obtain the set of Pareto-optimal solutions in each of the (DMOO) decision time steps using a Multi-Objective Particle Swarm Optimization (MOPSO) algorithm. For the sake of brevity, we refer to Reyes-Sierra and Coello-Coello (2006) [22] for a detailed review and explanation of the algorithm and different existing MOPSOs techniques. In my analysis, I use the Optimal MOPSO algorithm (OMOPSO) developed by Reyes-Sierra and Coello-Coello (2005) [109], which is acknowledged as a prominent and competitive formulation among their MOPSO peers and with respect to evolutionary formulations [52].

5.5 Results and Discussion

5.5.1 Management scenarios

To analyze the use of multiobjective concepts for optimal control of pumping rates and to evaluate the impact of the different dynamic decision rules, I set up four different test cases (A, B, C and D). In each of these cases, at each time horizon, I select pumping rates following the corresponding dynamic decision rules described in Section 5.5.2. Thus, I obtain dynamic decision paths for each rule (A, B, C and D). For simplicity, I prefer to keep the application scenarios straightforward and will not look at a possible change of decision preference over time.

For each decision rule, I analyze two scenarios: (1) assuming "well-known" hydraulic conductivity conditions and (2) admitting geological uncertainty. In the first version, I evaluate the four management scenarios over time (see Section 5.5.2), contrast the different decision rules (5.5.3), compare the performance to the simple "satisfying all demand (**D**)" rule (5.5.4) and scrutiny the resulting capture maps (5.5.5). In the second version, I investigate the impact of geological uncertainty for a fixed time horizon (5.5.6). Remarks concerning the assumptions made in my scenarios, their influence, possible generalizations and remaining restrictions will be bundled in Section 5.7.

5.5.2 Trade-offs in the multi-objective single decision horizon problem

As a first result, I present and discuss what are the achievable goal attainment levels and their trade-offs in a single decision horizon. To investigate this aspect, I show in Fig. 5.3 the three-dimensional Pareto front for the initial time horizon. Here, each sphere represents a multi-objective compromise solution over the considered three objective functions. Fig. 5.3 shows, additionally, the projections of the Pareto Front onto the planes of the coordinate system. For easier analysis of the trade-offs, the goal attainment levels are normalized to an interval [0, 1] that spans the lowest and highest goal attainment levels found in the current decision period, for each objective function axis. In addition, for reasons of clarity, I add to each axis label the obtained maximum and minimum values. For instance, the GW shortage axis in Fig. 5.3 denotes 90% of groundwater shortage as the largest value found during the optimization analysis. Just 10% of the current groundwater demand is fulfilled in the most extreme solution.

When looking at Fig. 5.3, I can observe the apparent conflict among the three selected objectives: Pareto solutions achieving a lower groundwater shortage entail larger pumping costs and a larger exceedance area. In the following, I will walk through the pairwise trade-offs one by one.

In the tension between meeting the groundwater demand and complying with the given WHPA, the actual groundwater demand can be virtually fulfilled ($\approx 0\%$ of groundwater shortage) by a wide range of Pareto solutions, all located at the upper part of the Pareto front. This set of Pareto solutions represents the ability of the well field to supply the actual groundwater demand through different pumping rate management strategies that re-distribute the overall pumping across the well field. In this specific time step, this leads to different sizes and shapes of the expected capture zone that all comply with the given WHPA (compare Section 5.5.5).

Among these Pareto solutions, I can find the management strategy based on average (fixed) pumping rates (decision rule D), highlighted with the smaller blue sphere. Solution D is always

a low-cost solution among all solutions with the same total pumping rate, because spatially uniform pumping leads to a quite uniform drawdown and costs rise with deeper drawdown. However, this strategy does not achieve the lowest possible penalty in exceedance area among all solutions that satisfy demand. Instead, solution A according to decision rule A (depicted in Fig. 5.3 with the large blue sphere) minimizes exceedance area while satisfying the demand. It achieves this trade-off by spatially re-distributing the pumping values in an optimal manner. The reduced exceedance area is a first benefit of spatial redistribution of pumping.

Now, I look at the trade-offs between costs and exceedance area (rear plane of Fig. 5.3). Here, the trade-off reveals a similar behavior to the aforementioned Pareto front. Similar low penalty values of area exceedance can be reached when adopting different cost-related pumping management strategies. Following decision rule B, the black sphere in Fig. 5.3 depicts the opposite alternative to solution A (big blue sphere). The black sphere represents the solution that risk-averse decision makers would select, totally avoiding the exceedance area while searching for the maximum possible groundwater supply.

When looking at the two-dimensional projection between costs and groundwater shortage (right face of Fig. 5.3), it shows a narrow range of behavior. In principle, it follows the energy cost versus pumping equation [61], which would be a clear parabola in homogeneous aquifers with identical pumping at all wells. The small scatter of the points is the consequence of spatially redistributed pumping.

Finally, I highlight the management alternative representing the best compromise solution (green sphere in Fig. 5.3 or decision rule C) between all three objectives. This solution is defined by the shortest distance to the origin of the normalized coordinates, highlighted with a white sphere. For many MOO problems, the best compromise solution might be suggested. However, in my case, the necessity for external water supply may suggest to select a compromise solution like A or D, unless when accompanied by demand-side management strategies.

To conclude, the use of spatially adaptive pumping within multi-objective concepts can provide a valuable set of decision options from which a decision maker can select the upcoming management strategy according to her/his preferences while considering three objectives of interest in WHPA management.

5.5.3 Dynamic decision paths following distinct decision rules

Here, I investigate how my dynamic MOO approach provides dynamic pumping schemes that react to a transient environment. To demonstrate this, I show in Fig. 5.4 the dynamic pumping rates of the eight wells composing the well field, plotted over the decision intervals τ_{dec} of 40 days. Each color in the stacked bars depicts the individual pumping rate of each well, and the sinusoidal function (black) shows the time-dependent groundwater demand. The figure shows the results of decision paths obtained by following decision rules A (left), B (center) and C (right).

First, I analyze scenario A. Apparently (as prescribed by rule A), the demand is satisfied at all times. However, the colors show that different wells contribute different fractions of demand at different times. The reason is as follows: in some time intervals, the mean flow direction extends the current abstraction zone to areas outside the given WHPA. Then, the optimal strategy reduces this expansion by assigning higher pumping rates to wells located in the opposite direction of the current flow direction. For instance, for time interval 8 with a mean

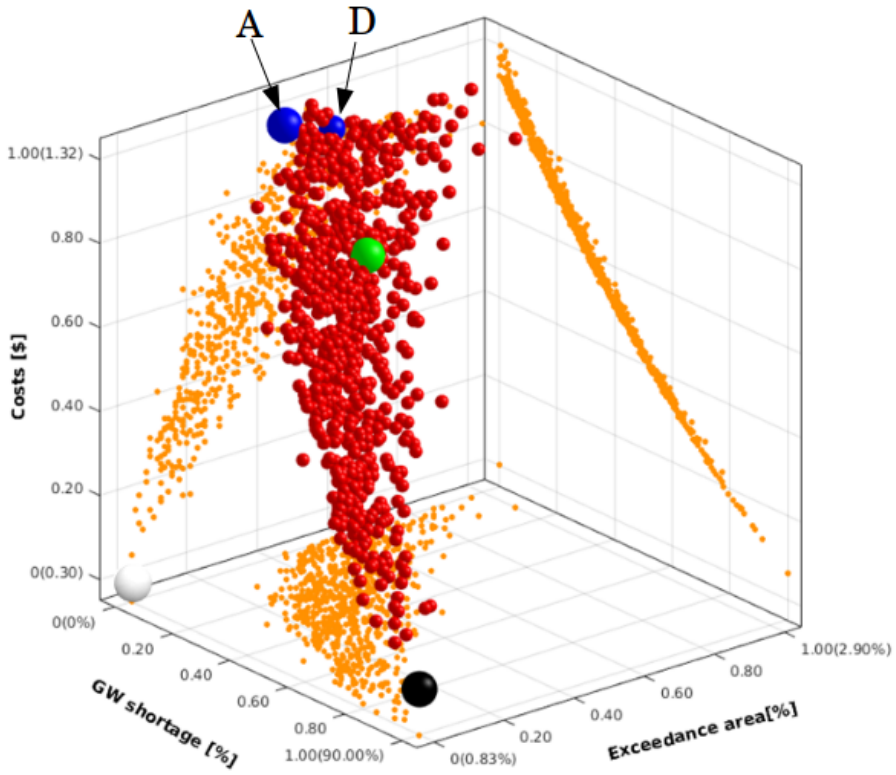

Figure 5.3: Pareto front in the initial time step. The red spheres represent optimal solutions. The blue sphere A depicts the decision path A fulfilling the current groundwater demand with the lowest penalty in exceeding the given WHPA. The blue sphere D represents uniform and constant pumping (rule D). The black sphere represents the solution that strictly adhere to the WHPA while meeting the groundwater demand (rule B). The green sphere highlights the best compromise solution among the three selected objectives. It shows the closest Euclidean distance to an idealistic solution represented by the white sphere located at the origin of the coordinate system. The orange dots depict the projection of the three-dimensional Pareto set onto the corresponding planes of the coordinate system.

flow direction coming from the north-west, southern wells, (yellow and red colors) contribute more to groundwater supply. On the other hand, for time intervals with lower groundwater demand, pumping rate conditions are more evenly distributed (e.g., time intervals 4 and 13). This is because the low demand leads to a buffer area between abstraction zone and WHPA that allows to use cost-optimal uniform pumping rates across all wells. The lower row of Fig. 5.4 summarizes, for each decision path, the pumping rates at each well. In general, the intermediate wells would provide most of the drinking well. This is expected, since most of the violation of the given WHPA is located in the transversal section.

Next, I look at the risk-averse pumping strategy of scenario B (center of Fig. 5.4). Apparently, there is a situation of undersupply at almost each time interval. The overall performance of this strategy would depend on the existing buffer area between actual abstraction zones and the given WHPA. The size of this buffer area depends on the demand, the WHPA size and geometry and the position of wells inside the WHPA. Possible remedies are water import or an enlarged WHPA, which is either costly or perhaps impossible to implement.

Finally, in Fig. 5.4c I look at the re-distribution of pumping rates for scenario C. Here, the decision path is a best compromise between all three objectives. Accordingly, I observe a mixture of the effects discussed above: groundwater demand is satisfied at most times, except for high-demand periods. In those periods, spatially adaptive pumping is used to comply, as good as reasonably possible, with the given WHPA. In periods of low demand, energy costs are minimized. Also, I observe that there is the possibility to shut down groundwater abstraction in well 8 for most of the time intervals. The periodically unsatisfied demand could be addressed by demand-side management, water import or enlarged WHPA delineation. If none of these options are available, one should choose a decision path like in scenario A.

In summary, these results demonstrate that optimal re-distribution of pumping can adapt to a transient environment by pumping more in those wells with best compliance to the given WHPA outline.

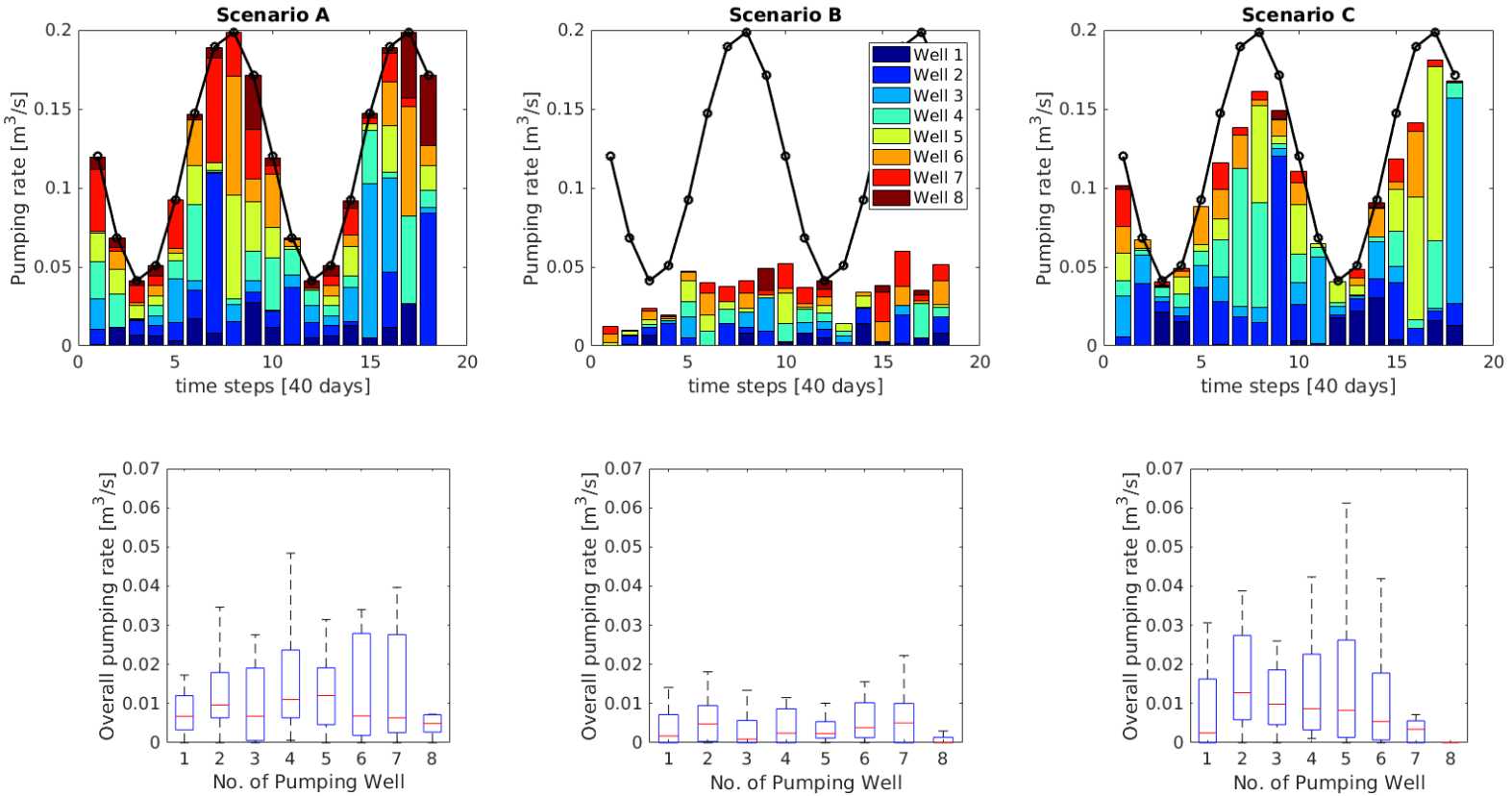

Figure 5.4: Comparison of pumping rate conditions over time for three decision path scenarios. a) prioritizes to supply groundwater shortage, b) prioritizes to reduce the extend of the current abstraction zone and c) links those Pareto solution depicting the best compromise among the three selected objective functions.

5.5.4 Overall performance of transient well field management

How does the overall performance of our optimal pumping approach compare to a conventional pumping scheme? To address this question, I compare in Fig. 5.5 the performances of transient optimization (decision scenarios A, B and C, in blue, black and green, respectively) with the performance of a spatially uniform pumping that simply follows the demand (decision scenario D in red). In the upper row, Fig 5.5a shows the exceedance area growing over time, while Fig. 5.5b-c show the objective function values over time for groundwater shortage (b) and costs (c). The exceedance area rises over time wherever the WHPA is exceeded at a new location. The lower row (Figs. 5.5d-f) shows the obtained total performance. For exceedance area, I show in Fig. 5.5d the worst (i.e., the final) value occurring over time in Fig. 5.5a and call it total exceedance. For total groundwater shortage, I compute the sum of shortage over time and normalize it by total demand. Total costs in Fig. 5.5f are simply the sum of pumping costs at all time steps in Fig. 5.5c.

First, I evaluate the exceedance area using Figs. 5.5a and d. The groundwater production in scenario A satisfies the dynamic demand just like Scenario D. However, it reduces the exceedance of the WHPA at all time intervals. Thus, by using rule A, I can reduce the total penalty in exceedance area from about 30% to above 20% (Fig. 5.5d). Once I accept an optimal compromise between groundwater shortage and exceedance area (scenario C), I can reduce exceedance area down to 4%.

Now, I analyze the groundwater shortage versus time using Figs. 5.5b and e. Obviously, scenarios A and D fulfill the groundwater demand at all times (0% total shortage). Here, scenario C (green) fulfills roughly $\approx 87\%$ of the total water demand while scenario B is only capable of supplying 30%.

Finally, Fig. 5.5c and e present the energy costs for the four considered scenarios. Comparing to the cost of the conventional scheme D, scenario A (supply first, safety later) is slightly more expensive, but the best-compromise scenario C brings the cost back down to the costs of D. B is cheapest because it puts safety first and so leads to very low groundwater abstraction and related energy costs.

In general, scenario C would be the recommended strategy if additional sources of water supply were available. With a similar cost as the conventional solution (scenario D), scenario C is safer (half the exceedance area) but still provides 87% of the total groundwater demand. Scenario A provides full water supply (0% of groundwater shortage), but is more expensive than D. Apparently, these are the costs of increased safety. In both A and C, one could consider mitigating the remaining safety issue (A) or the remaining shortage (C) by seeking to enlarge the existing WHPA. Such a decision, however, may be constrained by the land use activities around the existing WHPA. Therefore, A and C are valuable decision alternatives for well field management in densely populated areas. Finally, scenario B shows that, in our test case, the consequences of maximal safety are too high in water shortage.

To conclude, I could show that the optimal dynamic $\&$ spatial re-distribution of pumping rates can effectively reduce the expansion of the current abstraction zone caused by transiency-driven scenarios. However, the energy costs for pumping operation increases or one has to import some fraction of water.

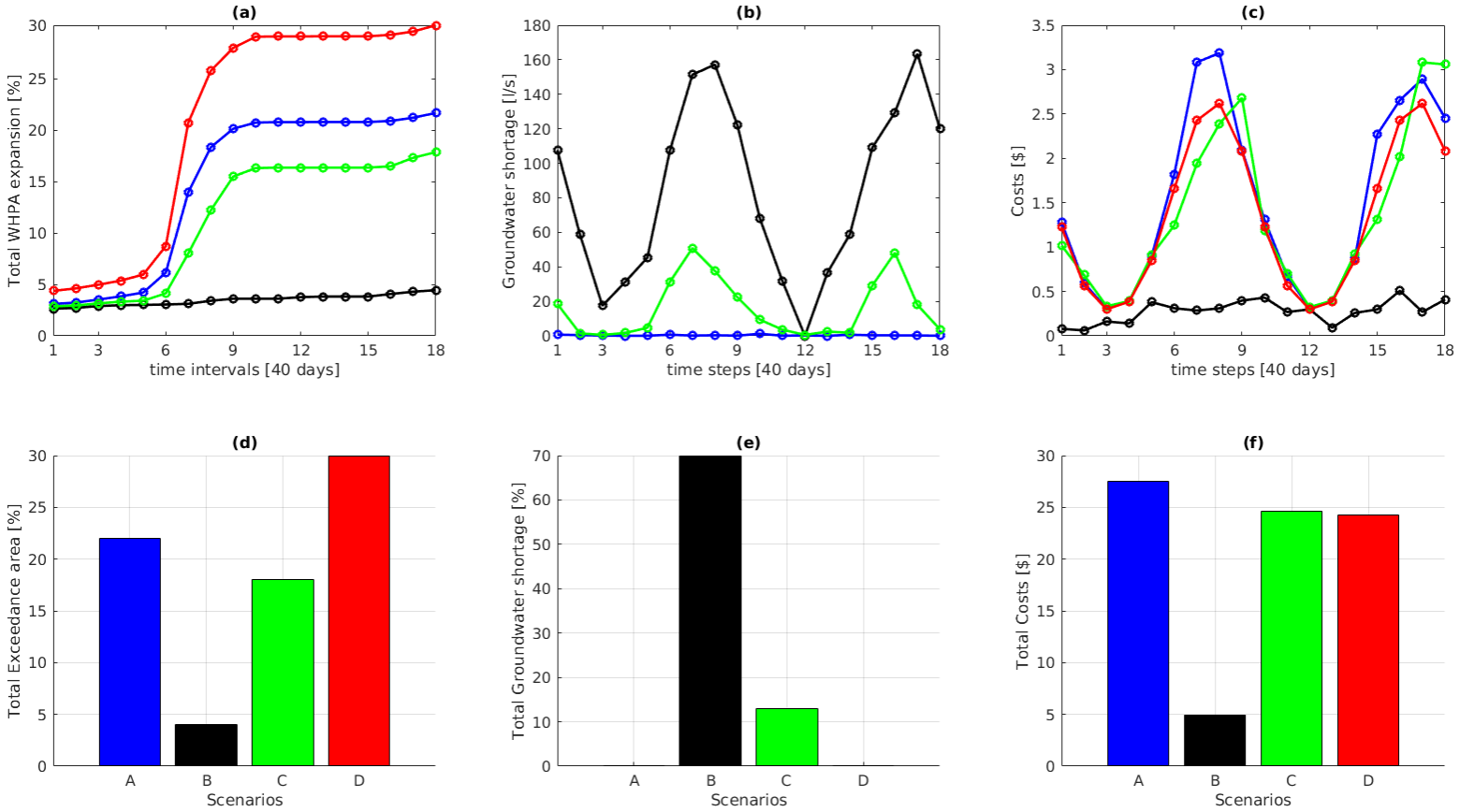

Figure 5.5: Comparison of pumping rate conditions from our dynamic optimization to conventional pumping over time for three optimal decision management scenarios. A) prioritizes to supply groundwater and then seeks the best possible safety, B) prioritizes safety at any level of shortage C) searches a best compromise between supply, safety and costs. Additionally, scenario D in red shows the performance of a conventional pumping rate strategy that follows the demand, but without spatial re-distribution. Top row: objective function values over time. Bottom row: aggregation for total values (see Section 5.5.4)

5.5.5 Impact of dynamic re-distribution on the capture maps

In this section, I compare the different pumping rate strategies on a map that shows capture areas. In order to visually illustrate the resulting differences, I show in Fig. 5.6 the dynamic capture map for each decision path (from left to right: scenarios A, B, C and D, respectively). For purposes of comparison, each figure highlights in white the total capture area of the corresponding strategy, in red the total capture area of the conventional case (scenario D) and in green the actually delineated WHPA.

The color shading in the background shows the percentage of the year in which each location on the map is part of the corresponding capture area. This kind of map has been called time reliability map by Rodriguez-Pretelin and Nowak [95] (see Chapter 2). The white outlines envelope all locations that belong to the capture area on any day of the year. It would be the WHPA one would need to have full protection over the entire year.

In principle, I can see two effects of adaptive pumping: (1) The total capture area can be smaller due to restricted pumping as in scenarios B and C and (2) the utilization of the WHPA is more dense in A and C, allowing to pump (almost) the same water from a more compact and smaller total capture area. The first effect is trivial and I will not pay further attention to it. Instead, I have a closer look at the second one.

As mentioned previously, scenarios A and D fulfill the groundwater demand at all time intervals. If I look at Fig. 5.6a, I see that most of the reduction in the total capture area (due to optimal pumping) in scenario A took place at the extremes in the transverse direction. This is because A pumps in the south when groundwater flow comes from the north-east and vice versa. Also, it reacts to the effect of aquifer heterogeneity on capture area. This leads to a stabilization of the dynamic capture zone within the more densely utilized core area that aligns better with the given WHPA.

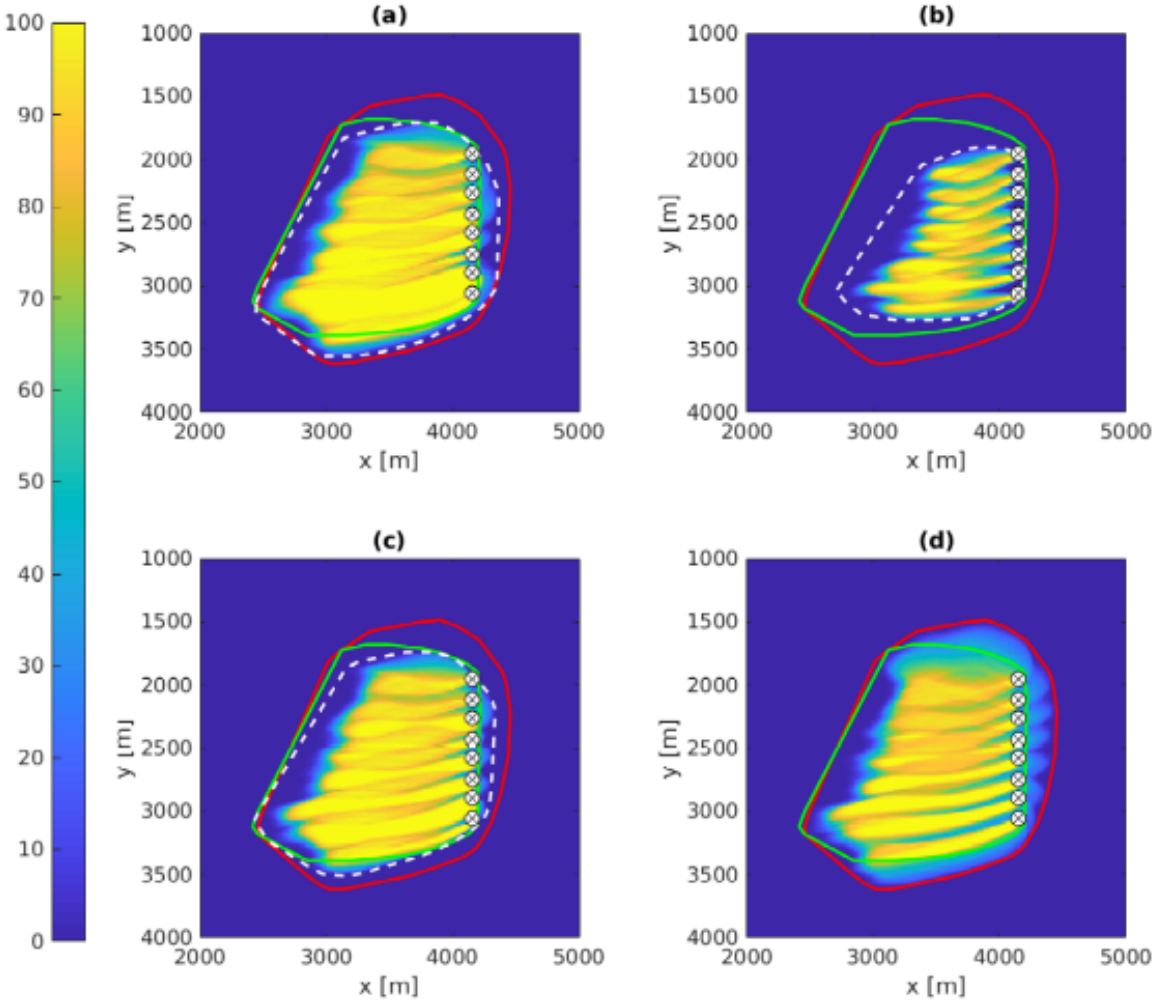

Figure 5.6: Comparison of the impact in WHPA delineation and time reliability values between each of the three distinctive decision path scenarios and the non-optimal transient simulation with average pumping among the eight drinking wells conforming the well field. In white, red and blue are highlighted the total capture area for the corresponding strategy, the total capture area of the conventional case and the actually delineated WHPA, respectively.

5.5.6 Robust optimization benefits when introducing geological uncertainties

In the previous sections, I discussed how an optimal re-distribution of pumping rates can provide flexible control to limit the expansion of the actual abstraction zone. However, I assumed a complete characterization of the hydraulic conductivity field. Now, I investigate the impact of geological uncertainty on our suggested approach. For this purpose, I repeat the entire MOO exercise, but now using Eq. 5.7 as objective function, i.e, the mean effective objective value over 100 conditioned hydraulic conductivity fields (see Section 5.4.1). The resulting trade-off solutions now account for geological uncertainty rather than relying on a single hydraulic conductivity assumption.

For the purpose of discussion, I show in Fig. 5.7 the Pareto fronts from three distinctive uncertainty scenarios within MOO. For simplicity, I show only the projection onto the shortage-exceedance plane. Scenario I (red) resembles full ignorance of the decision maker about geological uncertainty, i.e., the Pareto front from Section 5.5.2 Scenario II (blue) shows the performance of the same solutions, but evaluated on average over 100 realizations. This shows how a deterministic planner must expect to perform when confronted with an uncertain environment. Finally, scenario III (black) considers uncertainty in planning, i.e., it uses Eq. 5.7 as objective function.

The loss of performance from I to II shows the disadvantage of ignoring uncertainty as a deterministic planner. The gap in performance from II to III is the benefit of considering uncertainty in planning. This demonstrates that my suggested dynamic pumping can be used to reduce the impact of uncertainty. The loss from I to III are the plain consequences of being in an uncertain situation, and is not a problem of our specific approach. I can demonstrate this by looking at the conventional pumping scheme (scenario D, green spheres) in the three Pareto fronts: it suffers to the same degree from scenario I (red) to scenario II (blue), and it benefits to the same degree from II (blue) to III (black). Instead, it is the problem of trying to use a given WHPA that is too small to cope with uncertainty. For considering uncertainty more successfully, one could use methods like probabilistic delineation of WHPAs ([36], [95]) that eventually lead to a larger, more robust assessment of capture areas under geological uncertainty. This would provide my suggested approach with more freedom to adapt to uncertainties.

However, I do not show corresponding results of a combined approach, because the computational cost is already high enough. While the deterministic MOO in the previous sections took only 50 hours per decision horizon on a small computing cluster (using 20 cores), the use of 100 realizations to produce the results in Fig. 5.7 costs more by a factor of 100. To make such computations feasible for practical use, one will have to apply techniques of mathematical model reduction or improved Monte Carlo schemes. Such research, however, is beyond the scope of the current chapter. A contribution into this direction is provided in Chapter 6.

In general, my suggested approach opens up new opportunities to play with the given WHPA. However, if that WHPA is too tight (either due to uncertainty as shown here or due to too strong transients), then it is not provided with enough freedom to play. Hence, the given WHPA should not be too restrictive to host, at least, the uncertainty at hand.

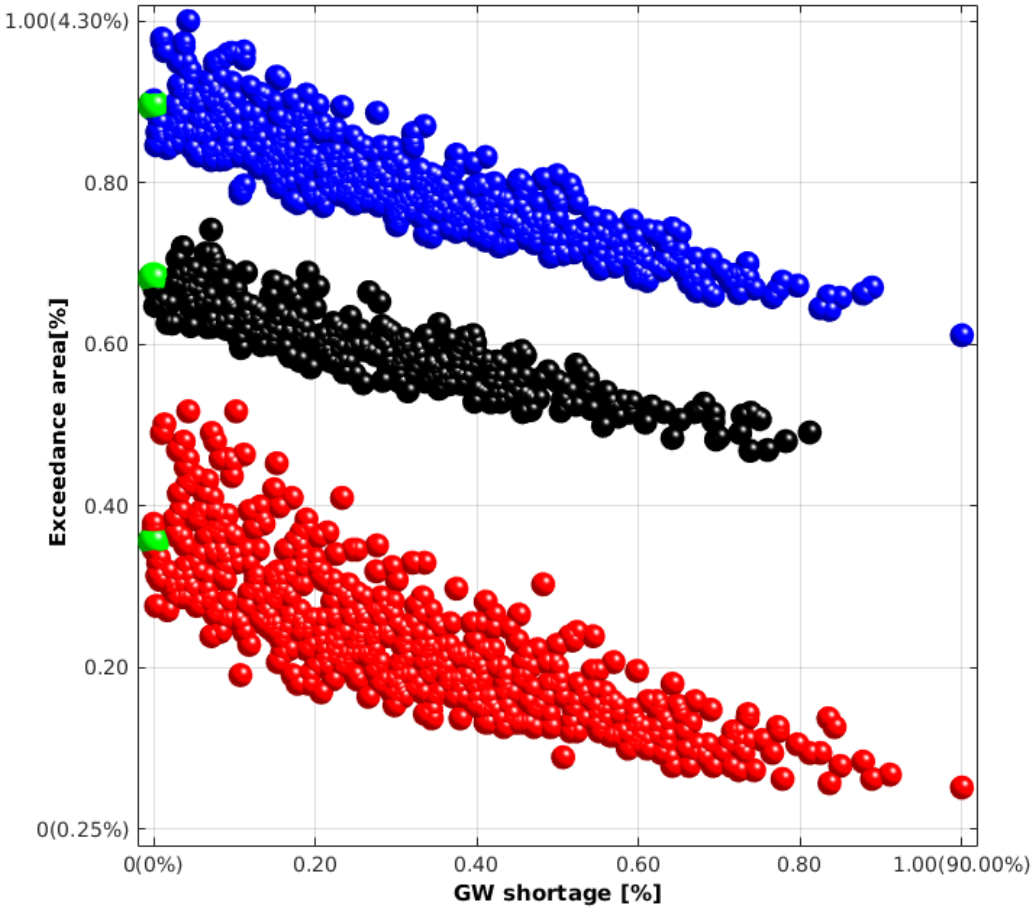

Figure 5.7: Pareto fronts for three distinctive scenarios to address uncertainty. The red Pareto front depicts scenario I which neglects the influence of geological uncertainty. The blue Pareto front (scenario II) describes the impact of neglecting geological uncertainty in scenario I. This set of blue Pareto solutions is obtained by averaging the obtained optimal management schemes over a set of hydraulic conductivity realizations. The black Pareto front (Scenario III) considers uncertainty conditions during the optimization problem.

5.5.7 Final remarks

The main focus of this study is to illustrate the possibility to control the influence of transient flow environments over WHPA delineation by re-adapting the current pumping rate management strategy (according to some decision maker's preferences) so that the expansion of the actual abstraction zone beyond the given WHPA can be reduced or even avoided. Consequently, I limited my MOO analysis to a single transient flow scenario in such a way that it facilitates us to illustrate the suitability of my approach. This assumption does not represent a limitation to my approach: for practical applications where insufficient information exists about transient flow behavior, additional uncertainty triggered by unknown future flow conditions can easily be included.

I am aware that the results and conclusions of my comparison are specific to the analyzed management scenarios and to the used selected decision criteria to manage the water well field over time. Hence, my analysis serves mainly to illustrate the flexibility of my intended approach rather than recommending which optimal strategy to use.

Furthermore, in order to provide real-time control of drinking water production within the assigned WHPA outline, my MOO formulation can be extended by implementing data assimilation techniques [73] in order to benefit from continuous monitoring of groundwater quality through the use of intelligent monitoring [129].

Additionally, I am aware that the results and conclusions of my study depend on the used decision criteria for selecting among Pareto solutions of similar performance (see Section 5.2.4). Obviously, the imposition of such control policies would affect the performance of subsequent system states [17] and might lead to sub-optimal solutions (not foreseen by the decision maker) in the long-term analysis.

Therefore, in future work one might investigate techniques that search for the optimal control policy so that the cumulated reward (e.g., the overall groundwater production for one year simulation) maximizes while correcting sub-optimal solutions through simulation (e.g., reinforcement learning techniques [119]).

5.6 Conclusions and Outlook

Wellhead Protection Areas are frequently delineated assuming steady-state capture areas at all times. However, the influence from nature's transient behavior or anthropogenic causes can lead to significant changes in the actual capture outline. Then, the given WHPA is not large enough to envelope the actual capture area at all times. In this study, I propose an engineered pumping management scheme that optimally adapts pumping rates, based on multi-objective optimization concepts. Its goal is to achieve robustness against transiency while, at the same time, considering additional management objectives. Thus, steady-state WHPAs be used as sufficient protection schemes. In summary, my findings are:

1. WHPA programs and pumping management can benefit from multi-objective optimization concepts. The competitiveness among the selected objectives lead to Pareto optimal solutions from which a decision maker can select the well field management strategy that best suits to upcoming management necessities and transient groundwater flow conditions.

2. An optimal pumping strategy that fulfills the overall groundwater demand can effectively reduce the expansion of the abstraction zone beyond the given WHPA when compared to a non-optimal management scheme. Optimal pumping reduces the influence of the time-variant flow environment by pumping more at those wells that currently yield a smaller influence in the expansion of the current abstraction zone.

3. Optimal pumping stabilizes the dynamic changes of the groundwater abstraction zone, leading to a densely utilized and more static core area that aligns better with the given WHPA.

4. Inappropriate WHPA delineations can not be treated even with my suggested approach. Thus, to address geological uncertainties, it is still preferable to use probabilistic WHPA outlines that are large enough to compensate for uncertainties.

6. Computational cost reduction via Unsupervised learning techniques

The content of this chapter is based on the manuscript *Unsupervised learning for probabilistic WHPA analysis: A novel approach to identify hydraulic conductivity fields that best approximate geological uncertainties* [1]. In the following, I am reusing parts of the text and figures of this manuscript.

A general approach to deal with model uncertainty in natural systems is to use an ensemble of many realizations or other multiple representation approaches. However, to represent such uncertainty by using a large ensemble of model realizations might result in prohibitive computational times. To mitigate issues with computing time in uncertain systems, one possible option is to utilize a smart but well-selected realizations that best represent the involved uncertainties. Thus, the goal of this chapter is to present a methodology to detect a limited subset of hydraulic conductivity fields that best approximate the geological uncertainty conditions of a model ensemble used to delineate wellhead protection areas. However, the selection of representative realizations has to be achieved without running the expensive transient optimizations, i.e. as a pre-processing of the most expensive step. Since geological uncertainty turned out to have a higher influence on WHPA delineation than (uncertain) transient flow conditions (see Chapter 4), the much cheaper steady-state simulation is still near-optimal to a transient selection. In this way, I can reduce the computational costs by limiting transient flow simulations to only K field realizations that best reproduce and propagate geological uncertainty.

6.1 Introduction

Typically, in order to deal with geological uncertainty during WHPA analysis, groundwater modelers use an ensemble of many hydraulic conductivity realizations or other multiple representation approaches to capture the influence of uncertain hydrogeological conditions, generally using Monte Carlo simulation [117]. Each of these realizations depicts a different hydraulic conductivity field that leads to distinctive contour lines and streamlines [53] and thus to different capture outline solutions. The straightforward analysis of such methods is statistical aggregation over the ensemble of capture realizations which summarizes the results to the decision maker in order to provide a simple communication of uncertainties. The obtained output is a well capture probability map with values ranging from 0 to 1 that expresses the probability of well pollution in case of spill events for each location inside the probabilistic WHPA delineation [36], [35], [95].

The involved Monte Carlo simulations are already expensive as they trigger a loop over many model calls. However, more complex analysis may trigger even more loops nested inside or outside the Monte Carlo loop. Such more complex aspects might be, in the case of WHPA delineation, transient simulation of transport towards a well (time loop inside the Monte Carlo loop) or optimization of adaptive pumping rates (optimization loop around the Monte Carlo loop). In such cases, it is tempting to represent uncertainty using a limited set of hydraulic conductivity realizations.

One possible strategy to reduce this computational cost is to substitute the Monte Carlo loop with a limited set of aquifer realizations according to the modeller own experience and knowledge. However, this manual interpretation of geological uncertainty might bring on bias into the overall result. This could lead for instance in over-confident management strategies for groundwater protection that perform worse in practice than what is expected during the optimization and decision making. A less subjective methodology that has been used to identify such representative subsets of realizations is unsupervised learning, for example clustering. Cluster analysis searches, within a low-dimensional representation of the ensemble, for commonalities among realizations based on some distance measures. The number of clusters required to represent the total ensemble is an indicator for the structure of knowledge in the chaos of uncertainty, and a small set of models (one at the center of each cluster) is used as condensed, yet comprehensive, set of hypothesis to represent the relevant aspects of uncertainty.

There have been previous studies addressing the use of cluster analysis to depict geological uncertainty through a subset of realizations, mostly in the field of oil reservoir production. For instance, in the context of uncertainty quantification, Scheidt and Caers (2009) [101] combined kernel k-means clustering with flow simulation to select a small number of representative realizations that represent relevant statistics for future oil production to replace a larger ensemble. The same authors [102] presented a distance kernel method to select a subgroup of realizations that represent ranges of uncertainty for time series of cumulative oil production. In the context of robust optimization problems, Wang et al. (2012) [128] applied k-mean clustering to detect representative realizations. They used this subgroup of realizations to search for robust optimal well placement solutions that maximize the expected oil production of the reservoir under study. When aiming to optimize well control strategies, for a similar purpose of robust optimization, Shirangi and Mukerji (2012) [108] used kernel clustering. In both studies, the authors significantly reduced the computational cost of performing robust optimization by depicting geological uncertainty with a limited number of reservoir realizations.

However, one problem remains: if the selection of that limited set is not performed properly, bias might arise that leads to unforeseen risk scenarios in WHPA analysis or to oversizing strategies in the context of optimizing groundwater protection [94]. This means that the low-dimensional representation of the ensemble (in which distances are defined for cluster analysis) has to be problem-specific and chosen properly. Recently, Shirangi and Durlosfsky (2016) [107] introduced a more general methodology to detect representative models for robust optimization. They investigated the use of flow-based and permeability-based cluster analysis for optimization problems such as optimal well location and optimal oil production. They conclude that the additional flow-based information was beneficial during the reduction process, despite the higher computational time spent for the additional flow simulation.

In this chapter, I apply clustering techniques to speed up WHPA analysis in a transient-transport context, combined with optimal pumping management. To the best knowledge of the authors, there is only one study addressing clustering in groundwater flow modeling. Alzraiee and Garcia (2012) [4] compared the cumulative distribution function of hydraulic heads between an ensemble of 400 hydraulic conductivity fields and distinctive subsets using different clustering algorithms and distance criteria. The authors concluded that, for the study under analysis, 25% of the total number of realizations was enough to achieve approximately the ensemble statistical response. I aim to deepen the use of clustering techniques in groundwater flow modeling, evaluating the effects in transport modelling, particularly for WHPA analysis.

6.2 Methodology

In the present section, I describe the novel methodology for the selection of representative model realizations to reduce computational time in WHPA analysis when addressing geological uncertainty.

6.2.1 Reducing the cost of Monte Carlo integration for expensive WHPA simulation

Solving a large number of realization scenarios is computationally very expensive, especially because transient flow simulation has to be performed for each realization. Here, a groundwater modeller might argue to reduce this additional computational cost of transient flow simulation by assuming steady-state conditions. However, Chapter 3 has shown that steady-state assumptions lead to risk scenarios. The computational cost in my framework rise even more due to the multiobjective optimization in Chapter 5 where I show how multiobjective optimization concepts help to counter transient flow conditions in groundwater production by optimally controlling pumping rates [94]. In this and in related kinds of problems, in order to achieve robustness against any source of uncertainty, a Monte Carlo simulation is commonly integrated as an inner loop within the optimization analysis [29].

One alternative to reduce the computer time is to find a subset of N_s hydraulic conductivity realizations that, chosen from the original ensemble of size N_r, approximates to a statistic of interest when aggregated for decision analysis [38]. In the case of probabilistic WHPA analysis, the subset outline solution W_t should reproduce approximately a chosen time-geological reliability outline W_t (see Chapter 4) obtained after aggregation over all N_s ensemble K field realizations:

$$\underbrace{\tilde{E}_r[R_t(\mathbf{x}_i, w_r)]}_{W_r} \approx \underbrace{\tilde{E}_s[R_t(\mathbf{x}_i, w_s)]}_{W_s} \tag{6.1}$$

Where,

$$\tilde{E}_s[R_t(\mathbf{x}_i, w_s)] = \frac{1}{N_s} \sum_{j=1}^{N_s} R_t(x_i, w_j) \tag{6.2}$$

and,

$$\tilde{E} \approx E \tag{6.3}$$

Here $\tilde{E}$ is the Monte Carlo approximation of the expected value E. In this way, I can reproduce the expected solution $\tilde{E}_r$ via $\tilde{E}_s$ using a much smaller constant set of K field scenarios ($N_s < N_r$) to represent the involved uncertain parameters w.

Furthermore, if I assume that transient flow has a much smaller influence when compared to geological uncertainty in probabilistic WHPA analysis, I can solve the more expensive probabilistic WHPA transient flow simulation, if I first solve all K field scenarios assuming steady-state conditions and then selecting the subset N_s of representative K field realizations much

cheaper based on clustering the steady-state realizations. What strategy suits best to find the limited set of realizations and what features to use to discriminate between ensemble scenarios will be explained on the following sections.

6.2.2 Using Feature extraction for low-dimensional representation of WHPAs

Regardless of the methodology used for selecting K field realizations, is necessary first to reduce the high-dimensional character of the hydraulic conductivity fields and respective capture membership map. Most clustering methodologies find such a low-dimensional representation via feature extraction. This avoids the *curse of dimensionality* (see Chapter 2), which would lead to trivial cluster solutions [118].

In my methodology, I get the low-dimensional representation of each K field realization K_i following the same approach as introduced by Wang et al. (2012) [128]. Using Eq. 6.4, I map each hydraulic conductivity scenario to its one-dimensional and non negative counterpart K_{dist} value:

$$K_{dist_i} = \|k_i - \hat{K}\| \tag{6.4}$$

Here, K_{dist} is the Euclidean distance between each hydraulic conductivity realization K_i and the ensemble average over all K field realizations $\hat{K}$.

Then, I address the low-dimensional representation of each capture outline using two different metrics. First, I use A_{area} to depict the total capture area. In my study, this is expressed as the total number of map pixels inside each capture outline. For the second metric, I use the same strategy as the one used for K_{dist}. Using Eq. 6.5, I obtain a unitary magnitude A_{dist} that expresses the difference between the binary outline of a WHPA outline A_i and the ensemble mean over all all WHPA realizations $\hat{A}$.

$$A_{dist_i} = \|A_i - \hat{A}\| \tag{6.5}$$

Finally, all three feature values are normalized with their respective maximum magnitude. With the above strategy, I can map the relation between each K field realization and respective WHPA outline using a three-dimensional feature space. Hence, each model realization is described by a vector composed of one geological feature and two transport-based quantities that I will use for clustering analysis [107].

6.2.3 Cluster analysis

The next step is to perform a cluster analysis. For this purpose, among the different techniques existing in the literature (see Chapter 2), I utilize a centroid-based strategy. Specifically, I use the k-medoids cluster approach (as implemented in MATLAB [104]), given its robustness to noise and outliers.

In summary, the k-medoids divides the low-dimensional data set into a predefined number of clusters that share a similar Euclidean distance to an initial randomly selected number M of realizations used as cluster centers. Then using the data set of each cluster, a new cluster center

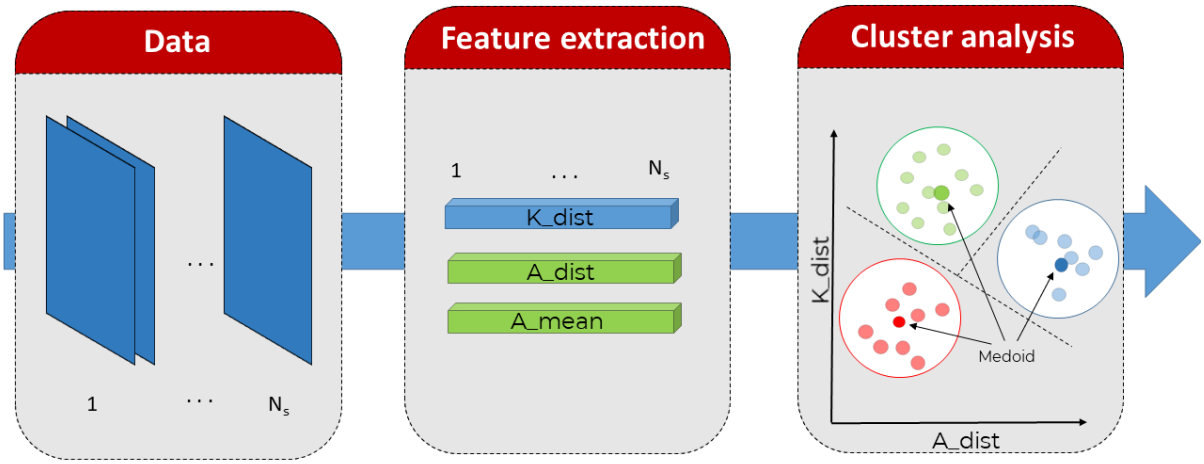

Figure 6.1: Conceptual framework and methodology used to highlight representative hydraulic conductivity fields and corresponding capture outlines to reduce the computational cost of dealing with geological uncertainty during probabilistic WHPA analysis. The low-dimensional representation of each K field scenario and capture outline uses three scalar metrics for feature extraction framework. K_{dist} for conductivity fields, and A_{dist} and A_{area} for the corresponding capture outline. Then, clustering is used to identify cluster centers as condensed set of realizations.

or medoid is suggested by measuring the mean distance among all data points. The process repeats until each center or medoid stabilizes.

In my analysis, the number of clusters (N_s in eq. 6.2) required to represent the desired statistic from the total ensemble is an indicator for the structure of knowledge in the chaos of uncertainty, and a small set of representations ($w_j.j - 1, \cdots N_s$ in eq. 6.2), each one at the center of each cluster, can be used as a condensed, yet comprehensive, set of hypothesis to represent the relevant aspects of uncertainty. Hence, the clustering analysis aggregates large number realizations into a limited set of representative meta-concerns. Each obtained medoid has the same importance, i.e., when aggregating over the obtained subset, I do not implement weight factors [38]. Figure 6.1 shows the conceptual framework explained above.

6.3 Results and Discussion

For the sake of clarity, I implement a numerical example to illustrate the suitability of my methodology using the scenario introduced in Section 5. First, I present the optimal selection, under steady-state conditions, of a subset N_s of hydraulic conductivity fields in order to approximate a computationally more expensive, ensemble-based transient WHPA solution. Then, I solve the multiobjective optimization problem explained in section 5 using the subset N_s previously obtained.

6.3.1 Low-dimensional representation using geological and transport features

First, I present the low-dimensional representation of an ensemble of 2000 K field scenarios. Fig. 6.2 shows the two-dimensional projection of each ensemble realization (light black) ac-

cording to the joint geological (K_{dist}) and transport feature magnitudes (A_{dist} and A_{area}) for WHPA solutions under steady-state conditions.

As can be seen in Fig. 6.2, rather than depicting well-defined clusters in the low-dimensional feature space, the feature extraction formed a densely packed cloud of WHPA realizations. In the case that a groundwater modeler has to select a specified number of representative scenarios in order to describe the overall structure of geological uncertainty, determining the optimal number of clusters becomes not a trivial task. An option for partitioning, is to arbitrarily assign a number of clusters which subdivides the data set, and then to investigate whether the used amount of clusters helps to properly identify enough representative K-field scenarios. For instance, Fig. 6.2 shows the partition of the data cloud using 100 clusters, highlighting in red the medoid of each cluster. Note that most of the selected scenarios are located at the center of each two-dimensional projection. This is mainly an effect of the very high density of realizations in the center. Nevertheless, the cluster analysis was able to recognize ensemble realizations with extreme feature performances such as those with larger WHPA outlines (high A_{area} value) and large A_{dist} magnitudes.

A combination of large magnitudes between both features can be understood as those realizations with overall higher hydraulic conductivity conditions which increase mean groundwater flow velocities, enabling to pump water from larger distances, and so reducing reliability values at those locations far away from the well gallery (i.e., lower time frequency exposition along the year).

Obviously, the greater the number of realizations included in the subset solution N_s, the smaller the error in the outline solution approximation. But, how does the size of N_s affect quantitatively the chosen reliability outline solution? I address this question in the next section.

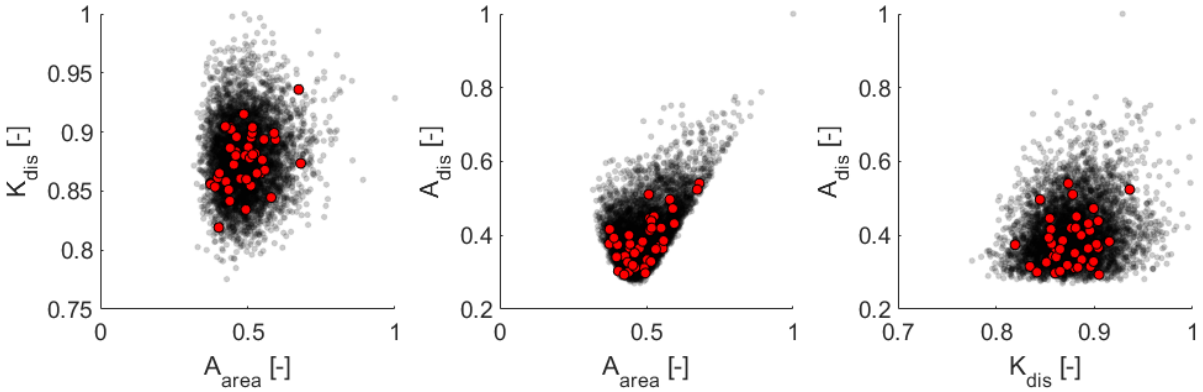

Figure 6.2: Two-dimensional representation of 2000 conditioned K-field realizations. To reduce the high-dimensional representation of each hydraulic conductivity field, three features are used: (1) K_{dist}, (2) A_{dist} and (3) A_{area}. The red dots highlight the medoids of the 100 clusters subdividing the feature solution space.

6.3.2 A well-selected subset of K-field scenarios can approximate the probabilistic ensemble solution for transient WHPA delineation

How does the selected WHPA solution obtained from a much smaller subset (under steady-state) differ from the full ensemble-based WHPA transient delineation? To investigate this

question, I compare in Fig. 6.3 the delineation between the 10%, 50% and 90% geological reliability outlines of the ensemble-based transient WHPA solution (highlighted in white) and the cluster-based WHPA solution (highlighted in red) for subsets N_s of 10 (left), 100 (center) and 300 (right) K field realizations. All shown probabilistic transient delineations are based on a 100% time reliability level.

In Fig. 6.3, each black cross indicates a pumping well location. Although visually perceivable for all reliability outlines, it is better appreciated when observing from left to right, that a clear trade-off exist between increasing the size of N_s (from left to right) and reducing the mismatch between outline resemblances, especially for the 90% geological reliability delineation. It is obvious that the greater the size of a subset N_S, the more geological uncertainty is captured, reducing the mismatch between reliability outlines.

Although this analysis is specific to this case study, it allows me to conclude that the proposed cluster-based methodology is a suitable strategy for selecting representative K field-scenarios for probabilistic WHPA analysis. As can be seen in Fig. 6.3, the proposed geological and transport features (K_{dist}, A_{dist} and A_{area}) can capture the shape of the contour lines for different geological reliability outlines, despite being defined under steady-state conditions. Now, a groundwater modeler can approach a highly expensive probabilistic WHPA transient analysis, as I perform in Chapters 4, using a much smaller set of Monte Carlo realizations chosen from the original ensemble.

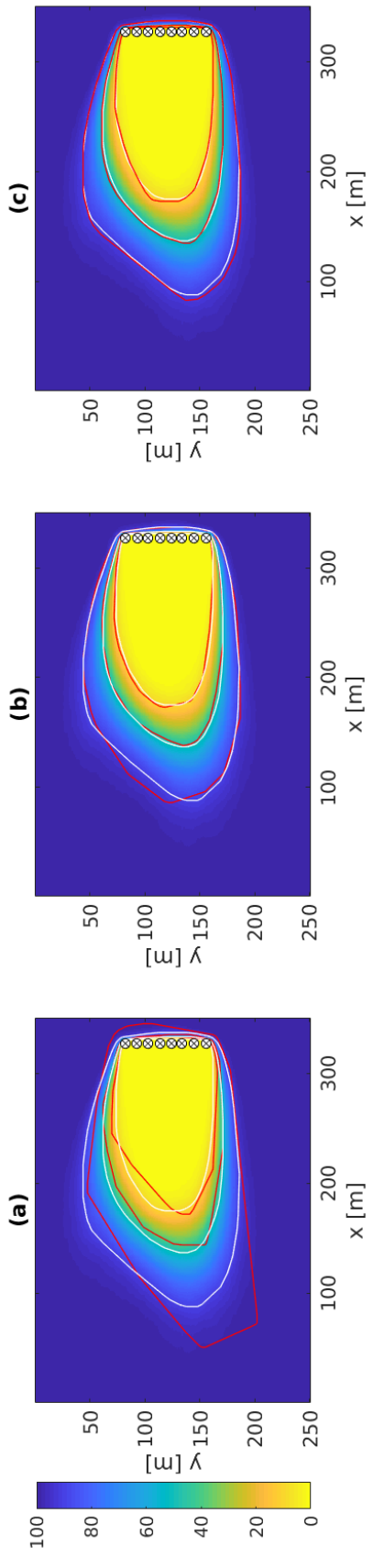

Figure 6.3: Comparison of the 10%, 50% and 90% geological reliability delineations between the ensemble mean solution (white) and the subset of K field realizations (red) using $N_s = 10$ (left), $N_s = 100$ (center) and $N_s = 300$ (right). The background shows the ensemble mean solution

6.3.3 The Approximating higher geological reliability levels requires a larger number N_s of the subset

How does the required number N_s of subsets depend on the chosen geological reliability level? First, in order to answer this question beyond the visual impression from section 6.3.2, I need to define an error measure E_{del} that evaluates the disagreement between different approximation of reliability outlines of same magnitude. One possibility is to compute (within the domain Ω) an error measure E_{del} that depicts the summation of both the area extent that the limited set solution failed to cover (false-negative error) and the excess area consumed without providing any additional protection (false-positive error). I express this comparison with:

$$E_{del}(\mathbf{x}) = \int_{\Omega} (1 - W(\mathbf{x}_i, \theta)) \cdot W(\mathbf{x}_i, \tilde{\theta})\, dx \tag{6.6}$$

By using Eq. 6.6, I define a pragmatic decision rule that links the number N_s of clusters subdividing the three-dimensional feature space with a performance metric that evaluates the resemblance between the ensemble based WHPA probabilistic delineation and its corresponding approximation.

Fig. 6.2 shows the trade-off between the 10% (blue), 50% (red) and 90% (black) geological reliability delineations for sizes of N_s between 1 and 2000. Within this range, a size of $N_s = 1$ indicates that the data cloud (see Fig. 6.2) is represented only by its own medoid located at the center of the data cloud. On the contrary, if $N_s = 2000$ it means that each Monte Carlo realization is directly used.

Overall, the three geological reliability delineations show a similar trade-off behavior: all three show an initial steeper increment in the reduction of E_{del}, which stabilizes when $N_s \approx 100$. Nevertheless, particularly relevant is the milder increase for the 90% geological reliability outline (black) which, in comparison to the 10% and 50% geological reliability outlines, reaches a reduction of E_{del} above 90% only once $N_s = 300$, a size three times greater for N_s when compared to the other two reliability levels ($N_s \approx 100$).

This behavior can be attributed to the difficulty for larger geological reliability delineations to find a proper combination of individual WHPA outlines that matches with the chosen reliability outline. This difficulty is reduced for lower reliability outlines because for positions near the well gallery, there are more opportunities to find the correct combination of individual WHPA delineations that on average approximate the aimed probabilistic outline solution. Thus, if highly accurate analysis requires to approximate transient WHPA transient probabilistic delineations, at high reliability level, there is an obvious need for choosing a larger number of clusters. It seems tat the magical statistical number 30, where many approximations in statistics simplify, is a good rule of thumb: select N_s such that the number of clusters that will represent the lack of reliability, are at least 30 (hence $N_s = 300$ for 100% - 90% = 10%).

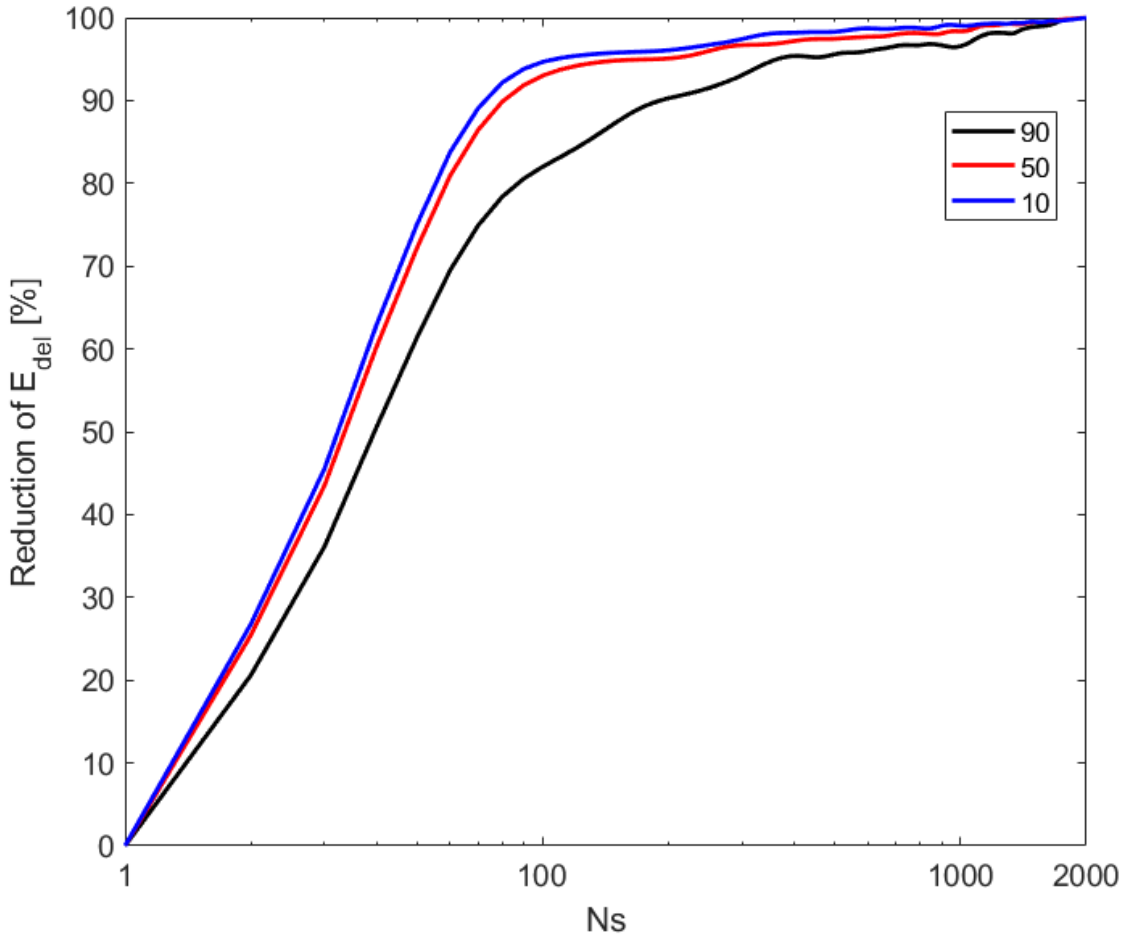

Figure 6.4: Size of N_s for the 10% (blue), 50% (red) and 90% (black) geological reliability delineations

6.3.4 Clustering outperforms the expected solution of subsets of randomly selected WHPA scenarios

How does the performance of my clustering approach compare to a plain Monte Carlo simulation? To give an answer to this question, I perform a resampling (with replacement) of N_s subset solutions comprised of randomly selected WHPA scenarios and compare the results and their scattering to the WHPA solutions obtained by clustering with the same N_s.

Fig. 6.5 shows in gray the speed-accuracy of the trade-offs computation for 10% (left), 50% (center) and 90% (right) geological reliability delineations for sizes of N_s between 1 and 2000. Accuracy is shown as error of delineation $E_{del}*$ (as defined in Eq. 6.6) divided by the respective A_{area} value of a reference solution (as defined in Section 6.2.2). Furthermore, to compare the expected performance between WHPA solutions of randomly selected WHPA realizations and the proposed clustering approach, I show the average over 1000 Monte Carlo repetitions of the resampling (in red) and the unique solution obtained after clustering analysis (in blue).

When inspecting the performance of each random repetition one can see a high variability in the $E_{del}*$ values. This indicates us it is difficult for the generated N_s subset scenarios to accurate approximate the selected WHPA outline. Furthermore, when contrasting the mean performance of the randomized repetition (in red) with the one obtained by clustering (in blue), I can observe a clear split in the performance along the "N_s" dimension.

First, when comparing the expected $E_{del}*$ values and the clustering-based curves for the same size of N_s in the low-CPU-time region ($N_s \leq 100$), for Figs. 6.5b and c, the plain Monte Carlo approach outperforms clustering performance. This behavior could be attributed to the low-variance representation of the ensemble via clustering, which neglects the influence of extremes because it represents each cluster by feature-wise average representatives (i.e., by the medoid WHPA scenarios per cluster).

Second, however, this negative behavior is reversed when $N_s \geq 100$, for all three geological reliability WHPA levels. By using the proposed clustering approach, the aimed approximation would require, for this scenario, only 100 realizations (5% of the total ensemble realizations) to achieve $\leq 5\%$ in $E_{del}*$ values. Of course, is not the best possible combination of ensemble realizations, but clustering reduces the random component of the error. Thus, it becomes an educated selection tool that outperforms the Monte Carlo alternative by obtaining better performance than average. Finally, at about $N_s > 500$, the clustering approach even outperforms every single Monte Carlo repetition.

Overall, I conclude that my clustering approach has an overall greater performance when compared to plain Monte Carlo strategies in order to reduce the computational cost of expensive computational simulations ($N_s \geq 100$). However, this is not the case for rather cheap simulations. One possibility to reduce such negative performance, would be to depict the obtained cluster through the combination of measurements that not only describe the mean cluster characteristics via the centroid, but also to integrate additional information that preserves the overall ensemble structure and distribution (with extremes).

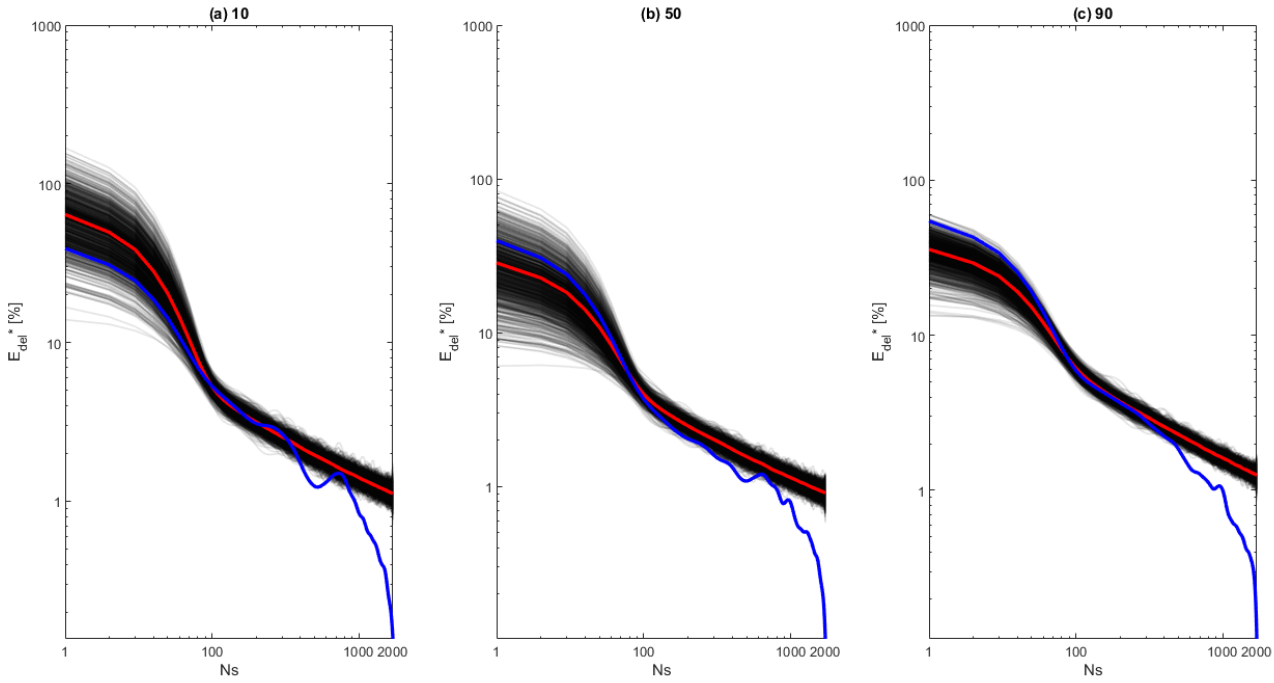

Figure 6.5: Comparison of N_s solutions of size N_s for the 10% (left), 50% (center) and 90% (right) geological reliability delineations between randomly selected realizations (gray), their mean penalty performance (red) and subset solutions obtained via clustering analysis (blue)

6.3.5 Approximate robust optimization using a limited subset N_s

In the previous sections, I discussed how clustering the probabilistic WHPA delineation under steady-state conditions can help to better approximate a computationally more demanding transient probabilistic WHPA solution. Now, I move a step forward and use the approximate subset solutions N_s in the entire MOO exercise as described in Chapter 5. In this analysis, I choose a 50% geological reliability and 100% time reliability.

Fig. 6.6 shows the projection of the resulting Pareto Front onto the shortage-exceedance plane, for the initial time horizon from three distinctive subset numbers N_s. Scenarios I (red), II (blue) and III (black) use N_s values of 10, 100 and 300 K-field realizations, respectively. For each scenario, the green sphere depicts the solution with the shortest distance to the origin of the normalized coordinates highlighted with a white sphere. While the visual evaluation of each WHPA approximation can be seen in Fig. 6.3, the trade-off performance between the size of N_s and the reduction of the E_{del} measure is indicated in Fig. 6.4. In Fig. 6.6, each sphere solution is normalized in an interval [0, 1] that indicates the lowest (0) and highest (1) goal attainment levels found in the current decision period.

Although all three subset solutions resemble transient outlines (see Fig. 6.3), reasonably well, one behavior becomes clear. The better the representation of geological uncertainty with increasing N_s, the lower is the alleged performance in the trade-off between groundwater shortage and exceedance area. This alleged loss of performance, however, is in fact an increased honesty and will shield the decision maker against undesired surprises.

Now, in order to analyze the consequences of saving in computational time, I compare the three scenarios using the best compromise solution (green sphere) between the two considered objectives for the three Pareto Fronts. While the decision to increase the size of N_s is straightforward when comparing the performance between the green spheres of I and II, the decision to increase the size of N_s by another 200% from II to III in order to slightly improve the reduction of E_{del} seems not justifiable. In terms of computational saving, the additional computational effort required in III does not pay off in terms of trade-off performance when comparing the two respective green spheres. In fact, this was already inducted by Fig. 6.4, where the 50% reliability level is approximated well with $N_s = 100$.

In general, my suggested approach opens up new opportunities to optimally reproduce geological uncertainty for further analysis in WHPA analysis such as expensive multiobjective optimization problems while avoiding the corresponding high computational time.

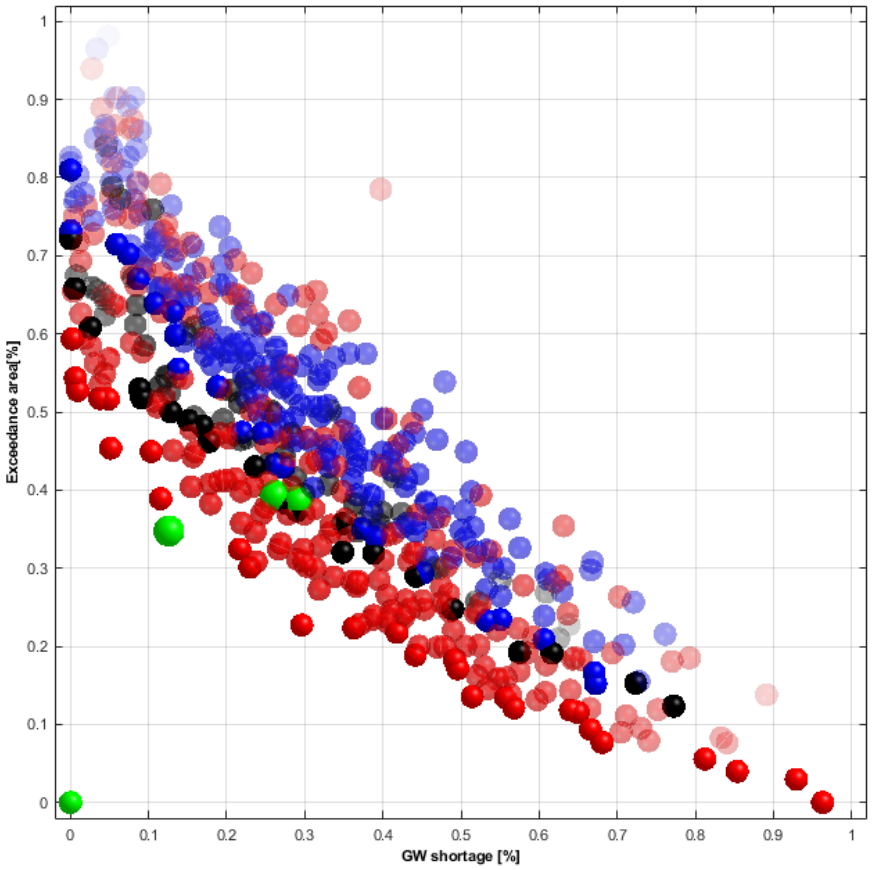

Figure 6.6: Pareto fronts for three distinctive N_s scenarios to address geological uncertainty. The red, blue and black Pareto fronts represent N_s scenarios of size 10 (red), 100 (black) and 300 (blue) Ensemble K-field realizations chosen via clustering, respectively. The green spheres highlight the best compromise solution among the two selected objectives for each Pareto Front depicting the shortest the distance to the origin of the normalized coordinates highlighted with a white sphere.

6.4 Conclusions and Outlook

In this study, I present a methodology that reduces the cost of using Monte Carlo simulation to quantify geological uncertainty in WHPA analysis. My methodology applies cluster analysis to detect a limited subset of hydraulic conductivity fields that best approximate the overall information of a larger ensemble of K scenarios. The classification and selection of each representative model realization is made according to some pixel-wise commonalities among all hydraulic conductivity fields (geological features) and respective WHPA solutions (transport features). In the end, my analysis reduces the required number of hydraulic conductivity fields to estimate the impact of geological uncertainty in (probabilistic) WHPA delineation. In this way, further analysis with high computational cost can be performed, such as transient multi-objective optimization problems.

1. In probabilistic WHPA analysis, the use of clustering becomes a suitable strategy to account for the influence of geological uncertainty while reducing the overall size of the needed ensemble of K field realizations.

2. The high dimensionality of hydraulic conductivity fields and respective WHPA solutions can be reduced into a low-dimensional feature space using three feature metrics, one for geological interpretation and two for depicting transport processes.

3. The number of representative ensemble realizations needed to statistically approximate a chosen reliability outline depends of the aimed reliability magnitude. Of course, the higher the reliability magnitude, greater the required number of ensemble realizations. By clustering, I can obtain a practical approximation of the ensemble result ($\geq 90\%$) using less than 20% of the total ensemble sample.

4. However, for low-CPU-time regions of high geological reliability levels, the proposed approach performed poorly. This behavior can be attributed to the decision of using k-medoids as clustering technique, since it lacks the representation of extremes (because clusters are represented by their medoids) so it underestimates WHPAs to some extent. Nevertheless, the proposed clustering approach reduces the random component of the error, becoming a numerically more reliable alternative than performing randomized Monte Carlo selection strategies.

7. Summary, Conclusions and Outlook

7.1 Summary

The main goal of this thesis is to develop new concepts and methodologies that permit to face the influence of transient groundwater flow in WHPA delineation so that groundwater production remains safe. To fulfill this main objective, I presented four contributions: 1) A new approximate solution to represent transiency based on a dynamic superposition of steady-state flow solutions. 2) Using this approximate solution, I extended the current probabilistic framework in WHPA delineation by integrating transient flow behavior as new dimension. 3) I introduced a new multiobjective optimization framework that allows optimal control of pumping rate schemes in a well gallery in order to stabilize changes in the groundwater abstraction zone triggered by transiency. 4) A clustering technique to reduce the computational cost of addressing geological uncertainties in probabilistic WHPA analysis. The aforementioned contributions have been presented in chapters 3 to 6. A summary of each contribution can be found below. General conclusions are presented in Section 7.2 and finally in Section 7.3 I provided of possible routes for future work.

1. In Chapter 3, I presented a groundwater simulator that is based on a linear(ized) form of the groundwater flow equation. The simulator assumes quasi-stationarity of groundwater storage in order to speed up computational analysis, so that Monte Carlo simulation becomes possible with less computational time restrictions. Using this formulation, I presented a time frequency map representation of WHPAs as well as the probabilistic WHPA solution for WHPAs considering additional uncertainty due to (a) imprecise information regarding aquifer parameters and (b) inexact knowledge about the behavior of the different transient drivers. Both sources of uncertainty are considered via Monte Carlo simulation of time reliability maps.

2. In Chapter 4, using the numerical formulation of Chapter 3, I investigated the effects of transient groundwater flow in WHPA delineation, distinguishing between the influence on deterministic WHPA delineation and the impact on probabilistic WHPA solutions. To represent transient flow conditions, I considered seasonal variations of the following boundary conditions: (I) regional groundwater flow direction, (II) regional strength of the hydraulic gradient, (III) natural groundwater recharge and (IV) pumping rate. The key analysis tools used in this investigation were joint frequency/probability maps that indicate the degree of membership to the area that should be protected.

3. In Chapter 5, I presented a dynamic multiobjective optimization framework that enables the optimal control of well galleries for those situations where the control of the current abstraction zone becomes of paramount importance, such as urban city areas with industrial zones surrounding the current well catchment delineation. I solved the management problem utilizing time-dependent multiobjective optimization (MOO) concepts in order to search for compromise solutions that consider three objectives: 1) to minimize the risk of pumping water from outside a given WHPA, 2) to minimize the gap between groundwater supply and demand and 3) to minimize the involved costs of pumping. Additionally, I address aquifer heterogeneity through scenarios representative of the uncertainty in hydraulic conductivity.

4. In Chapter 6, I proposed a methodology to reduce the computational cost of addressing the Monte Carlo simulation of time reliability maps (Chapter 4) and multiobjective optimization problems addressing the optimal control of well galleries in urban environments (Chapter 5). The proposed framework uses clustering techniques to recognize a subset of model realizations that represents relevant statistics of interest for WHPA analysis under the influence of geological uncertainties. To avoid clustering in a high-dimensional space, I proposed a problem-specific low-dimensional space and appropriate distance metrics for clustering. The distances I suggested are a combination of pixel-wise commonalities between hydraulic conductivity fields (permeability-based representation) and respective WHPA outlines (transport-based representation). My formulation permits the fast but accurate simulation of groundwater transient flow solutions based on limited subsets of hydraulic conductivity fields. To test my machine learning framework, I replicated the problems introduced in Chapters 4 and 5, reducing in both scenarios the number of realizations needed to approximate the previously obtained solutions.

7.2 Conclusions

The first contribution presented a novel numerical formulation for groundwater transient flow simulation which requires only limited code development for being compatible with commercial software such as ModFlow [54] and FeFlow [123]. This numerical tool allows groundwater modelers to simulate transient flow conditions for WHPA delineation under reduced computational times.

The second contribution showed that, transient flow conditions are an important source of uncertainty and that plays an important role when delineating WHPAs. From a global point of view, the major conclusions are: 1) Each considered transient driver results in a distinctive pattern of temporal catchment membership, with the ambient flow direction having the largest influence. 2) Transient analysis improves decision support for probabilistic WHPA delineation. It provides, as additional information, time reliability levels. Now, probabilistic WHPA delineation requires to select reliability levels for time and for geological conditions. 3) Time reliability depicts a different form of risk when contrasted to geological reliability. Lack of time reliability depicts a known risk to the well for a specific time period. The lack of geological reliability depicts lack of knowledge whether the well is at risk. 4) In the presence of uncertain transient and geological conditions, higher time reliability protection represents a cheaper condition compared to high geological reliability levels. 5) The use of time-geological reliability information combined with land use information lead to a better decision making process concerning sensitive locations within a WHPA.

The third contribution found that, multiobjective concepts represent a valid alternative for restricting the time-variant changes of the groundwater capture zone. For scenarios with strong restrictions in expanding a WHPA, the optimal control of the well gallery, can represent a useful alternative to deal with transient flow behavior. Overall, I showed that 1) WHPA programs and pumping management can benefit from multi-objective optimization concepts. The competitiveness among the selected objectives lead to Pareto optimal solutions from which a decision maker can select the well field management strategy that best suits to upcoming management necessities and transient groundwater flow conditions. 2) An optimal pumping strategy that fulfills the overall groundwater demand can effectively reduce the expansion of the abstraction zone beyond the given WHPA when compared to a non-optimal management scheme. Optimal

pumping reduces the influence of the time-variant flow environment by pumping more at those wells that currently yield a smaller influence in the expansion of the current abstraction zone. 3) Optimal pumping stabilizes the dynamic changes of the groundwater abstraction zone, leading to a densely utilized and more static core area that aligns better with the given WHPA. 4) Inappropriate WHPA delineations can not be treated even with my suggested approach. Thus, to address geological uncertainties, it is still preferable to use probabilistic WHPA outlines that are large enough to compensate for uncertainties.

The fourth contribution showed that, clustering techniques are a valid methodology to reduce the cost of using Monte Carlo simulation to quantify geological uncertainty in WHPA analysis. In summary, the major conclusions are: 1) In probabilistic WHPA analysis, clustering can detect a limited subset of hydraulic conductivity fields that best approximate the overall information of a larger ensemble of K scenarios. 2) The high dimensionality of hydraulic conductivity fields and respective WHPA solutions can be reduced into a low-dimensional feature space using three feature metrics, one for geological interpretation and two for depicting transport processes. 3) The number of representative ensemble realizations needed to statistically approximate a chosen reliability outline depends of the aimed reliability magnitude. Of course, the higher the reliability magnitude, the greater the required number of ensemble realizations. However, we can obtain a practical approximation of the ensemble response ($\geq 90\%$) using less than 20% of the total ensemble sample. 4) However, for low-CPU-time regions of high geological reliability levels (e.g., the 90%) the proposed approach performed poorly. This behavior can be attributed to the decision of implementing k-medoids as the chosen clustering technique since it lacks of integrating extremes influence (because clusters are represented by their medoids) so that it underestimates WHPA to some extent. Nevertheless, the proposed clustering approach reduces the random component of the error, avoiding to scatter the performance in the feature space and thus, becoming a numerically more reliable alternative.

7.3 Outlook

Based on the aforementioned conclusions, possibles routes for future research are:

1. In Chapter 3, I presented a formulation that achieves fast but asymptotically valid transient flow simulation. While, the implementation is being directed principally towards confined aquifers, in reality, most aquifers are unconfined. Thus, a straightforward further analysis is to extend the formulation to encompass unconfined aquifer scenarios. This is more challenging, because unconfined aquifers result in non-linear partial differential equations.

2. In Chapter 4, I evaluated the impact of transient flow behavior in WHPA analysis. I assumed constant mean and variance (stationarity process) for the time series behavior of each transient driver. One question remaining is the influence that non-stationarity conditions might have on WHPA delineation and its importance versus geological uncertainty conditions.

3. In Chapter 5, I searched for optimal pumping rate schemes to restrict the influence of transient flow in the actual groundwater abstraction zone. However, when considering uncertainty influencing the optimization formulation I focused on evaluating the influence of aquifer heterogeneity (by aggregating the objective function over a selected ensemble of hydraulic conductivity fields) while assuming an accurate characterization of each transient driver. The next logical step is to include uncertainty in transient flow behavior. This would require looking at fast assimilation and short-term forecasting systems for transient capture zones.

4. In Chapter 6, I investigated how to recognize, using cluster analysis, a subset of ensemble realizations that represent relevant statistics of interest for WHPA analysis under the influence of geological uncertainties. The three metrics used for clustering focused on depicting individual hydraulic conductivity fields. The idea for further research is to include metrics and modified clustering techniques that preserve the representation of extremes. For example, one could investigate how much accuracy is gained by representing the clusters not only by their means (centroids), but by something that preserves the distribution (with extremes) of the entire ensemble.

5. In chapter 6, I assumed, when compared to transient flow behavior, a stronger influence of geological uncertainty conditions driving changes in the probabilistic WHPA solution. This assumption allowed me to cluster probabilistic transient solutions using steady-state WHPA solutions, with little concern about the differences between WHPAs under steady-state and transient flow conditions. In future research, it would be necessary to evaluate how much accuracy is lost when the transient flow influence increases, or whether additional proxies for transient behavior features could be found.

6. Overall, both methodologies (chapter 5 and 6) were evaluated using synthetic model scenarios. Obviously, for practical application, future work should focus on implementing both frameworks into real case scenarios.

Bibliography

[1] A. Rodriguez-Pretelin and W. Nowak. “Unsupervised learning for probabilistic WHPA analysis: A novel approach to identify hydraulic conductivity fields that best approximate geological uncertainties”. In: *Prep* (2020).

[2] W. M. Alley et al. “Flow and storage in groundwater systems”. In: *Science* 296.5575 (2002), pp. 1985–1990.

[3] J. Almedeij and F. Al-Ruwaih. “Periodic behavior of groundwater level fluctuations in residential areas”. In: *Journal of Hydrology* 328.3-4 (2006), pp. 677–684.

[4] A. Alzraiee and L. A. Garcia. “Using cluster analysis of hydraulic conductivity realizations to reduce computational time for Monte Carlo simulations”. In: *Journal of Irrigation and Drainage Engineering* 138.5 (2012), pp. 424–436.

[5] R. Andricevic and P. K. Kitanidis. “Optimization of the pumping schedule in aquifer remediation under uncertainty”. In: *Water Resources Research* 26.5 (1990), pp. 875–885.

[6] R. Azzouz, S. Bechikh, and L. B. Said. *Dynamic Multi-objective Optimization Using Evolutionary Algorithms : A Survey*. Springer, 2017, pp. 31–70.

[7] P. M. Barlow and S. A. Leake. *Streamflow depletion by wells-Understanding and managing the effects of groundwater pumping on streamflow*. 2012, p. 84.

[8] F. Barry et al. “Groundwater flow and capture zone analysis of the Central Passaic River Basin, New Jersey”. In: *Environmental Geology* 56.8 (2009), pp. 1593–1603.

[9] J. W. Bell et al. “Monitoring aquifer-system response to groundwater pumping and artificial recharge”. In: *First Break* 26.8 (2008), pp. 85–91.

[10] A. Bellin, G. Dagan, and Y. Rubin. “The Impact of Head Gradient Transients on Transport in Heterogeneous Formations: Application to the Borden Site”. In: *Water resources research* 32.9 (1996), pp. 2705–2713.

[11] R. E. Bellman. *Adaptive control processes: a guided tour*. Princeton university press, 2015, p. 276.

[12] J. M. Bishop. “Stochastic searching networks”. In: *1989 First IEE International Conference on Artificial Neural Networks, (Conf. Publ. No. 313)* (1989), pp. 329–331.

[13] E. Borgonovo and E. Plischke. “Sensitivity analysis: A review of recent advances”. In: *European Journal of Operational Research* 248.3 (2016), pp. 869–887.

[14] C. Boutsidis and M. W. Mahoney. “Unsupervised Feature Selection for the k-means Clustering Problem”. In: *Advances in Neural Information Processing Systems* (2009), pp. 153–161.

[15] C. V. Campi and J. E. Outlaw Jr. “Stochastic Approach To Delineating Wellhead Protection Areas”. In: *Journal of Water Resources Planning and Management* 124.August (1998), pp. 199–209.

[16] F. Campolongo, J. Cariboni, and A. Saltelli. “An effective screening design for sensitivity analysis of large models”. In: *Environmental Modelling and Software* 22.10 (2007), pp. 1509–1518.

[17] A. Castelletti, F. Pianosi, and R. Soncini-Sessa. “Stochastic and robust control of water resource systems: Concepts, methods and applications”. In: *System identification, environmental modelling, and control system design* (2012), pp. 383 –401.

[18] O. A. Cirpka and S. Attinger. “Effective dispersion in heterogeneous media under random transient flow conditions”. In: *Water Resources Research* 39.9 (2003), pp. 1–15.

[19] M. Clerc. *Particle swarm optimization*. John Wiley & Sons, 2010, p. 243.

[20] Carlos A Coello Coello, Gary B Lamont, David A Van Veldhuizen, et al. *Evolutionary algorithms for solving multi-objective problems*. Springer, 2007, p. 800.

[21] C. A. Coello Coello, G. T. Pulido, and M. S. Lechuga. “Handling multiple objectives with particle swarm optimization”. In: *IEEE Transactions on Evolutionary Computation* 8.3 (2004), pp. 256–279.

[22] C. A. Coello Coello and M. Reyes-Sierra. “Multi-Objective Particle Swarm Optimizers: A Survey of the State-of-the-Art”. In: *International Journal of Computational Intelligence Research* 2.3 (2006), pp. 287–308.

[23] T. D. Conlon et al. *Ground-Water Hydrology of the Willamette Basin, Oregon*. Tech. rep. USGS, 2005, pp. 48–59.

[24] R. Cyriac and A. K. Rastogi. “Optimization of pumping policy using coupled finite element-particle swarm optimization modelling”. In: *ISH Journal of Hydraulic Engineering* 22.1 (2016), pp. 88–99.

[25] T. Dalgleish et al. “A "Random-Walk" Solute Transport Model for Selected Groundwater Quality Evaluations”. In: *Journal of Experimental Psychology: General* 136.1 (2007), pp. 23–42.

[26] A. Davidson et al. “Water safety plans: Managing drinking-water quality from catchment to consumer”. In: *Journal of environmental health* (2005), p. 244.

[27] K. Deb. “An investigation of niche and species formation in genetic function optimization”. In: *ICGA’89* (1989), pp. 42–50.

[28] K. Deb et al. “A fast and elitist multiobjective genetic algorithm: NSGA-II”. In: *IEEE Transactions on Evolutionary Computation* 6.2 (2002), pp. 182–197.

[29] Kalyanmoy Deb. “Introducing Robustness in Multi-Objective Optimization KalyanmoyDeb”. In: 14.4 (2006), pp. 463–494.

[30] J. E. Doherty and R. J. Hunt. *Approaches to highly parameterized inversion: a guide to using PEST for groundwater-model calibration*. Tech. rep. US Department of the Interior, US Geological Survey, 2010, p. 59.

[31] P. A. Domenico and F. W. Schwarz. *Physical and chemical hydrogeology, 2nd ed., John Wiley & Sons, Inc.*. 1998, pp. 32–60.

[32] M. Dorigo. “Optimization, learning and natural algorithms”. PhD thesis. Politecnico di Milano, 1992, p. 140.

[33] DVGW. *Richtlinien für Trinkwasserschutzgebiete; Teil 1: Schutzge- biete für Grundwasser. Deutscher Verein des Gas- und Wasserfaches e.V*. Tech. rep. Bonn, Germany., 2006.

[34] A. M. Elfeki, G. Uffink, and S. Lebreton. “Influence of temporal fluctuations and spatial heterogeneity on pollution transport in porous media”. In: *Hydrogeology Journal* 20.2 (2012), pp. 283–297.

[35] R. Enzenhoefer, T. Bunk, and W. Nowak. “Nine steps to risk-informed wellhead protection and management: a case study”. In: *Ground Water* 52 (2014), pp. 161–174.

[36] R. Enzenhoefer, W. Nowak, and R. Helmig. “Probabilistic exposure risk assessment with advective-dispersive well vulnerability criteria”. In: *Advances in Water Resources* 36 (2012), pp. 121–132.

[37] R. Enzenhöfer. “Heft 229 Rainer Enzenhöfer Risk Quantification and Management in Water Production and Supply Systems”. PhD thesis. Universität Stuttgart, 2013, p. 249.

[38] G. van Essen et al. “Robust Waterflooding Optimization of Multiple Geological Scenarios”. In: *SPE Journal* 14.1 (2009), pp. 24–27.

[39] S. Evers and D. N. Lerner. “How uncertain is our estimate of a wellhead protection zone?” In: *Ground water* 36.1 (1998), pp. 49–57.

[40] M. Farina, K. Deb, and P. Amato. “Dynamic Multiobjective Optimization Problems : Test Cases , Approximations , and Applications”. In: 8.5 (2004), pp. 425–442.

[41] A. D. Festger and G. R Walter. “The capture efficiency map: the capture zone under time-varying flow”. In: *Ground Water* 40.6 (2002), pp. 619–628.

[42] L. Feyen et al. “Bayesian methodology for stochastic capture zone delineation incorporating transmissivity measurements and hydraulic head observations”. In: *Journal of hydrology* 271.1-4 (2003), pp. 156–170.

[43] O. L. Franke et al. “Estimating areas contributing recharge to wells”. In: *USGS Circular* 1174 (1998), pp. 1–14.

[44] H. J. W. M. H. Franssen, F. Stauffer, and W. Kinzelbach. “Impact of spatio-temporally variable recharge on the characterization of well capture zones”. In: 277 (2002), pp. 470–477.

[45] S. Franzetti and A. Guadagnini. “Probabilistic estimation of well catchments in heterogeneous aquifers”. In: *Journal of Hydrology* 174.1-2 (1996), pp. 149–171.

[46] E. O. Frind, D. S. Muhammad, and J. W. Molson. “Delineation of Three-Dimensional Well Capture Zones for Complex Multi-Aquifer Systems”. In: *Ground Water* 40.6 (2002), pp. 586–598.

[47] J. Fritz, W. Nowak, and I. Neuweiler. “Application of FFT-based Algorithms for Large-Scale Universal Kriging Problems”. In: *Mathematical Geosciences* 41.5 (2009), pp. 509–533.

[48] S. Gaur et al. “Multiobjective fuzzy optimization for sustainable groundwater management using particle swarm optimization and analytic element method”. In: *Hydrological Processes* 29.19 (2015), pp. 4175–4187.

[49] L. W. Gelhar. *Stochastic subsurface hydrology: Prentice-Hall, Inc.* 1993, p. 390.

[50] D. J. Goode and L. F. Konikow. “Apparent dispersion in transient groundwater flow”. In: *Water Resources Research* 26.10 (1990), pp. 2339–2351.

[51] J. Van der Gun. *Groundwater and Global Change: Trends, Opportunities and Challenges*. UNESCO, SIDE Publications Series, 2012, p. 44.

[52] D. Hadka and P. Reed. “Borg: An Auto-Adaptive Many-Objective Evolutionary Computing Framework”. In: *Evolutionary Computation* 21.2004 (2012), pp. 1–30.

[53] H. M. Haitjema. *Analytical element modeling of groundwater flow*. Elsevier, 1995, p. 394.

[54] A. W. Harbaugh. "MODFLOW-2005, The U. S. Geological Survey Modular Ground-Water Model: the Ground-Water Flow Process". In: *US Geological Survey Reston* 92.3 (2005), p. 134.

[55] M. Helbig, K. Deb, and A. P. Engelbrecht. "Key Challenges and Future Directions of Dynamic Multi-objective Optimisation". In: *Proceedings of the IEEE Congress on Evolutionary Computation* (2016), pp. 1256–1261.

[56] M. Helbig and A. P. Engelbrecht. "Challenges of dynamic multi-objective optimisation". In: *Proceedings - 1st BRICS Countries Congress on Computational Intelligence, BRICS-CCI 2013* (2013), pp. 254–261.

[57] J. Hoffmann et al. "Seasonal subsidence and rebound in Las Vegas Valley, Nevada, observed by synthetic aperture radar interferometry". In: *Water Resources Research* 37.6 (2001), pp. 1551–1566.

[58] J. Holland. "Adaptation in natural and artificial systems: an introductory analysis with application to biology". In: *Control and artificial intelligence* (1975).

[59] C. Huang and A. S. Mayer. "Pump-and-treat optimization using well locations and pumping rates as decision variables". In: 33.5 (1997), pp. 1001–1012.

[60] S. J. Jeffrey et al. "Simulating water-quality trends in public-supply wells in transient flow systems". In: *Ground water* 52 (2014), pp. 53–62.

[61] K. L. Katsifarakis, I. A. Nikoletos, and C. Stavridis. "Minimization of Transient Groundwater Pumping Cost - Analytical and Practical Solutions". In: *Water Resources Management* (2017), pp. 1–17.

[62] L. Kaufman and P. J. Rousseeuw. *Finding groups in data: an introduction to cluster analysis*. John Wiley & Sons, 1990, p. 342.

[63] W. Kinzelbach. "The random walk method in pollutant transport simulation". In: *Groundwater flow and quality modelling* (1988), pp. 227–245.

[64] W. Kinzelbach, M. Marburger, and W. Chiang. "Determination of groundwater catchment areas in two and three spatial dimensions". In: *Journal of Hydrology* 134.1-4 (1992), pp. 221–246.

[65] S. Kirkpatrick, C. D. Gelatt, and M. P. Vecchi. "Optimization of Simulated Annealing". In: *science* 220.4598 (1983), pp. 671–680.

[66] M. van Leeuwen et al. "Stochastic determination of well capture zones". In: *Water Resources Research* 34.9 (1998), pp. 2215–2223.

[67] S. Leray et al. "Temporal evolution of age data under transient pumping conditions". In: *Journal of Hydrology* 511 (2014), pp. 555–566.

[68] D. N. Lerner. "Well Catchments and Time-of-Travel Zones in Aquifers With Recharge". In: *Water Resources Research* 28.10 (1992), pp. 2621–2628.

[69] J. Li et al. "Stochastic goal programming based groundwater remediation management under human-health-risk uncertainty". In: *Journal of Hazardous Materials* 279 (2014), pp. 257–267.

[70] A. Libera, F. P. J. de Barros, and A. Guadagnini. “Influence of pumping operational schedule on solute concentrations at a well in randomly heterogeneous aquifers”. In: *Journal of Hydrology* 546 (2017), pp. 490–502.

[71] A. Libera et al. “Solute concentration at a well in non-Gaussian aquifers under constant and time-varying pumping schedule”. In: *Journal of Contaminant Hydrology* 205 (2017), pp. 37–46.

[72] R. T. Marler and J. S. Arora. “Survey of multi-objective optimization methods for engineering”. In: *Structural and Multidisciplinary Optimization* 26.6 (2004), pp. 369–395.

[73] Beatrice S. Marti. “Real-time management and control of groundwater flow field and quality”. PhD thesis. 2014, p. 113.

[74] J. P. Masterson, D. A. Walter, and D. R. LeBlanc. “Transient analysis of the source of water to wells: Cape Cod, Massachusetts”. In: *Ground water* 42.1 (2004), pp. 126–134.

[75] Mi. Mavrovouniotis, C. Li, and S. Yang. “A survey of swarm intelligence for dynamic optimization : Algorithms and applications”. In: *Swarm and Evolutionary Computation* 33.January (2017), pp. 1–17.

[76] D. C. Mays and R. M. Neupauer. “Plume spreading in groundwater by stretching and folding”. In: *Water Resources Research* 48.May (2012), pp. 1–10.

[77] B. Minasny and A. B. McBratney. “The Matérn function as a general model for soil variograms”. In: *Geoderma* 128.3-4 SPEC. ISS. (2005), pp. 192–207.

[78] Max D Morris. “Factorial sampling plans for preliminary computational experiments”. In: *Technometrics* 33.2 (1991), pp. 161–174.

[79] P. Moscato et al. *On Evolution, Search, Optimization, Genetic Algorithms and Martial Arts Towards Memetic Algorithms Pablo Moscato Caltech Concurrent Computation Program*. Tech. rep. 1989, p. 67.

[80] M. Musa and M. W. Kemblowski. “Transient capture zone for a single well”. In: *Ground Water* 34.1 (1996), pp. 168–170.

[81] R. M. Neupauer and J. L. Wilson. “Backward probabilistic model of groundwater contamination in non-uniform and transient flow”. In: *Advances in Water Resources* 25.7 (2002), pp. 733–746.

[82] A. T. Nguyen and S. Reiter. “A performance comparison of sensitivity analysis methods for building energy models”. In: *Building Simulation* 8.6 (2015), pp. 651–664.

[83] H. Niu et al. “Analytical Study of Unsteady Nested Groundwater Flow Systems”. In: *Mathematical Problems in Engineering* 2015 (2015), pp. 1–9.

[84] W. Nowak. “Measures of Parameter Uncertainty in Geostatistical Estimation and Geostatistical Optimal Design”. In: *Mathematical Geosciences* 42.2 (2010), pp. 199–221.

[85] W. Nowak et al. “Probability density functions of hydraulic head and velocity in three-dimensional heterogeneous porous media”. In: *Water Resources Research* 44.8 (2008), pp. 1–15.

[86] A. N. Piscopo, J. R. Kasprzyk, and R. M. Neupauer. “An iterative approach to multi-objective engineering design: Optimization of engineered injection and extraction for enhanced groundwater remediation”. In: *Environmental Modelling & Software* 69 (2015), pp. 253–261.

[87] E. T. Psarropoulou and G. P. Karatzas. “Transient groundwater modelling with spatio-temporally variable fluxes in a complex aquifer system: new approach in defining boundary conditions for a transient flow model”. In: *Civil Engineering and Environmental Systems* 29.1 (2012), pp. 1–21.

[88] T. S. Ramanarayanan, D. E. Storm, and M. D. Smolen. “Seasonal Pumping Variation Effects on Wellhead Protection Area Delineation”. In: *Water Resources Bulletin* 31.3 (1995), pp. 421–430.

[89] I. Rechenberg. “Cybernetic solution path of an experimental problem”. In: *Royal Aircraft Establishment Library Translation 1122* (1965).

[90] T. E. Reilly, F. O. Lehn, and G. D. Bennett. *The principle of superposition and its application in ground-water hydraulics*. Tech. rep. 1984.

[91] T. E. Reilly and D. W. Pollock. “Sources of water to wells for transient cyclic systems”. In: *Ground Water* 34.6 (1996), pp. 979–988.

[92] A. Rein et al. “Influence of temporally variable groundwater flow conditions on point measurements and contaminant mass flux estimations”. In: *Journal of Contaminant Hydrology* 108.3-4 (2009), pp. 118–133.

[93] G. Rock and H. Kupfersberger. “Numerical delineation of transient capture zones”. In: *Journal of Hydrology* 269.3-4 (2002), pp. 134–149.

[94] A. Rodriguez-Pretelin and W. Nowak. “Dynamic re-distribution of pumping rates in well fields to counter transient problems in groundwater production”. In: *Groundwater for Sustainable Development* 8 (2019), pp. 606–616.

[95] A. Rodriguez-Pretelin and W. Nowak. “Integrating transient behavior as a new dimension to WHPA delineation”. In: *Advances in Water Resources* 119 (2018), pp. 178–187.

[96] P. Salamon and D. Fern. “On modeling contaminant transport in complex porous media using random walk particle tracking”. PhD thesis. Universidad Técnica de Valencia, 2006, pp. 1–146.

[97] A. Saltelli et al. *Global sensitivity analysis: the primer*. John Wiley & Sons, 2008, p. 292.

[98] A. Saltelli et al. *Sensitivity analysis in practice: a guide to assessing scientific models*. John Wiley & Sons, 2004, p. 219.

[99] X. Sanchez-Vila and D. Fernández-Garcia. “Debates—Stochastic subsurface hydrology from theory to practice: Why stochastic modeling has not yet permeated into practitioners?” In: *Water Resources Research* 52.12 (2016), pp. 9246–9258.

[100] A. E. Scheidegger. “Statistical hydrodynamics in porous media”. In: *Journal of Applied Physics* 25.8 (1954), pp. 997–1001.

[101] C. Scheidt and J. Caers. “Representing spatial uncertainty using distances and kernels”. In: *Mathematical Geosciences* 41.4 (2009), pp. 397–419.

[102] C. Scheidt, J. Caers, and Others. “Uncertainty Quantification in Reservoir Performance Using Distances and Kernel Methods–Application to a West Africa Deepwater Turbidite Reservoir”. In: *Society of Petroleum Engineers* 14.04 (2009), pp. 680–692.

[103] O. Schmoll et al. *WHO Drinking-water Quality Series Protecting Groundwater for Health Protecting Groundwater for Health*. Vol. 1843390795. 2006.

[104] G. A. F. Seber. *Multivariate Observations*. John Wiley & Sons, 1984, p. 686.

[105] S. E. Serrano and S. R. Workman. "Modeling transient stream/aquifer interaction with the non-linear Boussinesq equation and its analytical solution". In: *Journal of Hydrology* 206.l 998 (1998), pp. 245–255.

[106] S. E. Serrano et al. "Models of nonlinear stream aquifer transients". In: *Journal of Hydrology* 336.1-2 (2007), pp. 199–205.

[107] M. G. Shirangi and L. J. Durlofsky. "A general method to select representative models for decision making and optimization under uncertainty". In: *Computers and Geosciences* 96.February (2016), pp. 109–123.

[108] M. G. Shirangi and T. Mukerji. "Retrospective Optimization of Well Controls Under Uncertainty Using Kernel Clustering". In: *25th Annual SCRF Meeting* January (2012), pp. 1–36.

[109] M. R. Sierra and C. A. Coello Coello. "Improving PSO-Based Multi-objective Optimization Using Crowding, Mutation and E-Dominance". In: *Lecture Notes in Computer Science* 3410 (2005), pp. 505–519.

[110] A. Singh. "Simulation and Optimization Modeling for the Management of Groundwater Resources . II : Combined Applications". In: *Journal of Irrigation and Drainage Engineering* 140.4 (2014), pp. 1–9.

[111] A. Singh, C. M. Bürger, and O. A. Cirpka. "Optimized Sustainable Groundwater Extraction Management: General Approach and Application to the City of Lucknow, India". In: *Water Resources Management* 27.12 (2013), pp. 4349–4368.

[112] K. P. Singh, S. Gupta, and D. Mohan. "Evaluating influences of seasonal variations and anthropogenic activities on alluvial groundwater hydrochemistry using ensemble learning approaches". In: *Journal of Hydrology* 511 (2014), pp. 254–266.

[113] R. C. Smith. *Uncertainty quantification: theory, implementation, and applications*. SIAM, 2013, p. 400.

[114] M. Sobol. "Sensitivity estimates for nonlinear mathematical models". In: *Mathematical Modeling and Computational experiment* 1.4 (1993), pp. 407–414.

[115] M. R. Sousa, E. O. Frind, and D. L. Rudolph. "An integrated approach for addressing uncertainty in the delineation of groundwater management areas". In: *Journal of Contaminant Hydrology* 148 (2013), pp. 12–24.

[116] F. Stauffer, H. J. W. M. H. Franssen, and W. Kinzelbach. "Semianalytical uncertainty estimation of well catchments: Conditioning by head and transmissivity data". In: *Water Resources Research* 40.8 (2004), pp. 1–11.

[117] F. Stauffer et al. "Delineation of Source Protection Zones Using Statistical Methods". In: *Water Resources Management* 19.2 (2005), pp. 163–185.

[118] M. Steinbach, L. Ertöz, and V. Kumar. "The Challenges of Clustering High Dimensional Data". In: *New directions in statistical physics* (2004), pp. 273–309.

[119] R. S. Sutton and A. G. Barto. *Reinforcement learning: An introduction*. Vol. 9. 5. Cambridge, MA: MIT Press, 2011, p. 1054.

[120] E. G Talbi. *Metaheuristics: from design to implementation*. John Wiley & Sons, 2009, p. 624.

[121] L. R. Townley. “The response of aquifers to periodic forcing”. In: *Advances in Water Resources* 18.3 (1995), pp. 125–146.

[122] M. G. Trefry. “Periodic forcing in composite aquifers”. In: *Advances in Water Resources* 22.6 (1999), pp. 645–656.

[123] M. G. Trefry and C. Muffels. “FEFLOW: a Finite-Element Ground Water Flow and Transport Modeling Tool”. In: *Groundwater* 45.5 (2007), pp. 525–528.

[124] US EPA. “Guidelines for delineation of well-head protection areas, EPA - 440/5-93-001 ed.; 1993.” In: EPA-440/5-93-001 (1993).

[125] M. D. Varljen and J. M. Shafer. “Assesment of uncertainty in time-related capture zones using conditional simulation of hydraulic conductivity”. In: *Ground Water* 29.5 (1991), pp. 737–748.

[126] S. Vassolo, W. Kinzelbach, and W. Schäfer. “Determination of a well head protection zone by stochastic inverse modelling”. In: *Journal of Hydrology* 206.3-4 (1998), pp. 268–280.

[127] W. E. Walker et al. “A Conceptual Basis for Uncertainty Management in Model-Based Decision Support”. In: *Integrated assessment* 4.1 (2003), pp. 5–17.

[128] H. Wang et al. “Optimal Well Placement Under Uncertainty Using a Retrospective Optimization Framework”. In: *SPE Journal* 17.01 (2012), pp. 112–121.

[129] D. Wirtz and W. Nowak. “The rocky road to extended simulation frameworks covering uncertainty, inversion, optimization and control”. In: *Environmental Modelling and Software* 93 (2017), pp. 180–192.

[130] I. H. Witten et al. *Data Mining: Practical machine learning tools and techniques*. Morgan Kaufmann, 2016, p. 560.

[131] C. Xu and G. Gertner. “Understanding and comparisons of different sampling approaches for the Fourier Amplitudes Sensitivity Test (FAST)”. In: *Computational Statistics and Data Analysis* 55.1 (2011), pp. 184–198.

Lebenslauf

Persönliche Daten

Name:	Abelardo Rodriguez Pretelin
Geburtsdatum:	16.04.1985
Geburtsort:	Mexiko Stadt

Bildungsweg

04/2015 - 02/2020	Promotion im Rahmen des Exzellenzcluster *SimTech*, Universität Stuttgart
10/2010 - 01/2013	Master of Science: Water Resources Engineering and Management , Universität Stuttgart
06/2004 - 06/2009	Bachelor Bauingenieurwesen, Universidad Veracruzana, Veracruz, Mexiko

Arbeitserfahrung

01/2019 - Aktuell	Direktor für Eisenbahnstatistik am Secretaría de Comunicaciones y Transportes / Agencia Reguladora del Transporte Ferroviario (Ministerium für Kommunikations und Verkehr, Regulierungsbehörde für den Eisenbahnverkehr)
08/2015 - 12/2018	Wissenschaftlicher Mitarbeiter am Institut für Wasser- und Umweltsystemmodellierung der Universität Stuttgart, Lehrstuhl für Stochastische Simulation und Sicherheitsforschung für Hydrosysteme
04/2013 - 08/2014	Geotechnischer Ingenieur, Geotest Supervisión técnica

Institut für Wasser- und Umweltsystemmodellierung
Universität Stuttgart

Pfaffenwaldring 61
70569 Stuttgart (Vaihingen)
Telefon (0711) 685 - 60156
Telefax (0711) 685 - 51073
E-Mail: iws@iws.uni-stuttgart.de
http://www.iws.uni-stuttgart.de

Verzeichnis der Mitteilungshefte

5 Plate, Erich: *Beitrag zur Bestimmung der Windgeschwindigkeitsverteilung in der durch eine Wand gestörten bodennahen Luftschicht*, und
Röhnisch, Arthur; Marotz, Günter: *Neue Baustoffe und Bauausführungen für den Schutz der Böschungen und der Sohle von Kanälen, Flüssen und Häfen; Gestehungskosten und jeweilige Vorteile*, sowie
Unny, T.E.: *Schwingungsuntersuchungen am Kegelstrahlschieber*, 1967

6 Seiler, Erich: *Die Ermittlung des Anlagenwertes der bundeseigenen Binnenschiffahrtsstraßen und Talsperren und des Anteils der Binnenschiffahrt an diesem Wert*, 1967

7 *Sonderheft anläßlich des 65. Geburtstages von Prof. Arthur Röhnisch mit Beiträgen von* Benk, Dieter; Breitling, J.; Gurr, Siegfried; Haberhauer, Robert; Honekamp, Hermann; Kuz, Klaus Dieter; Marotz, Günter; Mayer-Vorfelder, Hans-Jörg; Miller, Rudolf; Plate, Erich J.; Radomski, Helge; Schwarz, Helmut; Vollmer, Ernst; Wildenhahn, Eberhard; 1967

8 Jumikis, Alfred: *Beitrag zur experimentellen Untersuchung des Wassernachschubs in einem gefrierenden Boden und die Beurteilung der Ergebnisse*, 1968

9 Marotz, Günter: *Technische Grundlagen einer Wasserspeicherung im natürlichen Untergrund*, 1968

10 Radomski, Helge: *Untersuchungen über den Einfluß der Querschnittsform wellenförmiger Spundwände auf die statischen und rammtechnischen Eigenschaften*, 1968

11 Schwarz, Helmut: *Die Grenztragfähigkeit des Baugrundes bei Einwirkung vertikal gezogener Ankerplatten als zweidimensionales Bruchproblem*, 1969

12 Erbel, Klaus: *Ein Beitrag zur Untersuchung der Metamorphose von Mittelgebirgsschneedecken unter besonderer Berücksichtigung eines Verfahrens zur Bestimmung der thermischen Schneequalität*, 1969

13 Westhaus, Karl-Heinz: *Der Strukturwandel in der Binnenschiffahrt und sein Einfluß auf den Ausbau der Binnenschiffskanäle*, 1969

14 Mayer-Vorfelder, Hans-Jörg: *Ein Beitrag zur Berechnung des Erdwiderstandes unter Ansatz der logarithmischen Spirale als Gleitflächenfunktion*, 1970

15 Schulz, Manfred: *Berechnung des räumlichen Erddruckes auf die Wandung kreiszylindrischer Körper*, 1970

16 Mobasseri, Manoutschehr: *Die Rippenstützmauer. Konstruktion und Grenzen ihrer Standsicherheit*, 1970

17 Benk, Dieter: *Ein Beitrag zum Betrieb und zur Bemessung von Hochwasserrückhaltebecken*, 1970

18 Gàl, Attila: *Bestimmung der mitschwingenden Wassermasse bei überströmten Fischbauchklappen mit kreiszylindrischem Staublech*, 1971, vergriffen

19 Kuz, Klaus Dieter: *Ein Beitrag zur Frage des Einsetzens von Kavitationserscheinungen in einer Düsenströmung bei Berücksichtigung der im Wasser gelösten Gase*, 1971, vergriffen

20 Schaak, Hartmut: *Verteilleitungen von Wasserkraftanlagen*, 1971

21 *Sonderheft zur Eröffnung der neuen Versuchsanstalt des Instituts für Wasserbau der Universität Stuttgart mit Beiträgen von* Brombach, Hansjörg; Dirksen, Wolfram; Gàl, Attila; Gerlach, Reinhard; Giesecke, Jürgen; Holthoff, Franz-Josef; Kuz, Klaus Dieter; Marotz, Günter; Minor, Hans-Erwin; Petrikat, Kurt; Röhnisch, Arthur; Rueff, Helge; Schwarz, Helmut; Vollmer, Ernst; Wildenhahn, Eberhard; 1972

22 Wang, Chung-su: *Ein Beitrag zur Berechnung der Schwingungen an Kegelstrahlschiebern*, 1972

23 Mayer-Vorfelder, Hans-Jörg: *Erdwiderstandsbeiwerte nach dem Ohde-Variationsverfahren*, 1972

24 Minor, Hans-Erwin: *Beitrag zur Bestimmung der Schwingungsanfachungsfunktionen überströmter Stauklappen*, 1972, vergriffen

25 Brombach, Hansjörg: *Untersuchung strömungsmechanischer Elemente (Fluidik) und die Möglichkeit der Anwendung von Wirbelkammerelementen im Wasserbau*, 1972, vergriffen

26 Wildenhahn, Eberhard: *Beitrag zur Berechnung von Horizontalfilterbrunnen*, 1972

27 Steinlein, Helmut: *Die Eliminierung der Schwebstoffe aus Flußwasser zum Zweck der unterirdischen Wasserspeicherung, gezeigt am Beispiel der Iller*, 1972

28 Holthoff, Franz Josef: *Die Überwindung großer Hubhöhen in der Binnenschiffahrt durch Schwimmerhebewerke*, 1973

29 Röder, Karl: *Einwirkungen aus Baugrundbewegungen auf trog- und kastenförmige Konstruktionen des Wasser- und Tunnelbaues*, 1973

30 Kretschmer, Heinz: *Die Bemessung von Bogenstaumauern in Abhängigkeit von der Talform*, 1973

31 Honekamp, Hermann: *Beitrag zur Berechnung der Montage von Unterwasserpipelines*, 1973

32 Giesecke, Jürgen: *Die Wirbelkammertriode als neuartiges Steuerorgan im Wasserbau*, und Brombach, Hansjörg: *Entwicklung, Bauformen, Wirkungsweise und Steuereigenschaften von Wirbelkammerverstärkern*, 1974

33 Rueff, Helge: *Untersuchung der schwingungserregenden Kräfte an zwei hintereinander angeordneten Tiefschützen unter besonderer Berücksichtigung von Kavitation*, 1974

34 Röhnisch, Arthur: *Einpreßversuche mit Zementmörtel für Spannbeton - Vergleich der Ergebnisse von Modellversuchen mit Ausführungen in Hüllwellrohren*, 1975

35 *Sonderheft anläßlich des 65. Geburtstages von Prof. Dr.-Ing. Kurt Petrikat mit Beiträgen von*: Brombach, Hansjörg; Erbel, Klaus; Flinspach, Dieter; Fischer jr., Richard; Gàl, Attila; Gerlach, Reinhard; Giesecke, Jürgen; Haberhauer, Robert; Hafner Edzard; Hausenblas, Bernhard; Horlacher, Hans-Burkhard; Hutarew, Andreas; Knoll, Manfred; Krummet, Ralph; Marotz, Günter; Merkle, Theodor; Miller, Christoph; Minor, Hans-Erwin; Neumayer, Hans; Rao, Syamala; Rath, Paul; Rueff, Helge; Ruppert, Jürgen; Schwarz, Wolfgang; Topal-Gökceli, Mehmet; Vollmer, Ernst; Wang, Chung-su; Weber, Hans-Georg; 1975

36 Berger, Jochum: *Beitrag zur Berechnung des Spannungszustandes in rotationssymmetrisch belasteten Kugelschalen veränderlicher Wandstärke unter Gas- und Flüssigkeitsdruck durch Integration schwach singulärer Differentialgleichungen*, 1975

37 Dirksen, Wolfram: *Berechnung instationärer Abflußvorgänge in gestauten Gerinnen mittels Differenzenverfahren und die Anwendung auf Hochwasserrückhaltebecken*, 1976

38 Horlacher, Hans-Burkhard: *Berechnung instationärer Temperatur- und Wärmespannungsfelder in langen mehrschichtigen Hohlzylindern*, 1976

39 Hafner, Edzard: *Untersuchung der hydrodynamischen Kräfte auf Baukörper im Tiefwasserbereich des Meeres*, 1977, ISBN 3-921694-39-6

40 Ruppert, Jürgen: *Über den Axialwirbelkammerverstärker für den Einsatz im Wasserbau*, 1977, ISBN 3-921694-40-X

41 Hutarew, Andreas: *Beitrag zur Beeinflußbarkeit des Sauerstoffgehalts in Fließgewässern an Abstürzen und Wehren*, 1977, ISBN 3-921694-41-8, *vergriffen*

42 Miller, Christoph: *Ein Beitrag zur Bestimmung der schwingungserregenden Kräfte an unterströmten Wehren*, 1977, ISBN 3-921694-42-6

43 Schwarz, Wolfgang: *Druckstoßberechnung unter Berücksichtigung der Radial- und Längsverschiebungen der Rohrwandung*, 1978, ISBN 3-921694-43-4

44 Kinzelbach, Wolfgang: *Numerische Untersuchungen über den optimalen Einsatz variabler Kühlsysteme einer Kraftwerkskette am Beispiel Oberrhein*, 1978, ISBN 3-921694-44-2

45 Barczewski, Baldur: *Neue Meßmethoden für Wasser-Luftgemische und deren Anwendung auf zweiphasige Auftriebsstrahlen*, 1979, ISBN 3-921694-45-0

46 Neumayer, Hans: *Untersuchung der Strömungsvorgänge in radialen Wirbelkammerverstärkern*, 1979, ISBN 3-921694-46-9

47 Elalfy, Youssef-Elhassan: *Untersuchung der Strömungsvorgänge in Wirbelkammerdioden und -drosseln*, 1979, ISBN 3-921694-47-7

48 Brombach, Hansjörg: *Automatisierung der Bewirtschaftung von Wasserspeichern*, 1981, ISBN 3-921694-48-5

49 Geldner, Peter: *Deterministische und stochastische Methoden zur Bestimmung der Selbstdichtung von Gewässern*, 1981, ISBN 3-921694-49-3, *vergriffen*

50 Mehlhorn, Hans: *Temperaturveränderungen im Grundwasser durch Brauchwassereinleitungen*, 1982, ISBN 3-921694-50-7, *vergriffen*

51 Hafner, Edzard: *Rohrleitungen und Behälter im Meer*, 1983, ISBN 3-921694-51-5

52 Rinnert, Bernd: *Hydrodynamische Dispersion in porösen Medien: Einfluß von Dichteunterschieden auf die Vertikalvermischung in horizontaler Strömung*, 1983, ISBN 3-921694-52-3, *vergriffen*

53 Lindner, Wulf: *Steuerung von Grundwasserentnahmen unter Einhaltung ökologischer Kriterien*, 1983, ISBN 3-921694-53-1, *vergriffen*

54 Herr, Michael; Herzer, Jörg; Kinzelbach, Wolfgang; Kobus, Helmut; Rinnert, Bernd: *Methoden zur rechnerischen Erfassung und hydraulischen Sanierung von Grundwasserkontaminationen*, 1983, ISBN 3-921694-54-X

55 Schmitt, Paul: *Wege zur Automatisierung der Niederschlagsermittlung*, 1984, ISBN 3-921694-55-8, *vergriffen*

56 Müller, Peter: *Transport und selektive Sedimentation von Schwebstoffen bei gestautem Abfluß*, 1985, ISBN 3-921694-56-6

57 El-Qawasmeh, Fuad: *Möglichkeiten und Grenzen der Tropfbewässerung unter besonderer Berücksichtigung der Verstopfungsanfälligkeit der Tropfelemente*, 1985, ISBN 3-921694-57-4, *vergriffen*

58 Kirchenbaur, Klaus: *Mikroprozessorgesteuerte Erfassung instationärer Druckfelder am Beispiel seegangsbelasteter Baukörper*, 1985, ISBN 3-921694-58-2

59 Kobus, Helmut (Hrsg.): *Modellierung des großräumigen Wärme- und Schadstofftransports im Grundwasser*, Tätigkeitsbericht 1984/85 (DFG-Forschergruppe an den Universitäten Hohenheim, Karlsruhe und Stuttgart), 1985, ISBN 3-921694-59-0, *vergriffen*

60 Spitz, Karlheinz: *Dispersion in porösen Medien: Einfluß von Inhomogenitäten und Dichteunterschieden*, 1985, ISBN 3-921694-60-4, *vergriffen*

61 Kobus, Helmut: *An Introduction to Air-Water Flows in Hydraulics*, 1985, ISBN 3-921694-61-2

62 Kaleris, Vassilios: *Erfassung des Austausches von Oberflächen- und Grundwasser in horizontalebenen Grundwassermodellen*, 1986, ISBN 3-921694-62-0

63 Herr, Michael: *Grundlagen der hydraulischen Sanierung verunreinigter Porengrundwasserleiter*, 1987, ISBN 3-921694-63-9

64 Marx, Walter: *Berechnung von Temperatur und Spannung in Massenbeton infolge Hydratation*, 1987, ISBN 3-921694-64-7

65 Koschitzky, Hans-Peter: *Dimensionierungskonzept für Sohlbelüfter in Schußrinnen zur Vermeidung von Kavitationsschäden*, 1987, ISBN 3-921694-65-5

66 Kobus, Helmut (Hrsg.): *Modellierung des großräumigen Wärme- und Schadstofftransports im Grundwasser*, Tätigkeitsbericht 1986/87 (DFG-Forschergruppe an den Universitäten Hohenheim, Karlsruhe und Stuttgart) 1987, ISBN 3-921694-66-3

67 Söll, Thomas: *Berechnungsverfahren zur Abschätzung anthropogener Temperaturanomalien im Grundwasser*, 1988, ISBN 3-921694-67-1

68 Dittrich, Andreas; Westrich, Bernd: *Bodenseeufererosion, Bestandsaufnahme und Bewertung*, 1988, ISBN 3-921694-68-X, *vergriffen*

69 Huwe, Bernd; van der Ploeg, Rienk R.: *Modelle zur Simulation des Stickstoffhaushaltes von Standorten mit unterschiedlicher landwirtschaftlicher Nutzung*, 1988, ISBN 3-921694-69-8, *vergriffen*

70 Stephan, Karl: *Integration elliptischer Funktionen*, 1988, ISBN 3-921694-70-1

71 Kobus, Helmut; Zilliox, Lothaire (Hrsg.): *Nitratbelastung des Grundwassers, Auswirkungen der Landwirtschaft auf die Grundwasser- und Rohwasserbeschaffenheit und Maßnahmen zum Schutz des Grundwassers*. Vorträge des deutsch-französischen Kolloquiums am 6. Oktober 1988, Universitäten Stuttgart und Louis Pasteur Strasbourg (Vorträge in deutsch oder französisch, Kurzfassungen zweisprachig), 1988, ISBN 3-921694-71-X

72 Soyeaux, Renald: *Unterströmung von Stauanlagen auf klüftigem Untergrund unter Berücksichtigung laminarer und turbulenter Fließzustände*,1991, ISBN 3-921694-72-8

73 Kohane, Roberto: *Berechnungsmethoden für Hochwasserabfluß in Fließgewässern mit überströmten Vorländern*, 1991, ISBN 3-921694-73-6

74 Hassinger, Reinhard: *Beitrag zur Hydraulik und Bemessung von Blocksteinrampen in flexibler Bauweise*, 1991, ISBN 3-921694-74-4, *vergriffen*

75 Schäfer, Gerhard: *Einfluß von Schichtenstrukturen und lokalen Einlagerungen auf die Längsdispersion in Porengrundwasserleitern*, 1991, ISBN 3-921694-75-2

76 Giesecke, Jürgen: *Vorträge, Wasserwirtschaft in stark besiedelten Regionen; Umweltforschung mit Schwerpunkt Wasserwirtschaft*, 1991, ISBN 3-921694-76-0

77 Huwe, Bernd: *Deterministische und stochastische Ansätze zur Modellierung des Stickstoffhaushalts landwirtschaftlich genutzter Flächen auf unterschiedlichem Skalenniveau*, 1992, ISBN 3-921694-77-9, *vergriffen*

78 Rommel, Michael: *Verwendung von Kluftdaten zur realitätsnahen Generierung von Kluftnetzen mit anschließender laminar-turbulenter Strömungsberechnung*, 1993, ISBN 3-92 1694-78-7

79 Marschall, Paul: *Die Ermittlung lokaler Stofffrachten im Grundwasser mit Hilfe von Einbohrloch-Meßverfahren*, 1993, ISBN 3-921694-79-5, *vergriffen*

80 Ptak, Thomas: *Stofftransport in heterogenen Porenaquiferen: Felduntersuchungen und stochastische Modellierung*, 1993, ISBN 3-921694-80-9, *vergriffen*

81 Haakh, Frieder: *Transientes Strömungsverhalten in Wirbelkammern,* 1993, ISBN 3-921694-81-7

82 Kobus, Helmut; Cirpka, Olaf; Barczewski, Baldur; Koschitzky, Hans-Peter: *Versuchseinrichtung zur Grundwasser- und Altlastensanierung VEGAS, Konzeption und Programmrahmen*, 1993, ISBN 3-921694-82-5

83 Zang, Weidong: *Optimaler Echtzeit-Betrieb eines Speichers mit aktueller Abflußregenerierung*, 1994, ISBN 3-921694-83-3, *vergriffen*

84 Franke, Hans-Jörg: *Stochastische Modellierung eines flächenhaften Stoffeintrages und Transports in Grundwasser am Beispiel der Pflanzenschutzmittelproblematik*, 1995, ISBN 3-921694-84-1

85 Lang, Ulrich: *Simulation regionaler Strömungs- und Transportvorgänge in Karstaquiferen mit Hilfe des Doppelkontinuum-Ansatzes: Methodenentwicklung und Parameteridentifikation*, 1995, ISBN 3-921694-85-X, *vergriffen*

86 Helmig, Rainer: *Einführung in die Numerischen Methoden der Hydromechanik*, 1996, ISBN 3-921694-86-8, *vergriffen*

87 Cirpka, Olaf: *CONTRACT: A Numerical Tool for Contaminant Transport and Chemical Transformations - Theory and Program Documentation -*, 1996, ISBN 3-921694-87-6

88 Haberlandt, Uwe: *Stochastische Synthese und Regionalisierung des Niederschlages für Schmutzfrachtberechnungen*, 1996, ISBN 3-921694-88-4

89 Croisé, Jean: *Extraktion von flüchtigen Chemikalien aus natürlichen Lockergesteinen mittels erzwungener Luftströmung*, 1996, ISBN 3-921694-89-2, *vergriffen*

90 Jorde, Klaus: *Ökologisch begründete, dynamische Mindestwasserregelungen bei Ausleitungskraftwerken*, 1997, ISBN 3-921694-90-6, *vergriffen*

91 Helmig, Rainer: *Gekoppelte Strömungs- und Transportprozesse im Untergrund - Ein Beitrag zur Hydrosystemmodellierung-*, 1998, ISBN 3-921694-91-4, *vergriffen*

92 Emmert, Martin: *Numerische Modellierung nichtisothermer Gas-Wasser Systeme in porösen Medien,* 1997, ISBN 3-921694-92-2

93 Kern, Ulrich: *Transport von Schweb- und Schadstoffen in staugeregelten Fließgewässern am Beispiel des Neckars*, 1997, ISBN 3-921694-93-0, *vergriffen*

94 Förster, Georg: *Druckstoßdämpfung durch große Luftblasen in Hochpunkten von Rohrleitungen 1997*, ISBN 3-921694-94-9

95 Cirpka, Olaf: *Numerische Methoden zur Simulation des reaktiven Mehrkomponententransports im Grundwasser*, 1997, ISBN 3-921694-95-7, *vergriffen*

96 Färber, Arne: *Wärmetransport in der ungesättigten Bodenzone: Entwicklung einer thermischen In-situ-Sanierungstechnologie*, 1997, ISBN 3-921694-96-5

97 Betz, Christoph: *Wasserdampfdestillation von Schadstoffen im porösen Medium: Entwicklung einer thermischen In-situ-Sanierungstechnologie*, 1998, SBN 3-921694-97-3

98 Xu, Yichun: *Numerical Modeling of Suspended Sediment Transport in Rivers*, 1998, ISBN 3-921694-98-1, *vergriffen*

99 Wüst, Wolfgang: *Geochemische Untersuchungen zur Sanierung CKW-kontaminierter Aquifere mit Fe(0)-Reaktionswänden,* 2000, ISBN 3-933761-02-2

100 Sheta, Hussam: *Simulation von Mehrphasenvorgängen in porösen Medien unter Einbeziehung von Hysterese-Effekten*, 2000, ISBN 3-933761-03-4

101 Ayros, Edwin: *Regionalisierung extremer Abflüsse auf der Grundlage statistischer Verfahren*, 2000, ISBN 3-933761-04-2, *vergriffen*

102 Huber, Ralf: *Compositional Multiphase Flow and Transport in Heterogeneous Porous Media*, 2000, ISBN 3-933761-05-0

103 Braun, Christopherus: *Ein Upscaling-Verfahren für Mehrphasenströmungen in porösen Medien*, 2000, ISBN 3-933761-06-9

104 Hofmann, Bernd: *Entwicklung eines rechnergestützten Managementsystems zur Beurteilung von Grundwasserschadensfällen*, 2000, ISBN 3-933761-07-7

105 Class, Holger: *Theorie und numerische Modellierung nichtisothermer Mehrphasenprozesse in NAPL-kontaminierten porösen Medien,* 2001, ISBN 3-933761-08-5

106 Schmidt, Reinhard: *Wasserdampf- und Heißluftinjektion zur thermischen Sanierung kontaminierter Standorte*, 2001, ISBN 3-933761-09-3

107 Josef, Reinhold: *Schadstoffextraktion mit hydraulischen Sanierungsverfahren unter Anwendung von grenzflächenaktiven Stoffen*, 2001, ISBN 3-933761-10-7

108 Schneider, Matthias: *Habitat- und Abflussmodellierung für Fließgewässer mit unscharfen Berechnungsansätzen*, 2001, ISBN 3-933761-11-5

109 Rathgeb, Andreas: *Hydrodynamische Bemessungsgrundlagen für Lockerdeckwerke an überströmbaren Erddämmen*, 2001, ISBN 3-933761-12-3

110 Lang, Stefan: *Parallele numerische Simulation instätionärer Probleme mit adaptiven Methoden auf unstrukturierten Gittern*, 2001, ISBN 3-933761-13-1

111 Appt, Jochen; Stumpp Simone: *Die Bodensee-Messkampagne 2001, IWS/CWR Lake Constance Measurement Program 2001*, 2002, ISBN 3-933761-14-X

112 Heimerl, Stephan: *Systematische Beurteilung von Wasserkraftprojekten,* 2002, ISBN 3-933761-15-8, *vergriffen*

113 Iqbal, Amin: *On the Management and Salinity Control of Drip Irrigation,* 2002, ISBN 3-933761-16-6

114 Silberhorn-Hemminger, Annette: *Modellierung von Kluftaquifersystemen: Geostatistische Analyse und deterministisch-stochastische Kluftgenerierung,* 2002, ISBN 3-933761-17-4

115 Winkler, Angela: *Prozesse des Wärme- und Stofftransports bei der In-situ-Sanierung mit festen Wärmequellen,* 2003, ISBN 3-933761-18-2

116 Marx, Walter: *Wasserkraft, Bewässerung, Umwelt - Planungs- und Bewertungsschwerpunkte der Wasserbewirtschaftung,* 2003, ISBN 3-933761-19-0

117 Hinkelmann, Reinhard: *Efficient Numerical Methods and Information-Processing Techniques in Environment Water,* 2003, ISBN 3-933761-20-4

118 Samaniego-Eguiguren, Luis Eduardo: *Hydrological Consequences of Land Use / Land Cover and Climatic Changes in Mesoscale Catchments*, 2003, ISBN 3-933761-21-2

119 Neunhäuserer, Lina: *Diskretisierungsansätze zur Modellierung von Strömungs- und Transportprozessen in geklüftet-porösen Medien*, 2003, ISBN 3-933761-22-0

120 Paul, Maren: *Simulation of Two-Phase Flow in Heterogeneous Poros Media with Adaptive Methods*, 2003, ISBN 3-933761-23-9

121 Ehret, Uwe: *Rainfall and Flood Nowcasting in Small Catchments using Weather Radar*, 2003, ISBN 3-933761-24-7

122 Haag, Ingo: *Der Sauerstoffhaushalt staugeregelter Flüsse am Beispiel des Neckars - Analysen, Experimente, Simulationen -,* 2003, ISBN 3-933761-25-5

123 Appt, Jochen: *Analysis of Basin-Scale Internal Waves in Upper Lake Constance,* 2003, ISBN 3-933761-26-3

124 Hrsg.: Schrenk, Volker; Batereau, Katrin; Barczewski, Baldur; Weber, Karolin und Koschitzky, Hans-Peter: *Symposium Ressource Fläche und VEGAS - Statuskolloquium 2003, 30. September und 1. Oktober 2003,* 2003, ISBN 3-933761-27-1

125 Omar Khalil Ouda: *Optimisation of Agricultural Water Use: A Decision Support System for the Gaza Strip,* 2003, ISBN 3-933761-28-0

126 Batereau, Katrin: *Sensorbasierte Bodenluftmessung zur Vor-Ort-Erkundung von Schadensherden im Untergrund*, 2004, ISBN 3-933761-29-8

127 Witt, Oliver: *Erosionsstabilität von Gewässersedimenten mit Auswirkung auf den Stofftransport bei Hochwasser am Beispiel ausgewählter Stauhaltungen des Oberrheins*, 2004, ISBN 3-933761-30-1

128 Jakobs, Hartmut: *Simulation nicht-isothermer Gas-Wasser-Prozesse in komplexen Kluft-Matrix-Systemen*, 2004, ISBN 3-933761-31-X

129 Li, Chen-Chien: *Deterministisch-stochastisches Berechnungskonzept zur Beurteilung der Auswirkungen erosiver Hochwasserereignisse in Flussstauhaltungen,* 2004, ISBN 3-933761-32-8

130 Reichenberger, Volker; Helmig, Rainer; Jakobs, Hartmut; Bastian, Peter; Niessner, Jennifer: *Complex Gas-Water Processes in Discrete Fracture-Matrix Systems: Up-scaling, Mass-Conservative Discretization and Efficient Multilevel Solution,* 2004, ISBN 3-933761-33-6

131 Hrsg.: Barczewski, Baldur; Koschitzky, Hans-Peter; Weber, Karolin; Wege, Ralf: *VEGAS - Statuskolloquium 2004,* Tagungsband zur Veranstaltung am 05. Oktober 2004 an der Universität Stuttgart, Campus Stuttgart-Vaihingen, 2004, ISBN 3-933761-34-4

132 Asie, Kemal Jabir: *Finite Volume Models for Multiphase Multicomponent Flow through Porous Media*. 2005, ISBN 3-933761-35-2

133 Jacoub, George: *Development of a 2-D Numerical Module for Particulate Contaminant Transport in Flood Retention Reservoirs and Impounded Rivers,* 2004, ISBN 3-933761-36-0

134 Nowak, Wolfgang: *Geostatistical Methods for the Identification of Flow and Transport Parameters in the Subsurface,* 2005, ISBN 3-933761-37-9

135 Süß, Mia: *Analysis of the influence of structures and boundaries on flow and transport processes in fractured porous media*, 2005, ISBN 3-933761-38-7

136 Jose, Surabhin Chackiath: *Experimental Investigations on Longitudinal Dispersive Mixing in Heterogeneous Aquifers,* 2005, ISBN: 3-933761-39-5

137 Filiz, Fulya: *Linking Large-Scale Meteorological Conditions to Floods in Mesoscale Catchments,* 2005, ISBN 3-933761-40-9

138 Qin, Minghao: *Wirklichkeitsnahe und recheneffiziente Ermittlung von Temperatur und Spannungen bei großen RCC-Staumauern*, 2005, ISBN 3-933761-41-7

139 Kobayashi, Kenichiro: *Optimization Methods for Multiphase Systems in the Subsurface - Application to Methane Migration in Coal Mining Areas*, 2005, ISBN 3-933761-42-5

140 Rahman, Md. Arifur: *Experimental Investigations on Transverse Dispersive Mixing in Heterogeneous Porous Media,* 2005, ISBN 3-933761-43-3

141 Schrenk, Volker: *Ökobilanzen zur Bewertung von Altlastensanierungsmaßnahmen,* 2005, ISBN 3-933761-44-1

142 Hundecha, Hirpa Yeshewatesfa: *Regionalization of Parameters of a Conceptual Rainfall-Runoff Model*, 2005, ISBN: 3-933761-45-X

143 Wege, Ralf: *Untersuchungs- und Überwachungsmethoden für die Beurteilung natürlicher Selbstreinigungsprozesse im Grundwasser,* 2005, ISBN 3-933761-46-8

144 Breiting, Thomas: *Techniken und Methoden der Hydroinformatik - Modellierung von komplexen Hydrosystemen im Untergrund*, 2006, ISBN 3-933761-47-6

145 Hrsg.: Braun, Jürgen; Koschitzky, Hans-Peter; Müller, Martin: *Ressource Untergrund: 10 Jahre VEGAS: Forschung und Technologieentwicklung zum Schutz von Grundwasser und Boden,* Tagungsband zur Veranstaltung am 28. und 29. September 2005 an der Universität Stuttgart, Campus Stuttgart-Vaihingen, 2005, ISBN 3-933761-48-4

146 Rojanschi, Vlad: *Abflusskonzentration in mesoskaligen Einzugsgebieten unter Berücksichtigung des Sickerraumes,* 2006, ISBN 3-933761-49-2

147 Winkler, Nina Simone: *Optimierung der Steuerung von Hochwasserrückhaltebeckensystemen,* 2006, ISBN 3-933761-50-6

148 Wolf, Jens: *Räumlich differenzierte Modellierung der Grundwasserströmung alluvialer Aquifere für mesoskalige Einzugsgebiete*, 2006, ISBN: 3-933761-51-4

149 Kohler, Beate: *Externe Effekte der Laufwasserkraftnutzung*, 2006, ISBN 3-933761-52-2

150 Hrsg.: Braun, Jürgen; Koschitzky, Hans-Peter; Stuhrmann, Matthias: *VEGAS-Statuskolloquium 2006,* Tagungsband zur Veranstaltung am 28. September 2006 an der Universität Stuttgart, Campus Stuttgart-Vaihingen, 2006, ISBN 3-933761-53-0

151 Niessner, Jennifer: *Multi-Scale Modeling of Multi-Phase - Multi-Component Processes in Heterogeneous Porous Media*, 2006, ISBN 3-933761-54-9

152 Fischer, Markus: *Beanspruchung eingeerdeter Rohrleitungen infolge Austrocknung bindiger Böden,* 2006, ISBN 3-933761-55-7

153 Schneck, Alexander: *Optimierung der Grundwasserbewirtschaftung unter Berücksichtigung der Belange der Wasserversorgung, der Landwirtschaft und des Naturschutzes*, 2006, ISBN 3-933761-56-5

154 Das, Tapash: *The Impact of Spatial Variability of Precipitation on the Predictive Uncertainty of Hydrological Models,* 2006, ISBN 3-33761-57-3

155 Bielinski, Andreas: *Numerical Simulation of CO_2 sequestration in geological formations*, 2007, ISBN 3-933761-58-1

156 Mödinger, Jens: *Entwicklung eines Bewertungs- und Entscheidungsunterstützungssystems für eine nachhaltige regionale Grundwasserbewirtschaftung*, 2006, ISBN 3-933761-60-3

157 Manthey, Sabine: *Two-phase flow processes with dynamic effects in porous media - parameter estimation and simulation,* 2007, ISBN 3-933761-61-1

158 Pozos Estrada, Oscar: *Investigation on the Effects of Entrained Air in Pipelines,* 2007, ISBN 3-933761-62-X

159 Ochs, Steffen Oliver: *Steam injection into saturated porous media – process analysis including experimental and numerical investigations*, 2007, ISBN 3-933761-63-8

160 Marx, Andreas: *Einsatz gekoppelter Modelle und Wetterradar zur Abschätzung von Niederschlagsintensitäten und zur Abflussvorhersage, 2007,* ISBN 3-933761-64-6

161 Hartmann, Gabriele Maria: *Investigation of Evapotranspiration Concepts in Hydrological Modelling for Climate Change Impact Assessment*, 2007, ISBN 3-933761-65-4

162 Kebede Gurmessa, Tesfaye: *Numerical Investigation on Flow and Transport Characteristics to Improve Long-Term Simulation of Reservoir Sedimentation*, 2007, ISBN 3-933761-66-2

163 Trifković, Aleksandar: *Multi-objective and Risk-based Modelling Methodology for Planning, Design and Operation of Water Supply Systems*, 2007, ISBN 3-933761-67-0

164 Götzinger, Jens: *Distributed Conceptual Hydrological Modelling - Simulation of Climate, Land Use Change Impact and Uncertainty Analysis*, 2007, ISBN 3-933761-68-9

165 Hrsg.: Braun, Jürgen; Koschitzky, Hans-Peter; Stuhrmann, Matthias: *VEGAS – Kolloquium 2007,* Tagungsband zur Veranstaltung am 26. September 2007 an der Universität Stuttgart, Campus Stuttgart-Vaihingen, 2007, ISBN 3-933761-69-7

166 Freeman, Beau: *Modernization Criteria Assessment for Water Resources Planning; Klamath Irrigation Project, U.S.*, 2008, ISBN 3-933761-70-0

167 Dreher, Thomas: *Selektive Sedimentation von Feinstschwebstoffen in Wechselwirkung mit wandnahen turbulenten Strömungsbedingungen*, 2008, ISBN 3-933761-71-9

168 Yang, Wei: *Discrete-Continuous Downscaling Model for Generating Daily Precipitation Time Series*, 2008, ISBN 3-933761-72-7

169 Kopecki, Ianina: *Calculational Approach to FST-Hemispheres for Multiparametrical Benthos Habitat Modelling,* 2008*,* ISBN 3-933761-73-5

170 Brommundt, Jürgen: *Stochastische Generierung räumlich zusammenhängender Niederschlagszeitreihen*, 2008, ISBN 3-933761-74-3

171 Papafotiou, *Alexandros: Numerical Investigations of the Role of Hysteresis in Heterogeneous Two-Phase Flow Systems*, 2008, ISBN 3-933761-75-1

172 He, Yi: *Application of a Non-Parametric Classification Scheme to Catchment Hydrology*, 2008, ISBN 978-3-933761-76-7

173 Wagner, Sven: *Water Balance in a Poorly Gauged Basin in West Africa Using Atmospheric Modelling and Remote Sensing Information*, 2008, ISBN 978-3-933761-77-4

174 Hrsg.: Braun, Jürgen; Koschitzky, Hans-Peter; Stuhrmann, Matthias; Schrenk, Volker: *VEGAS-Kolloquium 2008 Ressource Fläche III*, Tagungsband zur Veranstaltung am 01. Oktober 2008 an der Universität Stuttgart, Campus Stuttgart-Vaihingen, 2008, ISBN 978-3-933761-78-1

175 Patil, Sachin: *Regionalization of an Event Based Nash Cascade Model for Flood Predictions in Ungauged Basins*, 2008, ISBN 978-3-933761-79-8

176 Assteerawatt, Anongnart: *Flow and Transport Modelling of Fractured Aquifers based on a Geostatistical Approach,* 2008, ISBN 978-3-933761-80-4

177 Karnahl, Joachim Alexander: *2D numerische Modellierung von multifraktionalem Schwebstoff- und Schadstofftransport in Flüssen*, 2008, ISBN 978-3-933761-81-1

178 Hiester, Uwe: *Technologieentwicklung zur In-situ-Sanierung der ungesättigten Bodenzone mit festen Wärmequellen,* 2009, ISBN 978-3-933761-82-8

179 Laux, Patrick: *Statistical Modeling of Precipitation for Agricultural Planning in the Volta Basin of West Africa,* 2009, ISBN 978-3-933761-83-5

180 Ehsan, Saqib: *Evaluation of Life Safety Risks Related to Severe Flooding,* 2009, ISBN 978-3-933761-84-2

181 Prohaska, Sandra: *Development and Application of a 1D Multi-Strip Fine Sediment Transport Model for Regulated Rivers,* 2009, ISBN 978-3-933761-85-9

182 Kopp, Andreas: *Evaluation of CO_2 Injection Processes in Geological Formations for Site Screening,* 2009, ISBN 978-3-933761-86-6

183 Ebigbo, Anozie: *Modelling of biofilm growth and its influence on CO_2 and water (two-phase) flow in porous media,* 2009, ISBN 978-3-933761-87-3

184 Freiboth, Sandra: *A phenomenological model for the numerical simulation of multiphase multicomponent processes considering structural alterations of porous media*, 2009, ISBN 978-3-933761-88-0

185 Zöllner, Frank: *Implementierung und Anwendung netzfreier Methoden im Konstruktiven Wasserbau und in der Hydromechanik*, 2009, ISBN 978-3-933761-89-7

186 Vasin, Milos: *Influence of the soil structure and property contrast on flow and transport in the unsaturated zone*, 2010, ISBN 978-3-933761-90-3

187 Li, Jing: *Application of Copulas as a New Geostatistical Tool*, 2010, ISBN 978-3-933761-91-0

188 AghaKouchak, Amir: *Simulation of Remotely Sensed Rainfall Fields Using Copulas*, 2010, ISBN 978-3-933761-92-7

189 Thapa, Pawan Kumar: *Physically-based spatially distributed rainfall runoff modelling for soil erosion estimation*, 2010, ISBN 978-3-933761-93-4

190 Wurms, Sven: *Numerische Modellierung der Sedimentationsprozesse in Retentionsanlagen zur Steuerung von Stoffströmen bei extremen Hochwasserabflussereignissen*, 2011, ISBN 978-3-933761-94-1

191 Merkel, Uwe: *Unsicherheitsanalyse hydraulischer Einwirkungen auf Hochwasserschutzdeiche und Steigerung der Leistungsfähigkeit durch adaptive Strömungsmodellierung*, 2011, ISBN 978-3-933761-95-8

192 Fritz, Jochen: *A Decoupled Model for Compositional Non-Isothermal Multiphase Flow in Porous Media and Multiphysics Approaches for Two-Phase Flow*, 2010, ISBN 978-3-933761-96-5

193 Weber, Karolin (Hrsg.): *12. Treffen junger WissenschaftlerInnen an Wasserbauinstituten*, 2010, ISBN 978-3-933761-97-2

194 Bliefernicht, Jan-Geert: *Probability Forecasts of Daily Areal Precipitation for Small River Basins,* 2011, ISBN 978-3-933761-98-9

195 Hrsg.: Koschitzky, Hans-Peter; Braun, Jürgen: *VEGAS-Kolloquium 2010 In-situ-Sanierung - Stand und Entwicklung Nano und ISCO -,* Tagungsband zur Veranstaltung am 07. Oktober 2010 an der Universität Stuttgart, Campus Stuttgart-Vaihingen*,* 2010*,* ISBN 978-3-933761-99-6

196 Gafurov, Abror: *Water Balance Modeling Using Remote Sensing Information - Focus on Central Asia,* 2010, ISBN 978-3-942036-00-9

197 Mackenberg, Sylvia: *Die Quellstärke in der Sickerwasserprognose: Möglichkeiten und Grenzen von Labor- und Freilanduntersuchungen,* 2010, ISBN 978-3-942036-01-6

198 Singh, Shailesh Kumar: *Robust Parameter Estimation in Gauged and Ungauged Basins,* 2010, ISBN 978-3-942036-02-3

199 Doğan, Mehmet Onur: *Coupling of porous media flow with pipe flow,* 2011, ISBN 978-3-942036-03-0

200 Liu, Min: *Study of Topographic Effects on Hydrological Patterns and the Implication on Hydrological Modeling and Data Interpolation,* 2011, ISBN 978-3-942036-04-7

201 Geleta, Habtamu Itefa: *Watershed Sediment Yield Modeling for Data Scarce Areas,* 2011, ISBN 978-3-942036-05-4

202 Franke, Jörg: *Einfluss der Überwachung auf die Versagenswahrscheinlichkeit von Staustufen,* 2011, ISBN 978-3-942036-06-1

203 Bakimchandra, Oinam: *Integrated Fuzzy-GIS approach for assessing regional soil erosion risks,* 2011, ISBN 978-3-942036-07-8

204 Alam, Muhammad Mahboob: *Statistical Downscaling of Extremes of Precipitation in Mesoscale Catchments from Different RCMs and Their Effects on Local Hydrology,* 2011, ISBN 978-3-942036-08-5

205 Hrsg.: Koschitzky, Hans-Peter; Braun, Jürgen: *VEGAS-Kolloquium 2011 Flache Geothermie - Perspektiven und Risiken,* Tagungsband zur Veranstaltung am 06. Oktober 2011 an der Universität Stuttgart, Campus Stuttgart-Vaihingen*,* 2011*,* ISBN 978-3-933761-09-2

206 Haslauer, Claus: *Analysis of Real-World Spatial Dependence of Subsurface Hydraulic Properties Using Copulas with a Focus on Solute Transport Behaviour,* 2011, ISBN 978-3-942036-10-8

207 Dung, Nguyen Viet: *Multi-objective automatic calibration of hydrodynamic models – development of the concept and an application in the Mekong Delta,* 2011, ISBN 978-3-942036-11-5

208 Hung, Nguyen Nghia: *Sediment dynamics in the floodplain of the Mekong Delta, Vietnam,* 2011, ISBN 978-3-942036-12-2

209 Kuhlmann, Anna: *Influence of soil structure and root water uptake on flow in the unsaturated zone,* 2012, ISBN 978-3-942036-13-9

210 Tuhtan, Jeffrey Andrew: *Including the Second Law Inequality in Aquatic Ecodynamics: A Modeling Approach for Alpine Rivers Impacted by Hydropeaking,* 2012, ISBN 978-3-942036-14-6

211 Tolossa, Habtamu: *Sediment Transport Computation Using a Data-Driven Adaptive Neuro-Fuzzy Modelling Approach,* 2012, ISBN 978-3-942036-15-3

212 Tatomir, Alexandru-Bodgan: *From Discrete to Continuum Concepts of Flow in Fractured Porous Media,* 2012, ISBN 978-3-942036-16-0

213 Erbertseder, Karin: *A Multi-Scale Model for Describing Cancer-Therapeutic Transport in the Human Lung,* 2012, ISBN 978-3-942036-17-7

214 Noack, Markus: *Modelling Approach for Interstitial Sediment Dynamics and Reproduction of Gravel Spawning Fish,* 2012, ISBN 978-3-942036-18-4

215 De Boer, Cjestmir Volkert: *Transport of Nano Sized Zero Valent Iron Colloids during Injection into the Subsurface*, 2012, ISBN 978-3-942036-19-1

216 Pfaff, Thomas: *Processing and Analysis of Weather Radar Data for Use in Hydrology*, 2013, ISBN 978-3-942036-20-7

217 Lebrenz, Hans-Henning: *Addressing the Input Uncertainty for Hydrological Modeling by a New Geostatistical Method*, 2013, ISBN 978-3-942036-21-4

218 Darcis, Melanie Yvonne: *Coupling Models of Different Complexity for the Simulation of CO_2 Storage in Deep Saline Aquifers*, 2013, ISBN 978-3-942036-22-1

219 Beck, Ferdinand: *Generation of Spatially Correlated Synthetic Rainfall Time Series in High Temporal Resolution - A Data Driven Approach*, 2013, ISBN 978-3-942036-23-8

220 Guthke, Philipp: *Non-multi-Gaussian spatial structures: Process-driven natural genesis, manifestation, modeling approaches, and influences on dependent processes*, 2013, ISBN 978-3-942036-24-5

221 Walter, Lena: *Uncertainty studies and risk assessment for CO_2 storage in geological formations*, 2013, ISBN 978-3-942036-25-2

222 Wolff, Markus: *Multi-scale modeling of two-phase flow in porous media including capillary pressure effects,* 2013, ISBN 978-3-942036-26-9

223 Mosthaf, Klaus Roland: *Modeling and analysis of coupled porous-medium and free flow with application to evaporation processes,* 2014, ISBN 978-3-942036-27-6

224 Leube, Philipp Christoph: *Methods for Physically-Based Model Reduction in Time: Analysis, Comparison of Methods and Application*, 2013, ISBN 978-3-942036-28-3

225 Rodríguez Fernández, Jhan Ignacio: *High Order Interactions among environmental variables: Diagnostics and initial steps towards modeling*, 2013, ISBN 978-3-942036-29-0

226 Eder, Maria Magdalena: *Climate Sensitivity of a Large Lake*, 2013, ISBN 978-3-942036-30-6

227 Greiner, Philipp: *Alkoholinjektion zur In-situ-Sanierung von CKW Schadensherden in Grundwasserleitern: Charakterisierung der relevanten Prozesse auf unterschiedlichen Skalen*, 2014, ISBN 978-3-942036-31-3

228 Lauser, Andreas: *Theory and Numerical Applications of Compositional Multi-Phase Flow in Porous Media*, 2014, ISBN 978-3-942036-32-0

229 Enzenhöfer, Rainer: *Risk Quantification and Management in Water Production and Supply Systems*, 2014, ISBN 978-3-942036-33-7

230 Faigle, Benjamin: *Adaptive modelling of compositional multi-phase flow with capillary pressure*, 2014, ISBN 978-3-942036-34-4

231 Oladyshkin, Sergey: *Efficient modeling of environmental systems in the face of complexity and uncertainty*, 2014, ISBN 978-3-942036-35-1

232 Sugimoto, Takayuki: *Copula based Stochastic Analysis of Discharge Time Series*, 2014, ISBN 978-3-942036-36-8

233 Koch, Jonas: *Simulation, Identification and Characterization of Contaminant Source Architectures in the Subsurface*, 2014, ISBN 978-3-942036-37-5

234 Zhang, Jin: *Investigations on Urban River Regulation and Ecological Rehabilitation Measures, Case of Shenzhen in China*, 2014, ISBN 978-3-942036-38-2

235 Siebel, Rüdiger: *Experimentelle Untersuchungen zur hydrodynamischen Belastung und Standsicherheit von Deckwerken an überströmbaren Erddämmen,* 2014, ISBN 978-3-942036-39-9

236 Baber, Katherina: *Coupling free flow and flow in porous media in biological and technical applications: From a simple to a complex interface description,* 2014, ISBN 978-3-942036-40-5

237 Nuske, Klaus Philipp: *Beyond Local Equilibrium — Relaxing local equilibrium assumptions in multiphase flow in porous media,* 2014, ISBN 978-3-942036-41-2

238 Geiges, Andreas: *Efficient concepts for optimal experimental design in nonlinear environmental systems*, 2014, ISBN 978-3-942036-42-9

239 Schwenck, Nicolas: *An XFEM-Based Model for Fluid Flow in Fractured Porous Media*, 2014, ISBN 978-3-942036-43-6

240 Chamorro Chávez, Alejandro: *Stochastic and hydrological modelling for climate change prediction in the Lima region, Peru*, 2015, ISBN 978-3-942036-44-3

241 Yulizar: *Investigation of Changes in Hydro-Meteorological Time Series Using a Depth-Based Approach*, 2015, ISBN 978-3-942036-45-0

242 Kretschmer, Nicole: *Impacts of the existing water allocation scheme on the Limarí watershed – Chile, an integrative approach*, 2015, ISBN 978-3-942036-46-7

243 Kramer, Matthias: *Luftbedarf von Freistrahlturbinen im Gegendruckbetrieb*, 2015, ISBN 978-3-942036-47-4

244 Hommel, Johannes: *Modeling biogeochemical and mass transport processes in the subsurface: Investigation of microbially induced calcite precipitation*, 2016, ISBN 978-3-942036-48-1

245 Germer, Kai: *Wasserinfiltration in die ungesättigte Zone eines makroporösen Hanges und deren Einfluss auf die Hangstabilität*, 2016, ISBN 978-3-942036-49-8

246 Hörning, Sebastian: *Process-oriented modeling of spatial random fields using copulas*, 2016, ISBN 978-3-942036-50-4

247 Jambhekar, Vishal: *Numerical modeling and analysis of evaporative salinization in a coupled free-flow porous-media system,* 2016, ISBN 978-3-942036-51-1

248 Huang, Yingchun: *Study on the spatial and temporal transferability of conceptual hydrological models*, 2016, ISBN 978-3-942036-52-8

249 Kleinknecht, Simon Matthias: *Migration and retention of a heavy NAPL vapor and remediation of the unsaturated zone*, 2016, ISBN 978-3-942036-53-5

250 Kwakye, Stephen Oppong: *Study on the effects of climate change on the hydrology of the West African sub-region*, 2016, ISBN 978-3-942036-54-2

251 Kissinger, Alexander: *Basin-Scale Site Screening and Investigation of Possible Impacts of CO_2 Storage on Subsurface Hydrosystems*, 2016, ISBN 978-3-942036-55-9

252 Müller, Thomas: *Generation of a Realistic Temporal Structure of Synthetic Precipitation Time Series for Sewer Applications*, 2017, ISBN 978-3-942036-56-6

253 Grüninger, Christoph: *Numerical Coupling of Navier-Stokes and Darcy Flow for Soil-Water Evaporation*, 2017, ISBN 978-3-942036-57-3

254 Suroso: *Asymmetric Dependence Based Spatial Copula Models: Empirical Investigations and Consequences on Precipitation Fields*, 2017, ISBN 978-3-942036-58-0

255 Müller, Thomas; Mosthaf, Tobias; Gunzenhauser, Sarah; Seidel, Jochen; Bárdossy, András: *Grundlagenbericht Niederschlags-Simulator (NiedSim3)*, 2017, ISBN 978-3-942036-59-7

256 Mosthaf, Tobias: *New Concepts for Regionalizing Temporal Distributions of Precipitation and for its Application in Spatial Rainfall Simulation,* 2017, ISBN 978-3-942036-60-3

257 Fenrich, Eva Katrin: *Entwicklung eines ökologisch-ökonomischen Vernetzungsmodells für Wasserkraftanlagen und Mehrzweckspeicher,* 2018, ISBN 978-3-942036-61-0

258 Schmidt, Holger: *Microbial stabilization of lotic fine sediments*, 2018, ISBN 978-3-942036-62-7

259 Fetzer, Thomas: *Coupled Free and Porous-Medium Flow Processes Affected by Turbulence and Roughness – Models, Concepts and Analysis*, 2018, ISBN 978-3-942036-63-4

260 Schröder, Hans Christoph: *Large-scale High Head Pico Hydropower Potential Assessment*, 2018, ISBN 978-3-942036-64-1

261 Bode, Felix: *Early-Warning Monitoring Systems for Improved Drinking Water Resource Protection*, 2018, ISBN 978-3-942036-65-8

262 Gebler, Tobias: *Statistische Auswertung von simulierten Talsperrenüberwachungsdaten zur Identifikation von Schadensprozessen an Gewichtsstaumauern*, 2018, ISBN 978-3-942036-66-5

263 Harten, Matthias von: *Analyse des Zuppinger-Wasserrades – Hydraulische Optimierungen unter Berücksichtigung ökologischer Aspekte*, 2018, ISBN 978-3-942036-67-2

264 Yan, Jieru: *Nonlinear estimation of short time precipitation using weather radar and surface observations*, 2018, ISBN 978-3-942036-68-9

265 Beck, Martin: *Conceptual approaches for the analysis of coupled hydraulic and geomechanical processes*, 2019, ISBN 978-3-942036-69-6

266 Haas, Jannik: *Optimal planning of hydropower and energy storage technologies for fully renewable power systems*, 2019, ISBN 978-3-942036-70-2

267 Schneider, Martin: *Nonlinear Finite Volume Schemes for Complex Flow Processes and Challenging Grids*, 2019, ISBN 978-3-942036-71-9

268 Most, Sebastian Christopher: *Analysis and Simulation of Anomalous Transport in Porous Media*, 2019, ISBN 978-3-942036-72-6

269 Buchta, Rocco: *Entwicklung eines Ziel- und Bewertungssystems zur Schaffung nachhaltiger naturnaher Strukturen in großen sandgeprägten Flüssen des norddeutschen Tieflandes*, 2019, ISBN 978-3-942036-73-3

270 Thom, Moritz: *Towards a Better Understanding of the Biostabilization Mechanisms of Sediment Beds*, 2019, ISBN 978-3-942036-74-0

271 Stolz, Daniel: *Die Nullspannungstemperatur in Gewichtsstaumauern unter Berücksichtigung der Festigkeitsentwicklung des Betons*, 2019, ISBN 978-3-942036-75-7

272 Rodriguez Pretelin, Abelardo: *Integrating transient flow conditions into groundwater well protection*, 2020, ISBN: 978-3-942036-76-4

Die Mitteilungshefte ab der Nr. 134 (Jg. 2005) stehen als pdf-Datei über die Homepage des Instituts: www.iws.uni-stuttgart.de zur Verfügung.